Martin Seeber, Dipl.Ing.

The Electroencephalographic Sources of Repetitive Movements

DISSERTATION

zur Erlangung des akademischen Grades

Doktor der technischen Wissenschaften

eingereicht an der

Technischen Universität Graz

Betreuer

Univ.-Prof. Dipl-Ing. Dr.techn. Gernot R. Müller-Putz

Institut für Neurotechnologie

Mitbetreuer
Assoc.Prof. Dipl.-Ing. Dr.techn. Reinhold Scherer

Graz, Februar 2017

EIDESSTATTLICHE ERKLÄRUNG

AFFIDAVIT

Ich erkläre an Eides statt, dass ich die vorliegende Arbeit selbstständig verfasst, andere als die angegebenen Quellen/Hilfsmittel nicht benutzt, und die den benutzten Quellen wörtlich und inhaltlich entnommenen Stellen als solche kenntlich gemacht habe. Das in TUGRAZonline hochgeladene Textdokument ist mit der vorliegenden Dissertation identisch.

I declare that I have authored this thesis independently, that I have not used other than the declared sources/resources, and that I have explicitly indicated all material which has been quoted either literally or by content from the sources used. The text document uploaded to TUGRAZonline is identical to the present doctoral dissertation.

Datum / Date

Unterschrift / Signature

Abstract

Investigating cortical involvement in motoric functions could lead to important progress in the research of motor impairment after brain injury. Studying brain dynamics during full-body movements, including gait, is a great challenge due to limitations of neuroimaging methods.
This thesis provides multiple achievements towards the development of an EEG based neuroimaging tool capable to investigate cortical dynamics during actual, full-body movements. These achievements include, the capability to consider individual head and brain geometries, the reduction of muscular artifacts during movements and the integration of motion tracking data for modeling cortical sources of repetitive movements.
Furthermore, these innovative neuroimaging techniques were utilized for modeling the neurophysiology of repetitive movements. More specifically, EEG source oscillations were studied during gait and repetitive finger movements in young healthy volunteers. In the data analysis, sustained and movement phase-related EEG source amplitude modulations were separated, based on the movement sequences. Interestingly, the sources of sustained- and movement-phase related activities were identified to be different. Therefore, I suggest that these two phenomena represent two different types of large-scale networks. First, movement state related networks, which upregulate cortical excitability in areas, specific to the body part that is moved. Second, movement-phase related networks, which modulate their frequency-specific synchrony in relation to the movement sequences. These networks may be related with other functions, including top-down control, prediction and integration of sensorimotor information.
The distinction of different large-scale cortical networks introduced in this work facilitates the interpretation of EEG sources during repetitive movements. The methods and findings of this thesis may contribute to further progress in basic and clinical neuroscience research as well as to the improvement of Brain-Computer Interfaces.

Zusammenfassung

Die Untersuchung kortikaler Einflüsse auf die Ausübung motorischer Funktionen kann zu Fortschritten in der Erforschung von motorischen Beeinträchtigungen führen, welche als Folge von Gehirnschädigungen entstehen können. Die Erforschung von Gehirnaktivität während der Bewegung des ganzen Körpers, u.a. der Gangfunktion, ist allerdings eine Herausforderung die aus den methodischen Möglichkeiten bildgebender Verfahren resultiert. Diese Doktorarbeit enthält einige Beiträge zur Entwicklung von EEG basierenden, bildgebenden Verfahren, die die Untersuchung der Gehirnaktivität während Körperbewegungen ermöglichen. Diese Entwicklungen beinhalten die Berücksichtigung individueller Geometrie des Kopfes und Gehirns, die Unterdrückung von Muskelartefakten und die Integration von Bewegungstrajektorien für die Modellierung der kortikaler Quellen von repetitiven Bewegungen.
Weiters wurden diese innovativen Technologien dafür genutzt, um die Neurophysiologie während repetitiven Bewegungen zu modellieren. Hierzu wurden die EEG Quelldynamiken des Ganges sowie während rhythmischen Fingerbewegungen untersucht. In der Datenanalyse wurden andauernde von bewegungsphasen bezogene Modulationen der EEG Quellamplituden unterschieden. Interessanterweise wurden die Quellen der beiden Phänomene als unterschiedlich identifiziert. Diese Ergebnisse lassen vermuten, dass die beiden Modulationstypen unterschiedliche makroskopische kortikale Netzwerke repräsentieren. Zum einen, Bewegungszustands-Netzwerke die die kortikale Erregbarkeit in Gehirnregionen spezifisch zum bewegten Körperteil erhöhen. Zum Anderen, bewegungsphasen bezogene Netzwerke, die ihre Frequenz-spezifische Synchronizität in Relation zu den Bewegungssequenzen modulieren. Diese Netzwerke könnten mit anderen Funktionen in Verbindung stehen, wie etwa der hierarchischen Kontrolle, sowie der Prädiktion und Integration sensomotorischer Information. Die Unterscheidung verschiedener kortikaler Netzwerke, die in dieser Arbeit

eingeführt wurde, erleichtert die Interpretation von EEG Quellsignalen während repetitiven Bewegungen. Die Methoden und Ergebnisse der Arbeit können zu weiteren Fortschritten in der neurowissenschaftlichen Grundlagenforschung sowie in der klinischer Forschung, als auch zur Verbesserung von Gehirn-Computer Schnittstellen beitragen.

Acknowledgements

First of all, I want to cordially thank my supervisor Prof. Gernot R. Müller-Putz for his valuable guidance throughout and towards the completion of my PhD. Further, I would like to thank Prof. Reinhold Scherer, who always backed me up over the years and supported me with his additional mentorship. As principal investigator of most of the projects I worked on, he provided the possibility to develop my own ideas and research interests.

I am also very grateful to all of my colleagues at the Institute of Neural Engineering. Especially, I want to thank David Steyrl for being a magnificent office colleague and Johanna Wagner for many great discussions at scientific conferences.

Moreover, I would like to thank my friends for their support and their patience, when I was speaking about the brain a bit too much.
I also would like to thank my family especially my father, Reinhard Seeber, for supporting me in many ways over the years.

Finally, I like to acknowledge the financial support of the European Union research project BETTER (ICT-2009.7.2-247935), BioTechMed Graz and the Land Steiermark projects BCI4REHAB and rE(EG)map!

Contents

List of Figures

1. Introduction

1.1. A brief overview of Brain Mapping

In accordance with the Medical Subject Headings (MeSH) vocabulary, *Brain Mapping* is defined as "Imaging techniques used to colocalize sites of brain functions or physiological activity with brain structures."[1]. There are two types of signals, which are mainly used for studying brain functions.
First, hemodynamic response signals, which are suggested to represent energy consumption of brain cells in a certain region. These signals are recorded by functional magnetic resonance imaging (fMRI) [1–3] and functional near-infrared spectroscopy (fNIRS) [4, 5].
Second, electrophysiological signals which directly record electrical dynamics of single neurons or neural populations. Neural population signals can be recorded invasively as local field potentials (LFP) and, on a larger spatial scale, electrocorticography (ECoG). LFP are capturing fluctuations of membrane potentials. ECoG signals are recorded on the cortical surface and as spatio-temporal summation of underlying LFP [6–8]. The non-invasive, extracranial counterpart to ECoG signals can be recorded as electroencephalography (EEG) at the scalp [9, 10]. Magnetoencephalography (MEG), in distinction to EEG, records the magnetic fields originated by the dynamics of electrical currents in the brain [11, 12].
The temporal resolution of electrophysiological recording techniques is much higher in comparison to fMRI and fNIRS recordings. While the temporal resolution is in the milliseconds range for electrophysiological recordings, it is >1 second for fMRI and fNIRS. However, fMRI is the most frequently used brain mapping technique these days. An important advantage of fMRI is it's high spatial resolution, which is at around one

[1] **MeSH Unique ID: D001931**.

millimeter. Further, using fMRI recordings it is possible to scan activity of the whole brain, including deep structures. In other words the coverage of these recordings is high.
Electrophysiological recording techniques largely differ in their spatial resolution. LFP represents the electrical dynamics of about 1000 neurons within a radius of about 140 µm [7] to the electrode tip. On the other hand, the spatial resolution of the EEG is typically 1 cm, capturing the summed electrical activity of 10 to several 100 million of neurons [13]. However, there is a trade-off between spatial resolution and coverage. For example, LFP are capable to record nearby neuronal activity in great detail. But naturally, they are spatially limited to a very specific brain region. That is, the location of the electrode tips. However, using high density EEG it is easily possible to record brain activity from many brain regions simultaneously. In comparison to invasive recordings, the signal quality of EEG recordings is much lower. The lower signal to noise ratio is largely caused by the comparably greater distance of the EEG electrodes to the neuronal sources of the signal. The electrical field monotonically decreases with increasing distance to their sources. More precisely, it is distorted by the propagation through different kinds of tissues associated with different electrical conductivities.
Based on the above mentioned properties of each brain mapping technique it appears that every recording method has advantages and disadvantages. Therefore, the choice of a brain mapping technique is highly dependent on the research question itself. In this work, we aim to study the cortical dynamics linked to body movements. In the next section, I argue why high density EEG recordings in combination with inverse source reconstruction methods is the brain mapping technique of choice in this thesis.

1.2. EEG: A brain mapping technique capable to study body movements

The majority of recent brain mapping studies are using fMRI. For studying body movements in humans however, fMRI has some critical limitations. The tube of MRI scanners restricts subjects in their movements. Further, subjects have to lay in the MRI scanner having their heads fixated. Any head movement during fMRI measurements is lowering it's signal quality and in the worst case is causing misleading results. Due to the heavy weight and large dimensions of MRI scanners, this setting restricts mobile applications. Therefore, fMRI, despite it's great usefulness, is not well-suited for studying cortical dynamics in humans during body movements, e.g. walking.

For studying cortical dynamics linked to body movements, EEG brain mapping provides several advantages. First, EEG recordings provide high temporal resolution in the milliseconds range. This high temporal resolution enables to directly investigate cortical signals in relation to movement kinematics and trajectories. Second, EEG signals provide many features, e.g. oscillations in distinct frequency ranges that are suggested to signify different large-scale neuronal interactions [14–16]. Because of these manifold features and due to the good coverage, EEG recordings are well-suited for investigating different cortical systems. Third, EEG recording systems, due to their lightweight, enable ambulatory experimental setups, which allow studying body movements including walking [17, 18].
Further, advances in EEG recording hardware resulted in the availability of compact, high-density (64 or more electrodes) systems which can be set up and mounted in a reasonable amount of time. High-density EEG recordings in combination with advanced computational methods for signal processing are leading to the utilization of EEG as a brain imaging tool [19]. To do so, information from different data sources has to be integrated in computational models. For studying body movements such modeling is twofold. First, computational modeling is needed to reconstruct cortical sources from EEG scalp recordings [19–22]. Based on these reconstructed EEG sources a second modeling step is necessary to directly relate specific EEG phenomena to the movement parameters of an experiment.

To reconstruct cortical sources, high-density EEG signals are combined with their electrodes' locations and a realistic model of the head. This model considers the geometries and conductivities of different tissues of the head (e.g. grey and white brain matter, cerebrospinal fluid, skull, skin). The tissues' geometry can be obtained from individual structural MRI scans. Head models are used to determine how the electrical field propagates from cortical populations to the EEG recording sites. This relationship can be computationally inverted using physiological constraints, thus allowing reconstruction of the cortical dynamics directly from EEG recordings. In summary, advanced EEG source reconstruction techniques integrate information from high-density EEG recordings and sophisticated head models into brain images at a millisecond temporal resolution.

For studying body movements, the reconstructed cortical dynamics can be related in a second modeling step to the movement parameters of an experiment. Traditionally, brain imaging was restricted to fixed setups as a result of above mentioned reasons. Recently, brain imaging was enabled also in mobile experimental setups, because of the availability of portable EEG recording systems along with methodical progress in EEG brain imaging methods [17, 18]. These methodical developments crucially include sophisticated artifact handling. The novel possibilities in mobile brain imaging implicate also additional variables, which have to be considered in the experimental design with respect to brain imaging. For instance, movement kinematics could be used as regressors in a model to determine cortical sources which correlate significantly with these kinematics. Another example would be to consider the position of a subject during brain imaging in a spatial navigation experiment.

The interpretation of the resulting EEG brain images is highly dependent on the EEG phenomena which are studied and respectively are mapped in these images. These phenomena and the corresponding theories are discussed in the next section.

1.3. EEG phenomena, what do we map?

1.3.1. The genesis of the EEG

EEG signals are fluctuations of the electric potentials recorded at the scalp. These signals are mainly generated by the spatio-temporal superimposition of postsynaptic potentials (PSP) of neuronal populations in the cortex. PSPs are alterations of the neuronal membrane potentials, caused by successful synaptic transmissions. Excitatory postsynaptic potentials (EPSP) cause a depolarization of the membrane potential, while inhibitory postsynaptic potentials (IPSP) cause a hyperpolarization. Therefore, the former increase the spiking probability, the latter decrease it.

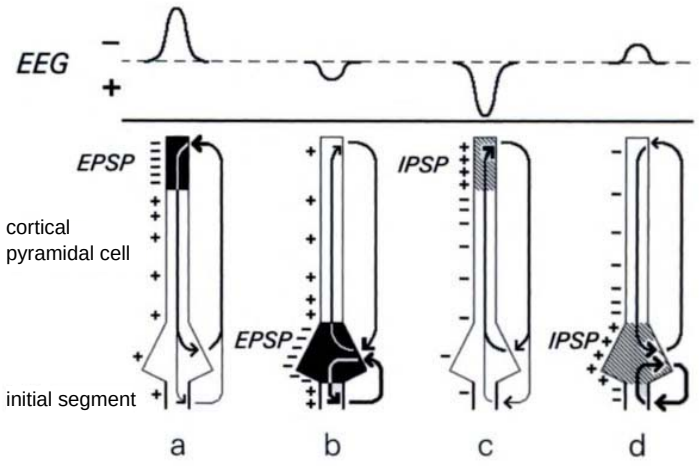

Figure 1.1.: The genesis of EEG fluctiations in dependence of different PSP. Modified from Zschocke [23] with permission from Springer.

Relevant for the genesis of EEG signals are the extracellular ionic current shifts resulting from the PSPs. EPSPs lower the number of positively charged ions located beneath the synapse. Relative to inactive membrane parts, the extracellular potential at the synapse is getting electrically negative and consequently forming an electrical dipole. The equivalent applies for IPSPs with inverted signs. Therefore, the orientation of these dipoles is dependent on the type of the PSP (excitatory/inhibitory) as well as the

position of the synapse at the neuron. For instance, an EPSP at the apical dendrites of a neuron will cause the same dipole orientation as an IPSP at the soma. This relationship is also illustrated in Figure 1.1. The synaptic activity of one single neuron, naturally cannot be detected in such large-scale recordings as EEG. At the cellular level, the extracellular field results from the activity of up to 10^4 synapses for one neuron. Since EEG is recording the activity of millions of neurons, these electrical fields are summed up additionally in the extracellular space for a large cortical population. To cause a macroscopic fluctuation of the scalp potential, which can be recorded as EEG, the synchronous activity of spatially aligned structures is necessary. Pyramidal neurons in the grey matter of the brain are largely spatially aligned, perpendicular to the cortical surface. Additionally to the spatial alignment the extracellular dipoles, they have to be electrically aligned at a given time point. Therefore, a fluctuation of the scalp potential depends on the temporal (synchrony) and spatial alignment of underlying large-scale neuronal populations. [10, 13, 23]

1.3.2. EEG oscillations

The observation of oscillatory phenomena in EEG recordings is directly linked with the discovery of the EEG itself. Prominent waves with a frequency between 8 and 13 Hz recorded over occipital areas were firstly described and therefore, were named 'alpha' waves. Large alpha amplitudes appeared when subjects closed their eyes and diminished, when the eyes were opened again [9]. Based on these findings, EEG oscillations are classically categorized into different frequency bands, that are, delta (0.5-4 Hz), theta (4-8 Hz), alpha (8-13 Hz), beta (13-30 Hz) and gamma (>30 Hz). These different EEG oscillations were roughly associated with different states of the brain, e.g. sleep, wakefulness, memory, motoric or cognitive processing, etc. [10]
However, this classical view on EEG signals has changed gradually over the years. For instance, it is necessary to distinguish between parieto-occipital alpha oscillations and central alpha, so called 'μ' rhythms [24, 25]. The generators of EEG oscillations are not well understood yet [26].

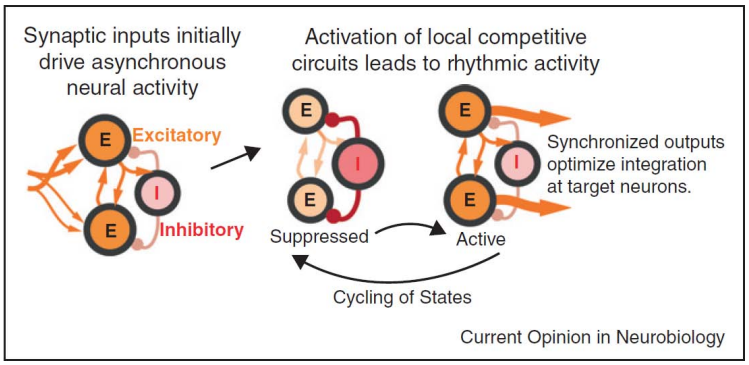

Figure 1.2.: Genesis of neuronal oscillations in a simple model. Initial, asynchronous activity (left) is replaced by alternating, synchronous suppression (middle) and activation (right) states due to interactions in neuronal circuitries. The resulting rhythmic fluctuations of the membrane potentials can be recorded extracellularly as neuronal oscillations. Reprinted from Miller and Buschman [27] with permission from Elsevier.

However, there are models suggesting that neuronal oscillations are mainly generated by recurrent connections in thalamocortical and cortico-cortical networks [14, 28, 29]. A very simple model capable to describe how neural oscillations could come about is illustrated in Figure 1.2. In this model, excitatory neurons (orange) are initially activated by asynchronous synaptic inputs (left). An active inhibitory interneuron (red) which is connected to both excitatory neurons suppresses these neurons simultaneously (middle). After suppression, both excitatory neurons are activated in parallel, which in turn charges the interneuron again. When the interneuron is active again, the cycle starts again. In local populations, the alternation between suppression and activation can be recorded as neuronal oscillations. Synchronous, rhythmic activity of the excitatory neurons increases the impact on downstream target neurons and thereby facilitates neural processing [27, 30].
Large-scale network interactions in the brain are naturally much more complex. Yet, this simple model illustrates how oscillations could be linked and therefore represent neuronal network interactions. Again, to generate an observable effect in macroscopic recordings as EEG, a large neuronal population is necessary to oscillate in synchrony.

1.3.3. Event-related desynchronization and synchronization

Similarly to the suppression of the alpha rhythm by eyes opening [9] μ rhythm (8-13 Hz) amplitudes recorded over motor areas decrease by the preparation, imagination and execution of movements [31–33]. This frequency-specific power decrease was suggested to reflect decreased synchrony of underlying neuronal populations and therefore is called event-related desynchronization (ERD) [31, 34]. The opposite scenario, namely power increase, is called event-related synchronization (ERS) and is considered to represent increased synchrony at a given frequency [34, 35]. ERD/ERS measures are defined by the comparison of the power during an active period (A) and a baseline or reference period (R) as indicated in equation 1.1. Thereby, ERD/ERS phenomena represent the modulation of oscillations in neuronal networks during an event in the active period in relation to the reference period.

$$ERD/ERS = \frac{A - R}{R} \cdot 100\% \tag{1.1}$$

In distinction from event-related potentials which appear phase-locked to an internal or external event, ERD/ERS are time-locked, but not phase-locked to the event. Therefore, some sort of power estimation in a defined frequency range is necessary when, as usually, multiple epochs are averaged to calculate the ERD/ERS measure. Otherwise, signals from different epochs would attenuate each other, due to their different phases.
The terms ERD and ERS are only meaningful, if there is a clear spectral peak at a given frequency, that is attenuated for ERD or is evolved for ERS [34]. ERD/ERS phenomena are extensively studied during movement experiments. It has been shown that μ rhythm ERD appears specific to right and left hand movements, on the contralateral hemisphere respectively. Further, foot movements induce ERD centrally over the sensorimotor areas [36]. These spatial localizations are in accordance with the somatotopic arrangement of the motor cortex [6] and were also reproduced using invasive, ECoG recordings [37]. Similarly, beta oscillations at around 20 Hz were also shown to desynchronize specifically to movements [37–39]. After movement, beta amplitudes increase in a short-lasting burst [33, 40, 41]. Therefore, ERD at μ and beta frequencies were suggested to reflect an increased excitability

level of neurons in respective cortical areas. On the contrary, beta ERS was interpreted as inhibition of neural circuitry [33, 34]. The description of ERD/ERS phenomena is of great importance for investigating EEG oscillatory dynamics, since it provides physiological interpretations for large-scale measures, i.e. EEG band power.

1.3.4. Frequency-specific cortical networks

Neuronal oscillations are studied in more detail using intracranial, invasive recordings. In addition to the LFP, microelectrode recordings are capable to record spiking activity of nearby neurons simultaneously. Therefore, the temporal relation of LFP signals and spike events can be studied. Indeed, this line of research found neuronal oscillations to be involved in the temporal coordination of neuronal populations. Especially, gamma oscillations (>30 Hz) in the visual system are related with the synchronization of neuronal groups [42–44]. Further, gamma oscillations are modulated by selective attention and were suggested to facilitate neuronal processing between distant cortical sites [45, 46]. More recently, oscillations in the high beta frequency range (20-40 Hz) were similarly found to mediate spike synchronization in neurons and selectively form neuronal assemblies [47–49]. In summary, neuronal oscillations are involved in forming frequency-specific networks [14]. Therefore, neural oscillations which are visible as spectral peaks in large-scale recordings (e.g. EEG) can be seen as markers of specific network interactions [15, 16]. Neuronal populations in a given cortical region may include several neuronal computations simultaneously. For instance, encoding and integrating information in local as well as long-range networks. Donner and Siegel [15] suggested that specific brain functions are linked to different frequency-specific network interactions (Figure 1.3). Separating specific neuronal oscillations by their different spectral profiles could therefore be use to identify these simultaneously active frequency-specific networks. So, different spectral profiles were proposed to signify frequency-specific network interactions which are related to distinct brain functions. To directly associate certain brain activity measures, in this case spectral profiles, with specific brain functions is crucially for interpreting large-scale recordings such as EEG.

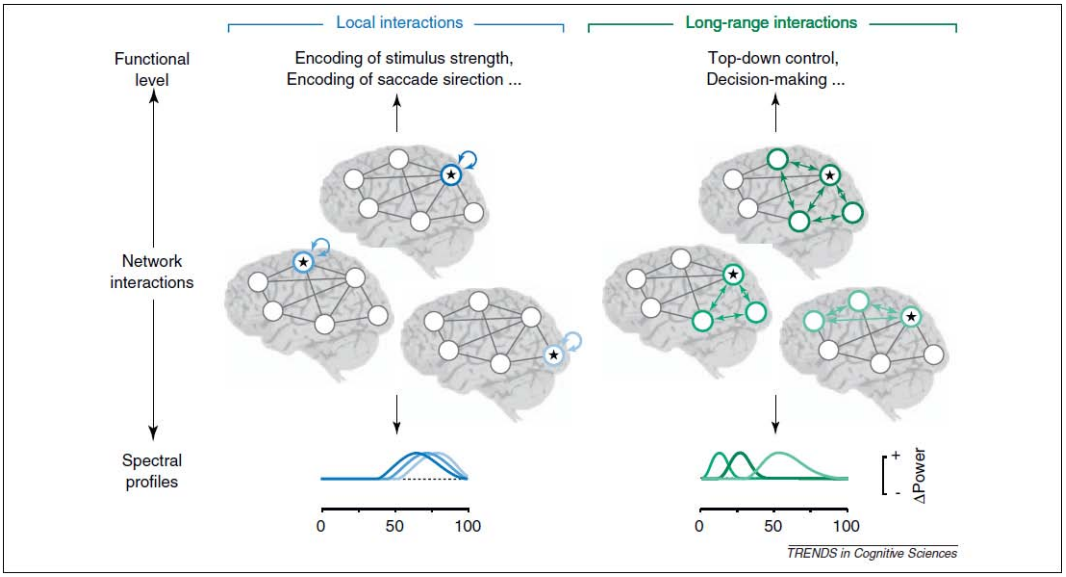

Figure 1.3.: Neuronal computations involve local as well as long-range network interactions. These different network interactions, mediated by neuronal oscillations, result in different spectral profiles in a cortical region. Therefore, different spectral peaks in cortical population signals were suggested to represent different frequency-specific network interactions subserving different functions. Reprinted from Donner and Siegel [15] with permission from Elsevier.

1.4. EEG source imaging

EEG is a very classical brain signal recording technique. Traditionally, the waveform of single channels were analyzed to characterize different brain states [10, 13]. In the last two decades however, more sophisticated methods for imaging EEG signals are evolving. Further, the availability and affordability of computational memory and power opens up novel methodical possibilities.

1.4.1. Forward modeling

In order to model the sources of EEG recordings, it is necessary to describe how bioelectrical potentials propagates from cortical sources to EEG electrodes at the scalp in a so-called *forward model*. The propagation of the electrical field in a medium with defined conductivity is well-described [50–53].
In brief, the bioelectric fields can be described from the quasistatic approximation of Maxwell's equations. In a media with defined conductivity, electrical potentials V can be determined from the primary current density J_p solving Poisson's equation 1.2.

$$\nabla \cdot (\sigma \nabla V) = \nabla \cdot J_p \tag{1.2}$$

For an unbounded homogeneous medium with constant conductivity σ, the solution of equation 1.2 is:

$$V(r) = \frac{1}{4\pi\sigma} \int_\Omega J_p(r') \cdot \frac{r - r'}{|r - r'|^3} \, d^3r' \tag{1.3}$$

Where V(r) is the electric potential at the recording location r in the volume Ω, while r′ is the source location.

For modeling the bioelectric potentials of the brain however, the assumption of only one homogeneous volume is too simplistic. Electric fields are

propagating through various kinds of tissues from their cortical sources to the scalp. Usually, several tissues (grey matter, cerebrospinal fluid, skull, skin) with different conductivities are modeled to describe the electrical field propagation in the head appropriately. The most common approach to solve such forward problems numerically is the boundary element method (BEM) [52–54]. This method is also capable to solve the forward problem for arbitrary head geometry. BEM models consist out of several surface layers with constant conductivities in the volumes between them. Only the electric potentials at the surfaces are computed solving equation 1.2 with certain boundary conditions.
First, the current across the boundary (surface S_k) at volume i to volume j is continuous (equation 1.4). Second, also the electric potentials on both sides of the surface S_k are equal (equation 1.5). Third, the outermost volume Ω_{N+1} expands from the skin surface to infinity, where σ_{N+1}=0. That means no currents are flowing outside of the head.

$$\sigma_i \nabla V_i \cdot dS_k = \sigma_j \nabla V_j \cdot dS_k \tag{1.4}$$

$$V_i(S_k) = V_j(S_k) \tag{1.5}$$

By discretizing the boundaries into meshes the BEM provides a solution describing scalp potentials as weighted sum of current densities. Using matrix notation the forward model can be written in the form:

$$V = G \cdot J \tag{1.6}$$

With G is the gain or *lead field matrix*. V is a vector containing the surface potentials (recordings) and J is a vector containing the source density currents. The dimension of V equals the number of used electrodes (recorded EEG signals), the dimension of J results from the number of modeled source vertices. The values in the lead field matrix represents the tissue conductivities and geometric distances between the cortical sources and each recording location.

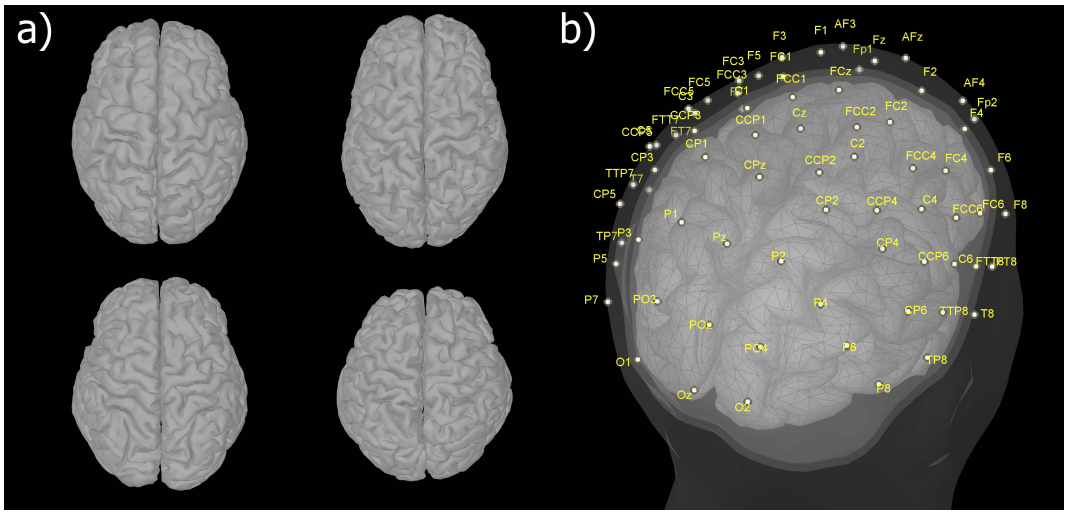

Figure 1.4.: a) Four individual cortical surfaces reconstructed from MRI scans. b) Exemplary individual head model, consisting of the cortex as solution space, skull and skin surfaces. Electrode positions (white dots) from a custom montage were integrated in this model.

Head geometry and brain surface are different for each individual. For accurate forward and source modeling, it is therefore necessary to use realistic head models based on individual anatomy. In Figure 1.4a) different brain surfaces are illustrated from four exemplary subjects. Brain, skull and head surfaces can be gained from individual T1 MRI scans using cortical reconstruction and volumetric segmentation tools, e.g. provided in the FreeSurfer image analysis suite [55, 56]. These surfaces along with co-registered EEG electrode positions results in realistic head models, capable for solving the forward problem with the BEM as described above. A realistic head model rendered from individual anatomy is shown for a custom electrodes montage in Figure 1.4b).

1.4.2. Inverse modeling

While the forward model is capable to describe the scalp potentials as a function of the electrocortical sources, inverse modeling aims the opposite (Figure 1.5). That is, to estimate the sources from scalp potentials, i.e. EEG recordings. Additional constraints are necessary for solving the inverse problem. Dependent on the number of sources that are modeled in an inverse problem, it is either overdetermined ($N_{sources} < N_{sensors}$) or underdetermined ($N_{sources} > N_{sensors}$). In the overdetermined case, usually a few dipoles are used to fit the scalp potentials. To do that, it is necessary to choose an appropriate number of dipoles, before their locations can be computed. The number of used dipoles directly influences the results, that is the location of the dipoles. It is challenging to determine the number of dipoles, since the scalp recordings in many cases do not show multipolar topographies which can be modeled with a few dipoles.

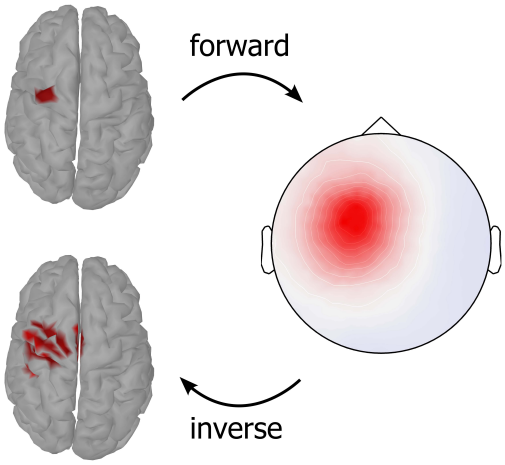

Figure 1.5.: An actual cortical source (top left) is causing (forward model) electric potentials on the scalp (right topography). The sources of scalp potentials can be reconstructed (bottom left) using certain assumptions (inverse model).

For underdetermined problems no unique solution exists, which means that an infinite number of source arrangements can explain the scalp recordings. Such problems are called ill-posed inverse problems. Mathematically, the challenge in solving the inverse problem is to invert the lead field

matrix G. In ill-posed inverse problems, the simple inversion of G is not defined. However, sources estimates that explain the recordings 'most likely' can be determined. A very common approach are minimum-norm estimates [57]. Generally, the aim is to estimate source densities from scalp recordings, based on their linear relationship provided by the forward model (equation 1.6). Minimum-norm estimates are calculated by minimizing the functional in equation 1.7.

$$F = ||V - G \cdot J||^2 \; + \; \lambda \cdot ||J||^2 \tag{1.7}$$

This leads to a solution which minimizes the model error in a least-squares sense, explaining the scalp recordings with minimum norms of the sources.

$$\hat{J} = T \cdot V \tag{1.8}$$

$$T = G^T (G \cdot G^T + \lambda \cdot C)^{-1} \tag{1.9}$$

In equation 1.8, $\hat{J}$ are the estimated current densities and T is the transformation matrix or inversion kernel (equation 1.9). λ>0 is the regularization parameter. This parameter is necessary to stabilize the inverse solution in the presence of noise. It is possible to find a mathematically exact solution with the inherent risk to fit to the noise of the data. Increasing λ leads to smoother current estimates and introduces a discrepancy between modeled and measured data for sake of robustness of the solution.
C is the data noise-covariance matrix which contains certain signal properties of the recordings. Diagonal entries of this matrix contain the variances of each channel which are estimates of their signal power. The off-diagonal entries contain the covariances of the channels. Given volume conduction, the covariance, for instance, is higher for lower distances of two channels. So, the noise-covariance matrix also provides information about the EEG montage to some extent. This matrix is commonly computed from resting state data while no specific task is performed. In this work, the implementation provided from the open-source toolbox Brainstorm [58] is used for computing the inverse kernel. In this implementation, the noise-covariance

is used for pre-whitening the leadfield matrix. In this case the 'whitened' inverse kernel $\tilde{T}$ is:

$$\tilde{T} = \tilde{G}^T(\tilde{G} \cdot \tilde{G}^T + \lambda \cdot I)^{-1} \tag{1.10}$$

$$\tilde{G} = C^{-1/2} \cdot G \tag{1.11}$$

$$\lambda \sim \frac{1}{SNR} \tag{1.12}$$

Where $\tilde{G}$ is the 'whitened' lead field matrix and I is the identity matrix. Pre-whitening orthogonalizes the recordings V based on the noise-covariance matrix C. For computing the 'whitened' inverse kernel a common choice for λ is written in equation 1.12, where SNR is the signal to noise ratio. This relation represents the practical notion that for noisy data (with low SNR) more regularization is needed.

sLORETA [59] stands for standardized low-resolution brain electromagnetic tomography and is a variant of the minimum norm solution in which the sources are normalized with the resolution matrix R (equation 1.13). The resolution matrix is expressing the bias between estimated and actual sources (equation 1.14). As discussed above, due to the presence of noise, some inaccuracies will remain in source estimation. However, the aim of standardizing the minimum norm estimates is to correct for the inherent modelling error of forward and inverse transformation.

$$R = T \cdot G \tag{1.13}$$

$$\hat{J} = R \cdot J \tag{1.14}$$

sLORETA estimates of the current density power at the l^{th} vertex are then computed as:

$$\hat{J}_l^T \cdot [R]_{ll}^{-1} \cdot \hat{J}_l \tag{1.15}$$

In this work, sLORETA is used for solving the inverse problem, because independent research groups validated sLORETA mathematically as well as with simulations [60, 61], in addition to the convincing results in the original publication [59].

1.5. Organization of the chapters

Chapter 1 'Introduction' contains a brief overview of brain mapping techniques and a rational, why EEG brain imaging is the method of choice in this thesis. Moreover, EEG phenomena, corresponding theories and EEG source imaging methods, which are relevant for this work are introduced.

In **Chapter 2 'Motivation and Aim of this Thesis'**, literature on which this work is based upon is briefly reviewed. Following these works, possible advancement in the field of brain imaging during body movements is discussed. Consequently, the objectives of this dissertation are defined.

In **Chapter 3 'Methods and Results'** the core publications and their contribution to this thesis are summarized.

Chapter 4 'Discussion and Conclusions' provides an overall discussion of the core publications and how they met the aims of the thesis. Moreover, the scientific progress in respect to the state of the art is argued.

2. Motivation and Aim of this Thesis

2.1. State of the Art

To image cortical dynamics during actual movements, high temporal resolution and a lightweight brain imaging technique allowing ambulant setups is needed. Both of these requirements can be met with EEG source imaging [19–22]. Especially, high density EEG systems and advanced signal processing methods can be combined to a brain imaging tool that, as described by Michel and Murray [19] "actually is the ultimate brain imaging tool for those who are interested in the temporal dynamics of large-scale brain networks in real-life situations". Furthermore, EEG source imaging methods are available in open-source toolboxes like, e.g. Brainstorm [58], CARTOOL [62], FieldTrip [63], MNE [64] and NFT [65]. In this work, Brainstorm was mainly used for source estimation. Brainstorm provides many compatible interfaces to other brain imaging tools. For instance, the Freesurfer image analysis suite [55, 56] was used for reconstructing the cortical surface from MRI scans and OpenMEEG [53, 54] was used for forward modelling herein.

Accurate source estimation of the EEG recordings is one challenge of EEG based brain imaging. Another, no less important issue in this thesis, is to interpret and model the reconstructed signals in relation to motor behavior. As discussed in section 1.3.3, previous literature report specific μ and beta ERD/ERS patterns for different isolated body movements (reviewed in Pfurtscheller and Lopes da Silva [34] and Neuper and Pfurtscheller [33]). These results were also replicated using ECoG recordings [37] and complemented with the finding that amplitudes in the high gamma (> 60 Hz)

frequency range increase prior to and during movements [39, 66, 67]. This high gamma increase appeared more focally than μ and beta ERD [39] and matched with fMRI activity more precisely [68, 69]. Furthermore, the time course of high gamma amplitudes resembles the flexion and extension sequences during finger tapping [70–72]. In summary, these studies showed that high gamma activity is important for studying motor functions of the cortex. Ball et al. [73] and Darvas et al. [74] showed that high gamma activity can also be detected in non-invasive EEG recordings during finger movements.

The above mentioned studies investigated finger movements at large. Here, we also aim to study the gait function. Traditionally, full-body movements are prevented during EEG measurements, because muscular activities cause major artifacts in the EEG recordings. In recent years however, the development of independent component analysis (ICA) based artifact reduction methods [75] led to first mobile brain imaging studies [76–78]. These studies used dipole fitting to localize independent components. Gwin et al. [77] reported that EEG spectral power in a wide frequency range is coupled to the gait cycle phase during walking. Wagner et al. [78] however, found power modulations in central midline areas, in a specific frequency range, at 25-40 Hz ('low gamma') to be related to the phases of the gait cycle. Interestingly, these modulation patterns did not match with those reported in Gwin et al. [77]. Similarly to results from studies investigating isolated foot movements [36, 79], Wagner et al. [78] showed a suppression of μ and beta oscillations (ERD) during walking in comparison to standing, which occurred in independent component clusters located in sensorimotor areas. While ICA based methods enabled much progress in mobile brain imaging, this approach however, has some limitations. First, the location of independent components is not necessarily consistent with certain EEG measures (e.g. ERD/ERS) which are used for interpreting the signals. Second, it is hard to evaluate if the artifact correction methods were successful. More detailed criteria are needed to ensure that the findings are caused by electrocortical activity, not from electromyographic (EMG) artifacts. Third, to the author's best knowledge, no mobile brain imaging study considered the individual head and brain geometry for EEG source localization.

2.2. Challenges

Several challenges are necessary to be faced in order to study cortical functions related to actual body movements. First, to provide a mobile neuroimaging tool capable to study cortical dynamics during movement, multiple methodical limitations had to be solved. Second, to achieve progress towards a neurophysiological model, that is linking EEG source signals to motoric actions, more conceptual work is needed.

Methodical

- Consider individual head and brain geometry in EEG source imaging based on available open-source toolboxes.
- Reduce motion artifacts during gait experiments based on the properties of electromuscular acitity.
- Integrate motion tracking parameters into EEG analysis expanding previous mobile brain imaging analysis methods.

Conceptual

- Describe differences in EEG source signals between experimental conditions, e.g. movement versus non-movement, following studies investigating ERD/ERS phenomena.
- Relate EEG source signals to movement parameters, i.e. link cortical with movement dynamics.
- Integrate these findings in a model in relation to existing frameworks and theories.

2.3. Aim of this Thesis

The general aim of this thesis is to develop brain imaging based methods and concepts that, in combination enable to investigate cortical involvement in motoric actions. These research tools should be capable to study brain dynamics related to movement sequences, including gait while guaranteeing natural body postures.
Imaging the brain's dynamics during movements is intended to achieve a deeper understanding of the relation between cortical and motor functions. This knowledge could lead to important progress in the research of motor impairment after brain injury. Models that are capable to describe motor behavior as a function of intact as well as injured cortical systems may subserve as basis for more advanced interventions or the development of novel rehabilitation strategies.
Because of this clinical perspective, an additional aim is that the developed methods and concepts of this work are capable to meet the requirements of clinical follow-up studies.

3. Methods and Results

3.1. EEG beta suppression and low gamma modulation are different elements of human upright walking

Seeber M., Scherer R., Wagner J., Solis-Escalante T., and Müller-Putz G.R. "EEG beta suppression and low gamma modulation are different elements of human upright walking." In: *Frontiers in Human Neuroscience* 8 (2014). DOI: 10.3389/fnhum.2014.00485 [80]
Seeber M., Scherer R., Wagner J., Solis-Escalante T., and Müller-Putz G.R. "Corrigendum: EEG beta suppression and low gamma modulation are different elements of human upright walking." In: *Frontiers in Human Neuroscience* 9 (2015). DOI: 10.3389/fnhum.2015.00542 [81]

The aim of the first work was to directly map ERD/ERS phenomena during human upright walking. Previous studies investigated EEG during gait using ICA and dipole localization. Dipole reconstruction of independent components however, does not necessarily match with the location of oscillatory sources, i.e. ERD/ERS. To consider different geometries of the subjects' heads and brains, individual head models were rendered from individual MRI scans. Based on these head models and high density EEG recordings (120 channels), we applied sLORETA for distributed source modeling. The data of ten healthy volunteers were available, which were walking in a robotic gait orthosis [78]. We found upper μ (10-12 Hz) and beta (18-30 Hz) to be suppressed (ERD) during walking in comparison to standing. The beta (18-30 Hz) ERD was located to central sensorimotor areas. These findings are also illustrated in Figure 3.1.

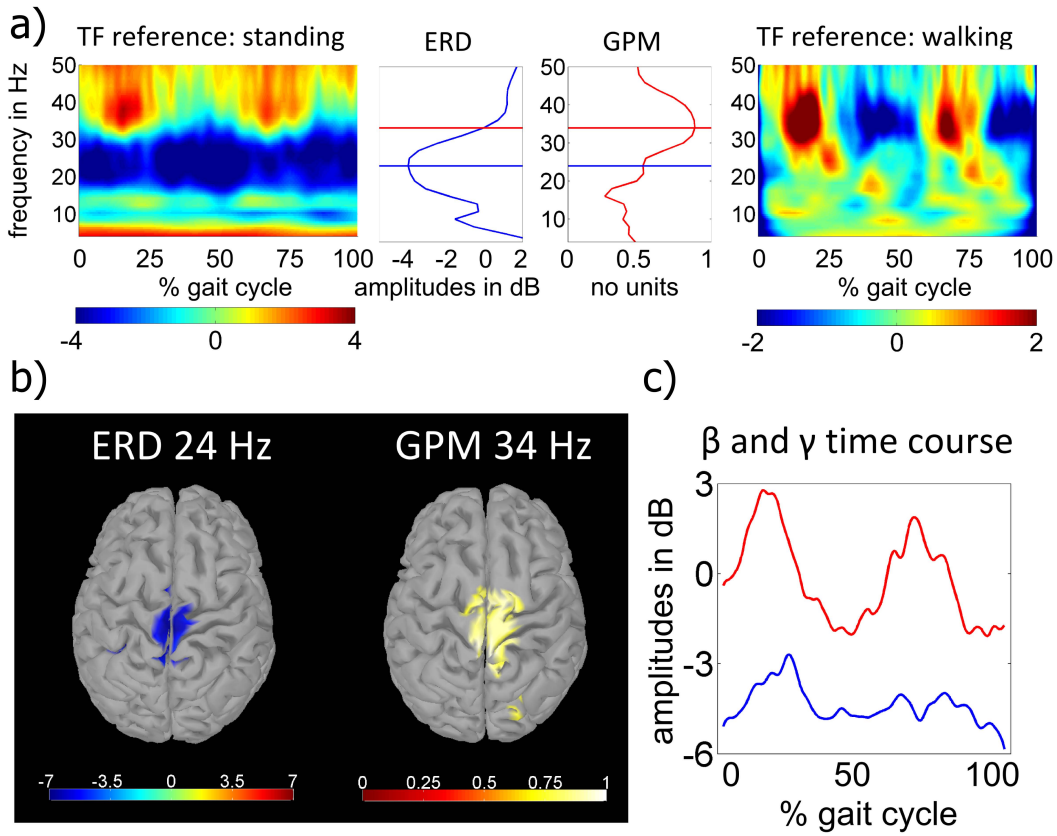

Figure 3.1.: a) Time-Frequency (TF) maps of identical data with different reference periods used for amplitude normalization. Either, sustained beta ERD (in blue, left TF) or low gamma GPM (right TF) can be seen better dependent on the normalization. Spectral profiles are shown in the middle. b) ERD and GPM source images. c) Time course at optimal frequencies for ERD and GPM.

We furthermore found amplitude modulations in the low gamma (24-40 Hz) frequency range to be related with the gait cycle. To determine the exact spectral profiles of these gait-phase related modulations (GPM), we introduced a measure. This measure is described in equation 3.1 and quantifies the relation between EEG source amplitude modulations and the gait phase as a function of their carrier frequency and cortical location.

$$GPM(f) = \frac{2}{\sqrt{2} \cdot \sigma_{A(f)} \cdot N} \cdot \sum_{n=0}^{N-1} A(n,f) \cdot e^{-2\pi i \cdot \frac{2 \cdot n}{N}} \tag{3.1}$$

In equation 3.1, $A(n,f)$ denotes the amplitude of an oscillation with the frequency f at a sample point n in the gait cycle. N is the total number of samples in a gait cycle. $\sigma_{A(f)}$ is the standard deviation of $A(n,f)$. The GPM measure is a complex number which magnitude would be 1 if $A(n,f)$ is modulated sinusoidally with the step frequency. The GPM phase describes the phase relation of the amplitude modulation of a certain brain oscillation and the gait cycle.

We conclude that μ and beta ERD reflect an increased excitability state in corresponding areas during walking, while the low gamma modulations may reflect sensorimotor processing or integration dependent on the gait phase. Because we identified the spectral profiles of ERD and gait-phase related modulations to be different, we suggest that these phenomena are associated with different frequency-specific network interactions.

Contribution to this thesis: Because it was the first work of this thesis, much engineering work was necessary to set up the methods for further investigations. The methodology, used in this study is fundamental for the entire thesis. It demonstrates how to enable EEG source imaging based on individual anatomy on the one hand. On the other hand, this study shows, the importance of distinguishing between different frequency-specific EEG phenomena, i.e. ERD and gait-phase related modulations. To the author's best knowledge this is the first EEG source imaging study investigating gait, which is based on distributed source models and individual anatomy.

3.2. High and low gamma EEG oscillations in central sensorimotor areas are conversely modulated during the human gait cycle

Seeber M., Scherer R., Wagner J., Solis-Escalante T., and Müller-Putz G.R. "High and low gamma EEG oscillations in central sensorimotor areas are conversely modulated during the human gait cycle." In: *NeuroImage* 112 (2015), pp. 318–326. DOI: 10.1016/j.neuroimage.2015.03.045 [82]

The objective of the second publication was to correct for electromuscular artifacts, which affect EEG recordings during gait movements. The idea of this work was to separate electromuscular (EMG) from true electrocortical activity. Successful artifact correction would solve some limitations of previous works and enables the investigation of EEG source signals at higher frequencies (>30 Hz). To do so, we developed a novel artifact correction method based on frequency spectral decomposition. EMG affects the recordings in a wide range of frequencies, especially for $>$ 30 Hz. Moreover, these artifacts have much larger amplitudes than EEG and are strongest at sites close to their origin, the muscles. The artifact correction approach in this study is based on these properties of EMG which makes it separable from EEG. Indeed, the principal spectral component with the largest magnitude met these criteria in every subject. Characteristic for this component is the broadband spectral profile and source activities which are located to dorsolateral sites, close to the neck muscles. Correcting for this component, revealed narrow band high gamma (60-80 Hz) oscillations which were increased during the whole gait cycle. The principle of this artifact correction approach is shown in Figure 3.2. After artifact correction, we additionally found that amplitudes at 70-90 Hz are modulated in relation to the gait cycle. Interestingly, these high gamma activities were conversely modulated to the previously reported low gamma (24-40 Hz) modulations. Both of the reported high gamma features were directly localized to functionally meaningful, central sensorimotor areas.

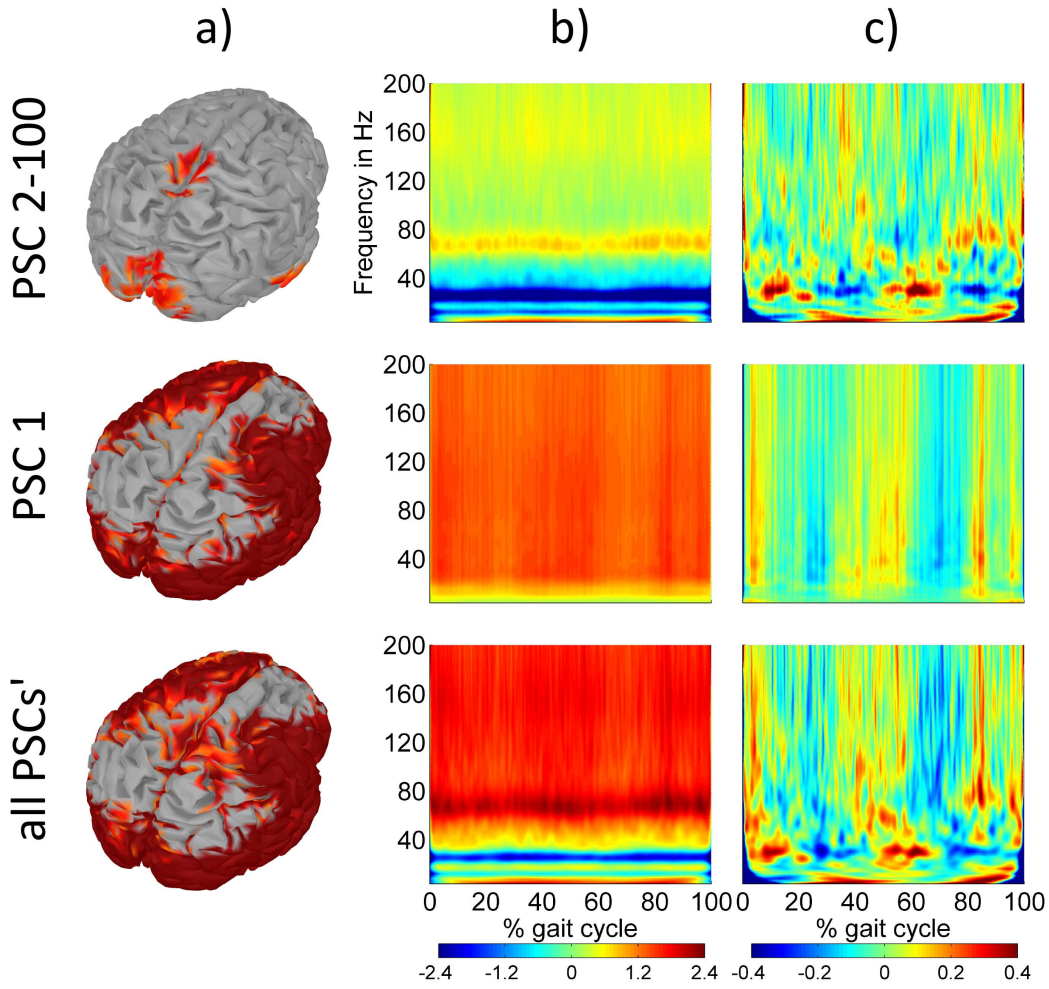

Figure 3.2.: Muscular artifact correction method. The rows in this Figure correspond to the corrected (top), removed (middle) and uncorrected (bottom) source estimates. a) EEG source images of normalized amplitude increase at the high gamma peak (68 Hz) of an exemplary subject. The central sensorimotor region in the corrected source image was used for illustrating the TF dynamics. b) TF plots showing a clear high gamma increase (relative to standing) for the corrected sources (top) and broadband activity for the removed component. c) Same as in b) but normalized for sustained effects. Gait phase-related amplitudes can be seen, which are conversely modulated to each other at high and low gamma frequencies.

Contribution to this thesis: This publication complements previous findings, by enabling the investigation of the high gamma activities due to the novel artifact correction approach. Furthermore, the correction method can be applied fully data driven and therefore is not dependent on user-driven artifact selection, which may be subjective. High gamma activities are reported to play an important role in motor preparation and execution. Similar to the distinction of sustained beta ERD and low gamma GPM, this study showed slightly different spectral peaks for high gamma increase and gait phase-related modulation. This finding additionally supports the idea that sustained and gait-phase related amplitude modulations are caused by different neuronal network oscillations.

3.3. EEG oscillations are modulated in different behavior-related networks during rhythmic finger movements

Seeber M., Scherer R., and Müller-Putz G.R. "EEG Oscillations Are Modulated in Different Behavior-Related Networks during Rhythmic Finger Movements." In: *Journal of Neuroscience* 36.46 (2016), pp. 11671–11681. DOI: 10.1523/jneurosci.1739-16.2016 [83]

The idea of the third paper was to investigate EEG source dynamics during rhythmic finger movements, based on the findings of the previous gait studies. In distinction to leg movements, finger movements are represented more laterally in sensorimotor areas. Therefore, we hypothesized to identify different spatial sources for sustained ERD/ERS and movement-phase related amplitudes (MPA), in addition to their different frequency spectra. EEG source imaging was applied based on the methods developed in the previous works. In the analysis we distinguished between sustained and movement-phase related amplitude modulations. To determine MPA, the finger movements were recorded with a data glove and related to EEG source amplitude envelopes. We actually found sustained ERD for alpha (10-12 Hz) and beta (18-24 Hz), as well as increased high gamma (60-80 Hz) amplitudes during the rhythmic finger movements in the hand representation area. Furthermore, we found significant MPA, most pronounced at high beta (24-30 Hz) frequencies in bilateral sensorimotor and prefrontal regions. We identified the frequency spectra and spatial sources of the sustained ERD/ERS and MPA phenomena to be different. These findings are summarized in Figure 3.3 and support our hypothesis that these two different phenomena are caused by different frequency-specific network interactions. First, we suggest that sustained ERD/ERS activities are representing static synchrony modulations in networks which may upregulate the excitably in associated cortical regions during movement. Second, we suggest that movement-phase related amplitude modulations reflect dynamic network synchrony modulations which could be associated with the prediction and integration of sensorimotor information linked to the movement sequences.

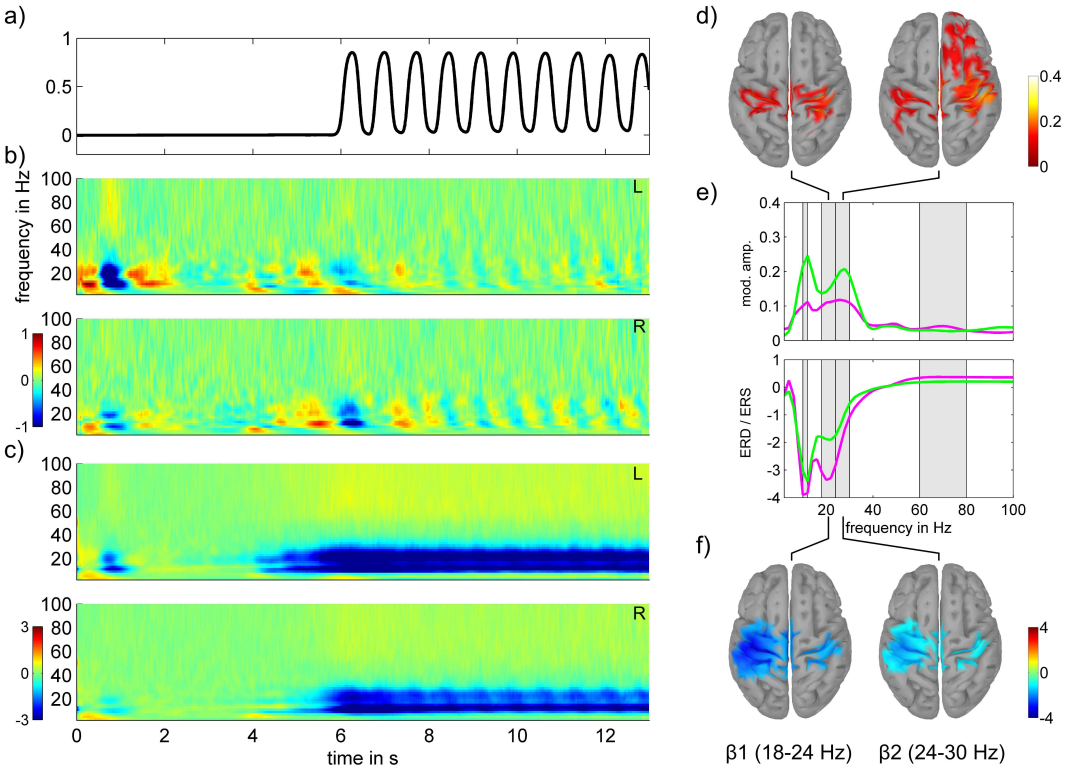

Figure 3.3.: a) Finger movements recorded with the data glove. b) TF plots of movement-phase related amplitudes in left (L) and right (R) sensorimotor regions. c) TF plots showing sustained amplitude modulation (ERD/ERS in blue/yellow) during movements. d) MPA source images at different beta frequencies. e) Frequency spectra of the ERD/ERS and MPA in the L/R region in magenta/green. f) ERD source images at different beta frequencies.

Contribution to this thesis: This study show that movement-phase related amplitude modulations appear also during repetitive finger movements. Furthermore, it supports and generalizes the viewpoint that sustained and movement-phase related modulations are generated by different types of network interactions. However, we also identified these frequency-specific network to partly overlap spatially as well as in their frequency spectra. Therefore, the distinction and identification of different large-scale networks, which is pointed out in this work, facilitates the interpretation of EEG sources during repetitive movements.

4. Discussion and Conclusions

The central aim of this thesis is to study cortical dynamics during repetitive movements, i.e. during walking and rhythmic finger movements. To do so, it was necessary to achieve progress towards an EEG based, mobile neuroimaging tool which enables the investigation the brain's dynamics during actual movements. Further, to facilitate the interpretation of EEG source signals, advancement in modeling the neurophysiology of movement dynamics was needed. In the following, the achievements of this thesis along these two lines are discussed.

4.1. Methodical progress - Towards a mobile brain imaging tool

In order to extend the possibilities of neuroimaging during actual movements, this work provides multiple contributions towards the development of a mobile brain imaging tool. Based on previous methods [19, 20] functional (EEG) was combined with structural (MRI) data to enable EEG source imaging. Individual head and brain geometry was considered using realistic head models (Seeber et al. [80]). This approach is important for clinical follow-up studies, because EEG source localization based on individual head models is more precisely than using template models [84]. In addition to EEG source reconstruction methods, the combination of multiple techniques are necessary to enable mobile brain imaging. First, that is to deal appropriately with motion and muscular artifacts in the recordings and the data analyses of movement experiments. Second, to include motion tracking data in the analyses of source reconstructed signals [17]. Third, to directly map and relate specific EEG phenomena to the motion tracking data.

For relating EEG source dynamics to movement tracking data, gait cycle patterns were recorded simultaneously with the EEG during the gait experiment. Based on this information the GPM measure (equation 3.1) was introduced in Seeber et al. [80] to quantify the relation of EEG source amplitude modulations to the gait cycle. So, with this measure it is possible to compute EEG source images indicating gait-phase related cortical activities. In Seeber et al. [82], a novel artifact correction method was developed, that is based on frequency spectral decomposition of source images. This advanced artifact correction approach revealed narrow-band high gamma activity during a gait experiment. Further, multiple criteria are indicated in this work, that can be used to identify muscular artifacts in EEG source images. That are, the frequency spectra, spatial patterns and magnitudes of remaining source activities. Electromuscular activity appear in a wide frequency range above 30 Hz [85, 86]. The distributed source modeling approach, used in this work, furthermore provides the benefit that remaining muscular artifacts can be recognized as spatially wide-spread patterns in the source images. Typically, these activities have large magnitudes at sites close to their true origin, that is mainly the neck and face muscles. The distinction of true electrocortical activity from movement artifacts is crucial in mobile brain imaging to prevent misleading results.
Utilizing the brain imaging methods of the previous works, EEG source dynamics were investigated in Seeber et al. [83] during repetitive finger movements. Movement-phase related activities were quantified and investigated similarly as in the previous gait studies. This study, revealed different EEG source images for movement-phase related and ERD/ERS sources. This finding demonstrates that the EEG phenomena which are used for brain imaging are of great importance. This is discussed in more detail in the next section.
Here, I would like to suggest that the techniques discussed above, only in combination result in a brain imaging tool that is capable to study the cortical dynamics during body movements.

4.2. Conceptual progress -Towards a neurophysiological model of repetitive movements

In this thesis, I focused on the analysis of EEG source oscillations. This approach is motivated by previous literature, reporting an important role for cortical oscillations in motor function (reviewed in Pfurtscheller and Lopes da Silva [34], and Jenkinson and Brown [87]). Further, oscillatory abnormalities are associated with various disorders of the brain, including motor deficits (reviewed in Brown [88], Schnitzler and Gross [89], Uhlhaas and Singer [90]). Especially, beta and high gamma activity were previously shown to be important for motor function [39, 67, 87, 91]. For example, in individuals suffering from Parkinson's disease, the suppression of exaggerated beta oscillations following drug treatment is correlated with the improvement of bradykinesia and rigidity [87]. After treatment with levodopa, high gamma synchrony between cortical and basal ganglia motor areas is increased and motor performance is improved [88]. Moreover, the role of beta and high gamma oscillations in motor performance was studied using transcranial alternating current stimulation to experimentally increase these oscillations. These studies found beta oscillations to promote tonic muscle contraction [92], while high gamma activity was suggested to facilitate motor processing [93].
In this work, suppressed beta oscillations along with high gamma increase are suggested to signify a state of increased cortical excitability in associated areas during movement execution. In the first two works investigating gait, i.e. repetitive leg movements, these activities were located to central sensorimotor regions (Seeber et al. [80], Seeber et al. [82]). During right finger movements, sustained beta ERD and high gamma amplitude increase was located to contralateral, left sensorimotor regions (Seeber et al. [83]). These findings are in accord with previous studies [36, 39] showing spatially specific patterns for the movement of different body parts, which match to the somatotopic arrangement of the motor cortex. Therefore, the upregulated excitability states during repetitive movements, reported in in this work, are further proposed to facilitate motor processing specific to the limb that is moved.

ERD/ERS phenomena per definition (equation 1.1) compare different states of spectral power at a given frequency, which are interpreted as representation of altered synchrony in underlying neuronal populations. Here, gait- or movement-phase related activities are investigated in addition to the well-established ERD/ERS phenomena. Gait phase-related amplitude modulations at 25-40 Hz were first reported by our group [78]. In Seeber et al. [80] we suggested that these phenomena are generated by different frequency-specific network interactions than sustained ERD/ERS activity. Furthermore, in Seeber et al. [82] we report GPM for high gamma (70-90 Hz) frequencies along with sustained high gamma (60-80 Hz) increase during the whole gait cycle. These findings generalize the results from Seeber et al. [80] for a different frequency range.
In Seeber et al. [83] repetitive finger movements were investigated because of their lateral representation in the motor cortex. We found the spatial sources of MPA and ERD/ERS activities to be different. This finding, in addition to the differences in their spectral profiles supports the viewpoint that sustained ERD/ERS and MPA are representing different frequency-specific networks. Narrow band amplitude modulation can be seen as a marker of modulated frequency-specific network synchrony [14–16]. Therefore, MPA are proposed to represent networks, which modulate their synchrony in relation to the movement sequences.
We found MPA to be well pronounced in bilateral sensorimotor areas and prefrontal areas at high beta (18-30 Hz) frequencies. Previous studies reported beta modulation in cortical motor areas to be associated with predictive timing of rhythmic, anticipated stimuli [94–96]. Moreover, studies using invasive recordings showed that high beta oscillations are forming specific neuronal assemblies between the left and right motor cortex [48] as well as in prefrontal areas [49, 97]. These results show that high beta oscillations mediate information processing between the hemispheres of the motor cortex [48] on the one hand. On the other hand, prefrontal activity was proposed to reflect top-down control [49, 97].
Based on these previous findings, high beta MPA in this work are suggested to be associated with top-down control, the prediction and integration of sensorimotor information.

4.3. Limitations and Recommendations

The EEG source imaging results in this work are limited in their spatial resolution. Due to the ill-posed inverse problem inherent in EEG source imaging, no unique source solution exists. The methods for EEG source modeling which were used in this work are validated in many respects and are well-accepted in the community. Yet, for interpreting EEG source images, it is important to keep the constraints of the methods in mind. Therefore, only large-scale spatial differences are discussed in this work, of course not such in the millimeter range. Moreover, sources of deep brain structures should be interpreted with great caution.
For studying cortical involvement in gait, a robotic orthosis was restricting the gait movements. This setup is naturally not mobile, but the methods we have developed and applied are capable for such setups. Furthermore, the findings of the gait studies were also replicated in follow-up treadmill studies. For the artifact correction method introduced in Seeber et al. [82], it is important to make sure that the spectral component that is removed, because it represents artifacts, shows the characteristic properties discussed above. Conversely, remaining activity, especially at higher frequencies, must not show these characteristics, to ensure that they are of cortical origin.
EEG source imaging results can be validated by comparing them with findings from ECoG. To support the results in this thesis they were compared with ECoG recordings wherever this was possible. An ongoing ECoG study moreover is aiming to replicate and validate the findings of this work.

4.4. Conclusions and Future Perspective

I consider this work to contribute multiple achievements towards the development of a neuroimaging tool that is capable for studying full-body movements. First, this included methodical achievements that are, the capability to consider individual head and brain geometries, the reduction of artifacts during movements and the integration of motion tracking data for modeling the cortical sources of repetitive movements.

Second, the main conceptual achievement of this thesis is to distinguish between movement state (sustained ERD/ERS) and movement phase-related (GPM, MPA) activities.
Here, I propose that these two phenomena are representing two different types of large-scale networks. Movement state related networks to upregulate excitability in cortical areas that are specific to the body part that is moved. Movement-phase related networks to modulate their synchrony in relation to the movement sequences which may reflect other functions. For movement-phase related activities at high beta frequencies these may include top-down control, prediction and integration of sensorimotor information. The innovative neuroimaging methodology in combination with this preliminary model of cortical dynamics during repetitive movements, developed in this thesis, could lead to further progress in basic and clinical neuroscience research as well as to further improvements of Brain-Computer Interfaces [98–100].
In basic neuroscience, the function of the proposed two different network types can be investigated in greater detail. Especially, with a focus on the multiple frequency-specific networks which are reported herein. For instance, follow-up studies could test each of the preliminary functions which were suggested for the different large-scale networks.
In clinical neuroscience, different large-scale networks could be investigated in respect to specific brain disorders. Motor deficits would be of primary interest following this thesis. So it would be interesting, if a distinct dysfunction could be associated with a certain abnormality in a specific cortical network. Such knowledge could be utilized for calculating defined network measures, which could be used to identify cortical dysfunctions more specifically. Based on this knowledge, novel rehabilitation strategies, therapies or interventions could be developed to recover normal network states and dynamics. To do so, frequency-specific electrical brain stimulation or neurofeedback strategies may be helpful.
For Brain-Computer Interfaces, the different phenomena and cortical signals which are described and separated in this thesis, could provide innovative features. For instance, to select an active state or action versus controlling the parameters in this state or action.

Bibliography

[1] Ogawa S., Lee T. M., Kay A. R., and Tank D. W. "Brain magnetic resonance imaging with contrast dependent on blood oxygenation." In: *Proceedings of the National Academy of Sciences* 87.24 (Dec. 1990), pp. 9868–9872. DOI: 10.1073/pnas.87.24.9868 (cit. on p. 1).

[2] Friston K. J., Jezzard P., and Turner R. "Analysis of functional MRI time-series." In: *Human Brain Mapping* 1.2 (1994), pp. 153–171. DOI: 10.1002/hbm.460010207 (cit. on p. 1).

[3] Logothetis N. K. "What we can do and what we cannot do with fMRI." In: *Nature* 453.7197 (June 2008), pp. 869–878. DOI: 10.1038/nature06976 (cit. on p. 1).

[4] Jobsis F. "Noninvasive, infrared monitoring of cerebral and myocardial oxygen sufficiency and circulatory parameters." In: *Science* 198.4323 (Dec. 1977), pp. 1264–1267. DOI: 10.1126/science.929199 (cit. on p. 1).

[5] Villringer A., Planck J., Hock C., Schleinkofer L., and Dirnagl U. "Near infrared spectroscopy (NIRS): A new tool to study hemodynamic changes during activation of brain function in human adults." In: *Neuroscience Letters* 154.1-2 (May 1993), pp. 101–104. DOI: 10.1016/0304-3940(93)90181-j (cit. on p. 1).

[6] Jasper H. and Penfield W. "Electrocorticograms in man: Effect of voluntary movement upon the electrical activity of the precentral gyrus." In: *Archiv für Psychiatrie und Nervenkrankheiten* 183.1-2 (1949), pp. 163–174. DOI: 10.1007/bf01062488 (cit. on pp. 1, 8).

[7] Buzsáki G. "Large-scale recording of neuronal ensembles." In: *Nature Neuroscience* 7.5 (May 2004), pp. 446–451. DOI: 10.1038/nn1233 (cit. on pp. 1, 2).

[8] Buzsáki G., Anastassiou C. A., and Koch C. "The origin of extracellular fields and currents — EEG, ECoG, LFP and spikes." In: *Nature Reviews Neuroscience* 13.6 (May 2012), pp. 407–420. DOI: 10.1038/nrn3241 (cit. on p. 1).

[9] Berger H. "Über das Elektrenkephalogramm des Menschen." In: *Archiv für Psychiatrie und Nervenkrankheiten* 87.1 (Dec. 1929), pp. 527–570. DOI: 10.1007/bf01797193 (cit. on pp. 1, 6, 8).

[10] Niedermeyer E. and Lopes da Silva F. *Electroencephalography: basic principles, clinical applications, and related fields*. Lippincott Williams & Wilkins, 2005 (cit. on pp. 1, 6, 11).

[11] Cohen D. "Magnetoencephalography: Detection of the Brain's Electrical Activity with a Superconducting Magnetometer." In: *Science* 175.4022 (Feb. 1972), pp. 664–666. DOI: 10.1126/science.175.4022.664 (cit. on p. 1).

[12] Hämäläinen M., Hari R., Ilmoniemi R. J., Knuutila J., and Lounasmaa O. V. "Magnetoencephalography—theory, instrumentation, and applications to noninvasive studies of the working human brain." In: *Reviews of Modern Physics* 65.2 (Apr. 1993), pp. 413–497. DOI: 10.1103/revmodphys.65.413 (cit. on p. 1).

[13] Nunez P. L. and Srinivasan R. *Electric Fields of the Brain*. Oxford University Press (OUP), Jan. 2006. DOI: 10.1093/acprof:oso/9780195050387.001.0001 (cit. on pp. 2, 6, 11).

[14] Buzsáki G. and Draguhn A. "Neuronal Oscillations in Cortical Networks." In: *Science* 304.5679 (June 2004), pp. 1926–1929. DOI: 10.1126/science.1099745 (cit. on pp. 3, 7, 9, 33).

[15] Donner T. H. and Siegel M. "A framework for local cortical oscillation patterns." In: *Trends in Cognitive Sciences* 15.5 (May 2011), pp. 191–199. DOI: 10.1016/j.tics.2011.03.007 (cit. on pp. 3, 9, 10, 33).

[16] Siegel M., Donner T. H., and Engel A. K. "Spectral fingerprints of large-scale neuronal interactions." In: *Nature Reviews Neuroscience* (Jan. 2012). DOI: 10.1038/nrn3137 (cit. on pp. 3, 9, 33).

[17] Makeig S., Gramann K., Jung T.-P., Sejnowski T. J., and Poizner H. "Linking brain, mind and behavior." In: *International Journal of Psychophysiology* 73.2 (Aug. 2009), pp. 95–100. DOI: 10.1016/j.ijpsycho.2008.11.008 (cit. on pp. 3, 4, 30).

[18] Gramann K., Ferris D. P., Gwin J., and Makeig S. "Imaging natural cognition in action." In: *International Journal of Psychophysiology* 91.1 (Jan. 2014), pp. 22–29. DOI: 10.1016/j.ijpsycho.2013.09.003 (cit. on pp. 3, 4).

[19] Michel C. M. and Murray M. M. "Towards the utilization of EEG as a brain imaging tool." In: *NeuroImage* 61.2 (June 2012), pp. 371–385. DOI: 10.1016/j.neuroimage.2011.12.039 (cit. on pp. 3, 18, 30).

[20] Baillet S., Mosher J., and Leahy R. "Electromagnetic brain mapping." In: *IEEE Signal Processing Magazine* 18.6 (2001), pp. 14–30. DOI: 10.1109/79.962275 (cit. on pp. 3, 18, 30).

[21] Michel C. M., Murray M. M., Lantz G., Gonzalez S., Spinelli L., and Peralta R. G. de. "EEG source imaging." In: *Clinical Neurophysiology* 115.10 (Oct. 2004), pp. 2195–2222. DOI: 10.1016/j.clinph.2004.06.001 (cit. on pp. 3, 18).

[22] Darvas F., Pantazis D., Kucukaltun-Yildirim E., and Leahy R. "Mapping human brain function with MEG and EEG: methods and validation." In: *NeuroImage* 23 (Jan. 2004), S289–S299. DOI: 10.1016/j.neuroimage.2004.07.014 (cit. on pp. 3, 18).

[23] Zschocke S. *Klinische Elektroenzephalographie*. Ed. by H.-C. Hansen. Springer Nature, 2002. DOI: 10.1007/978-3-662-08106-8 (cit. on pp. 5, 6).

[24] Klimesch W., Doppelmayr M., Russegger H., Pachinger T., and Schwaiger J. "Induced alpha band power changes in the human EEG and attention." In: *Neuroscience Letters* 244.2 (Mar. 1998), pp. 73–76. DOI: 10.1016/s0304-3940(98)00122-0 (cit. on p. 6).

[25] Pfurtscheller G., Neuper C., and Krausz G. "Functional dissociation of lower and upper frequency mu rhythms in relation to voluntary limb movement." In: *Clinical Neurophysiology* 111.10 (Oct. 2000), pp. 1873–1879. DOI: 10.1016/s1388-2457(00)00428-4 (cit. on p. 6).

[26] Klimesch W., Sauseng P., and Hanslmayr S. "EEG alpha oscillations: The inhibition–timing hypothesis." In: *Brain Research Reviews* 53.1 (Jan. 2007), pp. 63–88. DOI: 10.1016/j.brainresrev.2006.06.003 (cit. on p. 6).

[27] Miller E. K. and Buschman T. J. "Cortical circuits for the control of attention." In: *Current Opinion in Neurobiology* 23.2 (Apr. 2013), pp. 216–222. DOI: 10.1016/j.conb.2012.11.011 (cit. on p. 7).

[28] Steriade M., Gloor P., Llinás R., Lopes da Silva F., and Mesulam M.-M. "Basic mechanisms of cerebral rhythmic activities." In: *Electroencephalography and Clinical Neurophysiology* 76.6 (Dec. 1990), pp. 481–508. DOI: 10.1016/0013-4694(90)90001-z (cit. on p. 7).

[29] Lopes da Silva F. "Neural mechanisms underlying brain waves: from neural membranes to networks." In: *Electroencephalography and Clinical Neurophysiology* 79.2 (Aug. 1991), pp. 81–93. DOI: 10.1016/0013-4694(91)90044-5 (cit. on p. 7).

[30] Womelsdorf T., Schoffelen J.-M., Oostenveld R., Singer W., Desimone R., Engel A. K., and Fries P. "Modulation of Neuronal Interactions Through Neuronal Synchronization." In: *Science* 316.5831 (June 2007), pp. 1609–1612. DOI: 10.1126/science.1139597 (cit. on p. 7).

[31] Pfurtscheller G. and Aranibar A. "Event-related cortical desynchronization detected by power measurements of scalp EEG." In: *Electroencephalography and Clinical Neurophysiology* 42.6 (June 1977), pp. 817–826. DOI: 10.1016/0013-4694(77)90235-8 (cit. on p. 8).

[32] Pfurtscheller G. and Neuper C. "Motor imagery activates primary sensorimotor area in humans." In: *Neuroscience Letters* 239.2-3 (Dec. 1997), pp. 65–68. DOI: 10.1016/s0304-3940(97)00889-6 (cit. on p. 8).

[33] Neuper C. and Pfurtscheller G. "Event-related dynamics of cortical rhythms: frequency-specific features and functional correlates." In: *International Journal of Psychophysiology* 43.1 (Dec. 2001), pp. 41–58. DOI: 10.1016/s0167-8760(01)00178-7 (cit. on pp. 8, 9, 18).

[34] Pfurtscheller G. and Lopes da Silva F. "Event-related EEG/MEG synchronization and desynchronization: basic principles." In: *Clinical Neurophysiology* 110.11 (Nov. 1999), pp. 1842–1857. DOI: 10.1016/s1388-2457(99)00141-8 (cit. on pp. 8, 9, 18, 32).

[35] Pfurtscheller G. "Event-related synchronization (ERS): an electrophysiological correlate of cortical areas at rest." In: *Electroencephalography and Clinical Neurophysiology* 83.1 (July 1992), pp. 62–69. DOI: 10.1016/0013-4694(92)90133-3 (cit. on p. 8).

[36] Pfurtscheller G., Neuper C., Andrew C., and Edlinger G. "Foot and hand area mu rhythms." In: *International Journal of Psychophysiology* 26.1-3 (June 1997), pp. 121–135. DOI: 10.1016/s0167-8760(97)00760-5 (cit. on pp. 8, 19, 32).

[37] Crone N. "Functional mapping of human sensorimotor cortex with electrocorticographic spectral analysis. I. Alpha and beta event- related desynchronization." In: *Brain* 121.12 (Dec. 1998), pp. 2271–2299. DOI: 10.1093/brain/121.12.2271 (cit. on pp. 8, 18).

[38] Pfurtscheller G. "Central beta rhythm during sensorimotor activities in man." In: *Electroencephalography and Clinical Neurophysiology* 51.3 (Mar. 1981), pp. 253–264. DOI: 10.1016/0013-4694(81)90139-5 (cit. on p. 8).

[39] Miller K. J., Leuthardt E. C., Schalk G., Rao R. P. N., Anderson N. R., Moran D. W., Miller J. W., and Ojemann J. G. "Spectral Changes in Cortical Surface Potentials during Motor Movement." In: *Journal of Neuroscience* 27.9 (Feb. 2007), pp. 2424–2432. DOI: 10.1523/jneurosci.3886-06.2007 (cit. on pp. 8, 19, 32).

[40] Pfurtscheller G., Stancák A., and Neuper C. "Post-movement beta synchronization. A correlate of an idling motor area?" In: *Electroencephalography and Clinical Neurophysiology* 98.4 (Apr. 1996), pp. 281–293. DOI: 10.1016/0013-4694(95)00258-8 (cit. on p. 8).

[41] Müller-Putz G. R., Zimmermann D., Graimann B., Nestinger K., Korisek G., and Pfurtscheller G. "Event-related beta EEG-changes during passive and attempted foot movements in paraplegic patients." In: *Brain Research* 1137 (Mar. 2007), pp. 84–91. DOI: 10.1016/j.brainres.2006.12.052 (cit. on p. 8).

[42] Gray C. M., König P., Engel A. K., and Singer W. "Oscillatory responses in cat visual cortex exhibit inter-columnar synchronization which reflects global stimulus properties." In: *Nature* 338.6213 (Mar. 1989), pp. 334–337. DOI: 10.1038/338334a0 (cit. on p. 9).

[43] Engel A., König P., Kreiter A., and Singer W. "Interhemispheric synchronization of oscillatory neuronal responses in cat visual cortex." In: *Science* 252.5009 (May 1991), pp. 1177–1179. DOI: 10.1126/science.252.5009.1177 (cit. on p. 9).

[44] Singer W. "Synchronization of Cortical Activity and Its Putative Role in Information Processing and Learning." In: *Annual Review of Physiology* 55.1 (Jan. 1993), pp. 349–374. DOI: 10.1146/annurev.physiol.55.1.349 (cit. on p. 9).

[45] Fries P., Reynolds J. H., Rorie A. E., and Desimone R. "Modulation of Oscillatory Neuronal Synchronization by Selective Visual Attention." In: *Science* 291.5508 (Feb. 2001), pp. 1560–1563. DOI: 10.1126/science.1055465 (cit. on p. 9).

[46] Fries P. "A mechanism for cognitive dynamics: neuronal communication through neuronal coherence." In: *Trends in Cognitive Sciences* 9.10 (Oct. 2005), pp. 474–480. DOI: 10.1016/j.tics.2005.08.011 (cit. on p. 9).

[47] Siegel M., Warden M. R., and Miller E. K. "Phase-dependent neuronal coding of objects in short-term memory." In: *Proceedings of the National Academy of Sciences* 106.50 (Nov. 2009), pp. 21341–21346. DOI: 10.1073/pnas.0908193106 (cit. on p. 9).

[48] Canolty R. T., Ganguly K., Kennerley S. W., Cadieu C. F., Koepsell K., Wallis J. D., and Carmena J. M. "Oscillatory phase coupling coordinates anatomically dispersed functional cell assemblies." In: *Proceedings of the National Academy of Sciences* 107.40 (Sept. 2010), pp. 17356–17361. DOI: 10.1073/pnas.1008306107 (cit. on pp. 9, 33).

[49] Buschman T. J., Denovellis E., Diogo C., Bullock D., and Miller E. "Synchronous Oscillatory Neural Ensembles for Rules in the Prefrontal Cortex." In: *Neuron* 76.4 (Nov. 2012), pp. 838–846. DOI: 10.1016/j.neuron.2012.09.029 (cit. on pp. 9, 33).

[50] Geselowitz D. B. "On Bioelectric Potentials in an Inhomogeneous Volume Conductor." In: *Biophysical Journal* 7.1 (Jan. 1967), pp. 1–11. DOI: 10.1016/s0006-3495(67)86571-8 (cit. on p. 11).

[51] Sarvas J. "Basic mathematical and electromagnetic concepts of the biomagnetic inverse problem." In: *Physics in Medicine and Biology* 32.1 (Jan. 1987), pp. 11–22. DOI: 10.1088/0031-9155/32/1/004 (cit. on p. 11).

[52] Mosher J., Leahy R., and Lewis P. "EEG and MEG: forward solutions for inverse methods." In: *IEEE Transactions on Biomedical Engineering* 46.3 (Mar. 1999), pp. 245–259. DOI: 10.1109/10.748978 (cit. on pp. 11, 12).

[53] Kybic J., Clerc M., Abboud T., Faugeras O., Keriven R., and Papadopoulo T. "A common formalism for the Integral formulations of the forward EEG problem." In: *IEEE Transactions on Medical Imaging* 24.1 (Jan. 2005), pp. 12–28. DOI: 10.1109/tmi.2004.837363 (cit. on pp. 11, 12, 18).

[54] Gramfort A., Papadopoulo T., Olivi E., and Clerc M. "OpenMEEG: opensource software for quasistatic bioelectromagnetics." In: *BioMedical Engineering OnLine* 9.1 (2010), p. 45. DOI: 10.1186/1475-925x-9-45 (cit. on pp. 12, 18).

[55] Dale A. M., Fischl B., and Sereno M. I. "Cortical Surface-Based Analysis." In: *NeuroImage* 9.2 (Feb. 1999), pp. 179–194. DOI: 10.1006/nimg.1998.0395 (cit. on pp. 13, 18).

[56] Fischl B. "FreeSurfer." In: *NeuroImage* 62.2 (Aug. 2012), pp. 774–781. DOI: 10.1016/j.neuroimage.2012.01.021 (cit. on pp. 13, 18).

[57] Hämäläinen M. and Ilmoniemi R. J. "Interpreting magnetic fields of the brain: minimum norm estimates." In: *Medical & Biological Engineering & Computing* 32.1 (Jan. 1994), pp. 35–42. DOI: 10.1007/bf02512476 (cit. on p. 15).

[58] Tadel F., Baillet S., Mosher J. C., Pantazis D., and Leahy R. M. "Brainstorm: A User-Friendly Application for MEG/EEG Analysis." In: *Computational Intelligence and Neuroscience* 2011 (2011), pp. 1–13. DOI: 10.1155/2011/879716 (cit. on pp. 15, 18).

[59] Pascual-Marqui R. D. et al. "Standardized low-resolution brain electromagnetic tomography (sLORETA): technical details." In: *Methods Find Exp Clin Pharmacol* 24.Suppl D (2002), pp. 5–12 (cit. on p. 16).

[60] Wagner M., Fuchs M., and Kastner J. "Evaluation of sLORETA in the Presence of Noise and Multiple Sources." In: *Brain Topography* 16.4 (2003), pp. 277–280. DOI: 10.1023/b:brat.0000032865.58382.62 (cit. on p. 16).

[61] Sekihara K., Sahani M., and Nagarajan S. S. "Localization bias and spatial resolution of adaptive and non-adaptive spatial filters for MEG source reconstruction." In: *NeuroImage* 25.4 (May 2005), pp. 1056–1067. DOI: 10.1016/j.neuroimage.2004.11.051 (cit. on p. 16).

[62] Brunet D., Murray M. M., and Michel C. M. "Spatiotemporal Analysis of Multichannel EEG: CARTOOL." In: *Computational Intelligence and Neuroscience* 2011 (2011), pp. 1–15. DOI: 10.1155/2011/813870 (cit. on p. 18).

[63] Oostenveld R., Fries P., Maris E., and Schoffelen J.-M. "FieldTrip: Open Source Software for Advanced Analysis of MEG, EEG, and Invasive Electrophysiological Data." In: *Computational Intelligence and Neuroscience* 2011 (2011), pp. 1–9. DOI: 10.1155/2011/156869 (cit. on p. 18).

[64] Gramfort A., Luessi M., Larson E., Engemann D. A., Strohmeier D., Brodbeck C., Parkkonen L., and Hämäläinen M. S. "MNE software for processing MEG and EEG data." In: *NeuroImage* 86 (Feb. 2014), pp. 446–460. DOI: 10.1016/j.neuroimage.2013.10.027 (cit. on p. 18).

[65] Acar Z. A. and Makeig S. "Neuroelectromagnetic Forward Head Modeling Toolbox." In: *Journal of Neuroscience Methods* 190.2 (July 2010), pp. 258–270. DOI: 10.1016/j.jneumeth.2010.04.031 (cit. on p. 18).

[66] Crone N. "Functional mapping of human sensorimotor cortex with electrocorticographic spectral analysis. II. Event-related synchronization in the gamma band." In: *Brain* 121.12 (Dec. 1998), pp. 2301–2315. DOI: 10.1093/brain/121.12.2301 (cit. on p. 19).

[67] Pfurtscheller G., Graimann B., Huggins J., Levine S., and Schuh L. "Spatiotemporal patterns of beta desynchronization and gamma synchronization in corticographic data during self-paced movement."

In: *Clinical Neurophysiology* 114.7 (July 2003), pp. 1226–1236. DOI: 10.1016/s1388-2457(03)00067-1 (cit. on pp. 19, 32).

[68] Hermes D., Miller K. J., Vansteensel M. J., Aarnoutse E. J., Leijten F. S., and Ramsey N. F. "Neurophysiologic correlates of fMRI in human motor cortex." In: *Human Brain Mapping* 33.7 (June 2011), pp. 1689–1699. DOI: 10.1002/hbm.21314 (cit. on p. 19).

[69] Siero J. C., Hermes D., Hoogduin H., Luijten P. R., Ramsey N. F., and Petridou N. "BOLD matches neuronal activity at the mm scale: A combined 7T fMRI and ECoG study in human sensorimotor cortex." In: *NeuroImage* 101 (Nov. 2014), pp. 177–184. DOI: 10.1016/j.neuroimage.2014.07.002 (cit. on p. 19).

[70] Kubánek J., Miller K. J., Ojemann J. G., Wolpaw J. R., and Schalk G. "Decoding flexion of individual fingers using electrocorticographic signals in humans." In: *Journal of Neural Engineering* 6.6 (Oct. 2009), p. 066001. DOI: 10.1088/1741-2560/6/6/066001 (cit. on p. 19).

[71] Miller K. J., Zanos S., Fetz E. E., Den Nijs M., and Ojemann J. G. "Decoupling the Cortical Power Spectrum Reveals Real-Time Representation of Individual Finger Movements in Humans." In: *Journal of Neuroscience* 29.10 (Mar. 2009), pp. 3132–3137. DOI: 10.1523/jneurosci.5506-08.2009 (cit. on p. 19).

[72] Hermes D., Siero J. C. W., Aarnoutse E. J., Leijten F. S. S., Petridou N., and Ramsey N. F. "Dissociation between Neuronal Activity in Sensorimotor Cortex and Hand Movement Revealed as a Function of Movement Rate." In: *Journal of Neuroscience* 32.28 (July 2012), pp. 9736–9744. DOI: 10.1523/jneurosci.0357-12.2012 (cit. on p. 19).

[73] Ball T., Demandt E., Mutschler I., Neitzel E., Mehring C., Vogt K., Aertsen A., and Schulze-Bonhage A. "Movement Related Activity in the High Gamma Range of the Human Electroencephalogram." In: *NeuroImage* 47 (July 2009), S74. DOI: 10.1016/s1053-8119(09)70474-4 (cit. on p. 19).

[74] Darvas F., Scherer R., Ojemann J., Rao R., Miller K., and Sorensen L. "High gamma mapping using EEG." In: *NeuroImage* 49.1 (Jan. 2010), pp. 930–938. DOI: 10.1016/j.neuroimage.2009.08.041 (cit. on p. 19).

[75] Gwin J. T., Gramann K., Makeig S., and Ferris D. P. "Removal of Movement Artifact From High-Density EEG Recorded During Walking and Running." In: *Journal of Neurophysiology* 103.6 (Apr. 2010), pp. 3526–3534. DOI: 10.1152/jn.00105.2010 (cit. on p. 19).

[76] Gramann K., Gwin J. T., Bigdely-Shamlo N., Ferris D. P., and Makeig S. "Visual Evoked Responses During Standing and Walking." In: *Frontiers in Human Neuroscience* 4 (2010). DOI: 10.3389/fnhum.2010.00202 (cit. on p. 19).

[77] Gwin J. T., Gramann K., Makeig S., and Ferris D. P. "Electrocortical activity is coupled to gait cycle phase during treadmill walking." In: *NeuroImage* 54.2 (Jan. 2011), pp. 1289–1296. DOI: 10.1016/j.neuroimage.2010.08.066 (cit. on p. 19).

[78] Wagner J., Solis-Escalante T., Grieshofer P., Neuper C., Müller-Putz G. R., and Scherer R. "Level of participation in robotic-assisted treadmill walking modulates midline sensorimotor EEG rhythms in able-bodied subjects." In: *NeuroImage* 63.3 (Nov. 2012), pp. 1203–1211. DOI: 10.1016/j.neuroimage.2012.08.019 (cit. on pp. 19, 22, 33).

[79] Salmelin R., Hämäläinen M., Kajola M., and Hari R. "Functional Segregation of Movement-Related Rhythmic Activity in the Human Brain." In: *NeuroImage* 2.4 (Dec. 1995), pp. 237–243. DOI: 10.1006/nimg.1995.1031 (cit. on p. 19).

[80] Seeber M., Scherer R., Wagner J., Solis-Escalante T., and Müller-Putz G. R. "EEG beta suppression and low gamma modulation are different elements of human upright walking." In: *Frontiers in Human Neuroscience* 8 (July 2014). DOI: 10.3389/fnhum.2014.00485 (cit. on pp. 22, 30–33).

[81] Seeber M., Scherer R., Wagner J., Solis-Escalante T., and Müller-Putz G. R. "Corrigendum: EEG beta suppression and low gamma modulation are different elements of human upright walking." In: *Frontiers in Human Neuroscience* 9 (Oct. 2015). DOI: 10.3389/fnhum.2015.00542 (cit. on p. 22).

[82] Seeber M., Scherer R., Wagner J., Solis-Escalante T., and Müller-Putz G. R. "High and low gamma EEG oscillations in central sensorimotor areas are conversely modulated during the human gait cycle." In:

NeuroImage 112 (May 2015), pp. 318–326. DOI: 10.1016/j.neuroimage.2015.03.045 (cit. on pp. 25, 31–34).

[83] Seeber M., Scherer R., and Müller-Putz G. R. "EEG Oscillations Are Modulated in Different Behavior-Related Networks during Rhythmic Finger Movements." In: *Journal of Neuroscience* 36.46 (Nov. 2016), pp. 11671–11681. DOI: 10.1523/jneurosci.1739-16.2016 (cit. on pp. 28, 31–33).

[84] Brodbeck V., Spinelli L., Lascano A. M., Wissmeier M., Vargas M.-I., Vulliemoz S., Pollo C., Schaller K., Michel C. M., and Seeck M. "Electroencephalographic source imaging: a prospective study of 152 operated epileptic patients." In: *Brain* 134.10 (Oct. 2011), pp. 2887–2897. DOI: 10.1093/brain/awr243 (cit. on p. 30).

[85] Muthukumaraswamy S. D. "Functional Properties of Human Primary Motor Cortex Gamma Oscillations." In: *Journal of Neurophysiology* 104.5 (Sept. 2010), pp. 2873–2885. DOI: 10.1152/jn.00607.2010 (cit. on p. 31).

[86] Castermans T., Duvinage M., Cheron G., and Dutoit T. "About the cortical origin of the low-delta and high-gamma rhythms observed in EEG signals during treadmill walking." In: *Neuroscience Letters* 561 (Feb. 2014), pp. 166–170. DOI: 10.1016/j.neulet.2013.12.059 (cit. on p. 31).

[87] Jenkinson N. and Brown P. "New insights into the relationship between dopamine, beta oscillations and motor function." In: *Trends in Neurosciences* 34.12 (Dec. 2011), pp. 611–618. DOI: 10.1016/j.tins.2011.09.003 (cit. on p. 32).

[88] Brown P. "Oscillatory nature of human basal ganglia activity: Relationship to the pathophysiology of Parkinson's disease." In: *Movement Disorders* 18.4 (Apr. 2003), pp. 357–363. DOI: 10.1002/mds.10358 (cit. on p. 32).

[89] Schnitzler A. and Gross J. "Normal and pathological oscillatory communication in the brain." In: *Nature Reviews Neuroscience* 6.4 (Apr. 2005), pp. 285–296. DOI: 10.1038/nrn1650 (cit. on p. 32).

[90] Uhlhaas P. J. and Singer W. "Neural Synchrony in Brain Disorders: Relevance for Cognitive Dysfunctions and Pathophysiology." In: *Neuron* 52.1 (Oct. 2006), pp. 155–168. DOI: 10.1016/j.neuron.2006.09.020 (cit. on p. 32).

[91] Hutchison W. D., Dostrovsky J., Walters J., Courtemanche R., Boraud T., Goldberg J., and Brown P. "Neuronal Oscillations in the Basal Ganglia and Movement Disorders: Evidence from Whole Animal and Human Recordings." In: *Journal of Neuroscience* 24.42 (Oct. 2004), pp. 9240–9243. DOI: 10.1523/jneurosci.3366-04.2004 (cit. on p. 32).

[92] Pogosyan A., Gaynor L. D., Eusebio A., and Brown P. "Boosting Cortical Activity at Beta-Band Frequencies Slows Movement in Humans." In: *Current Biology* 19.19 (Oct. 2009), pp. 1637–1641. DOI: 10.1016/j.cub.2009.07.074 (cit. on p. 32).

[93] Joundi R., Jenkinson N., Brittain J.-S., Aziz T., and Brown P. "Driving Oscillatory Activity in the Human Cortex Enhances Motor Performance." In: *Current Biology* 22.5 (Mar. 2012), pp. 403–407. DOI: 10.1016/j.cub.2012.01.024 (cit. on p. 32).

[94] Saleh M., Reimer J., Penn R., Ojakangas C. L., and Hatsopoulos N. G. "Fast and Slow Oscillations in Human Primary Motor Cortex Predict Oncoming Behaviorally Relevant Cues." In: *Neuron* 65.4 (Feb. 2010), pp. 461–471. DOI: 10.1016/j.neuron.2010.02.001 (cit. on p. 33).

[95] Fujioka T., Trainor L. J., Large E. W., and Ross B. "Internalized Timing of Isochronous Sounds Is Represented in Neuromagnetic Beta Oscillations." In: *Journal of Neuroscience* 32.5 (Feb. 2012), pp. 1791–1802. DOI: 10.1523/jneurosci.4107-11.2012 (cit. on p. 33).

[96] Arnal L. H. and Giraud A.-L. "Cortical oscillations and sensory predictions." In: *Trends in Cognitive Sciences* 16.7 (July 2012), pp. 390–398. DOI: 10.1016/j.tics.2012.05.003 (cit. on p. 33).

[97] Buschman T. J. and Miller E. K. "Top-Down Versus Bottom-Up Control of Attention in the Prefrontal and Posterior Parietal Cortices." In: *Science* 315.5820 (Mar. 2007), pp. 1860–1862. DOI: 10.1126/science.1138071 (cit. on p. 33).

[98] Pfurtscheller G. and Neuper C. "Motor imagery and direct brain-computer communication." In: *Proceedings of the IEEE* 89.7 (July 2001), pp. 1123–1134. DOI: 10.1109/5.939829 (cit. on p. 35).

[99] Wolpaw J. R., Birbaumer N., McFarland D. J., Pfurtscheller G., and Vaughan T. M. "Brain–computer interfaces for communication and control." In: *Clinical Neurophysiology* 113.6 (June 2002), pp. 767–791. DOI: 10.1016/s1388-2457(02)00057-3 (cit. on p. 35).

[100] Müller-Putz G. R., Leeb R., Tangermann M., Hohne J., Kübler A., Cincotti F., Mattia D., Rupp R., Müller K.-R., and Millan J. R. "Towards Noninvasive Hybrid Brain-Computer Interfaces: Framework, Practice, Clinical Application, and Beyond." In: *Proceedings of the IEEE* 103.6 (June 2015), pp. 926–943. DOI: 10.1109/jproc.2015.2411333 (cit. on p. 35).

Appendix

Appendix A.

Core Publications

frontiers in
HUMAN NEUROSCIENCE

ORIGINAL RESEARCH ARTICLE
published: 08 July 2014
doi: 10.3389/fnhum.2014.00485

EEG beta suppression and low gamma modulation are different elements of human upright walking

***Martin Seeber*[1,2], *Reinhold Scherer*[1,2,3]*, *Johanna Wagner*[1,2], *Teodoro Solis-Escalante*[1,2,4] and *Gernot R. Müller-Putz*[1,2]**

[1] *Laboratory of Brain-Computer Interfaces, Institute for Knowledge Discovery, Graz University of Technology, Graz, Austria*
[2] *BioTechMed-Graz, Graz, Austria*
[3] *Rehabilitation Clinic Judendorf-Strassengel, Judendorf-Strassengel, Austria*
[4] *Department of Biomechanical Engineering, Delft University of Technology, Delft, Netherlands*

Edited by:
Sophie Molholm, Albert Einstein College of Medicine, USA

Reviewed by:
Pierfilippo De Sanctis, Albert Einstein College of Medicine, USA
Adam C. Snyder, University of Pittsburgh, USA
Kristine Lynne Snyder, University of Michigan, USA

***Correspondence:**
Reinhold Scherer, Laboratory of Brain-Computer Interfaces, Institute for Knowledge Discovery, Graz University of Technology, 8010 Graz, Austria;
Rehabilitation Clinic Judendorf-Strassengel, Grazer Straße 15, Judendorf-Strassengel, Austria
e-mail: reinhold.scherer@tugraz.at

Cortical involvement during upright walking is not well-studied in humans. We analyzed non-invasive electroencephalographic (EEG) recordings from able-bodied volunteers who participated in a robot-assisted gait-training experiment. To enable functional neuroimaging during walking, we applied source modeling to high-density (120 channels) EEG recordings using individual anatomy reconstructed from structural magnetic resonance imaging scans. First, we analyzed amplitude differences between the conditions, walking and upright standing. Second, we investigated amplitude modulations related to the gait phase. During active walking upper μ (10–12 Hz) and β (18–30 Hz) oscillations were suppressed [event-related desynchronization (ERD)] compared to upright standing. Significant β ERD activity was located focally in central sensorimotor areas for 9/10 subjects. Additionally, we found that low γ (24–40 Hz) amplitudes were modulated related to the gait phase. Because there is a certain frequency band overlap between sustained β ERD and gait phase related modulations in the low γ range, these two phenomena are superimposed. Thus, we observe gait phase related amplitude modulations at a certain ERD level. We conclude that sustained μ and β ERD reflect a movement related state change of cortical excitability while gait phase related modulations in the low γ represent the motion sequence timing during gait. Interestingly, the center frequencies of sustained β ERD and gait phase modulated amplitudes were identified to be different. They may therefore be caused by different neuronal rhythms, which should be taken under consideration in future studies.

Keywords: electroencephalography (EEG), gait, brain mapping, motor cortex, magnetic resonance imaging

INTRODUCTION

Investigating neural dynamics during natural motor behavior is necessary to gain new knowledge about cortical involvement during motor control. This knowledge is fundamental for studying motor impairment after brain injury. We aim to develop a neurophysiological model of human gait. To address this problem, we focused on the analysis of neuronal oscillations (Buzsáki and Draguhn, 2004) gained from high-density electroencephalographic (EEG) recordings. The excellent temporal resolution of EEG recordings enables the analysis of electrocortical activity as it relates to the gait cycle phases. The spatial interpretability of the EEG can substantially be improved by applying source modeling (Baillet et al., 2001; Michel et al., 2004) to high-density EEG data. Yet, electrocortical oscillations during human upright walking are not well-studied.

Previous studies have shown that EEG spectral power in the μ and β band decreases over sensorimotor areas (Jasper and Penfield, 1949) during isolated foot movements (Pfurtscheller et al., 1997; Crone et al., 1998; Miller et al., 2007), motor preparation and motor imagery (Pfurtscheller and Neuper, 1997; Müller-Putz et al., 2007), walking on the treadmill (Severens et al., 2012) and robot-assisted walking (Wagner et al., 2012), when compared to a rest (non-movement) condition. These phenomena are classically described as event-related desynchronization and synchronization (ERD/ERS; Pfurtscheller and Aranibar, 1977; Pfurtscheller and Lopes da Silva, 1999). After the movement, β band power increases in a short-lasting burst called post-movement β synchronization (Pfurtscheller et al., 1996; Müller-Putz et al., 2007; Solis-Escalante et al., 2012). The presence of β oscillations at rest and the elevated state after movement led to the view that β oscillations represent an idling state of the motor cortex (Pfurtscheller et al., 1996). This theory has been revised with the hypothesis that β oscillations promote the maintenance of the current motor set at the expense of new movements (Engel and Fries, 2010; Jenkinson and Brown, 2011). A recent study reported significant coupling between EEG recordings over the leg motor area and electromyography (EMG) from the anterior tibialis muscle at 24–40 Hz during treadmill walking (Petersen et al., 2012). This frequency range is very similar to gait cycle modulated low γ oscillations (25–40 Hz) located in central midline areas shown from Wagner et al. (2012). Contrary to this evidence, Gwin et al. (2011) reported gait cycle phase coupled electrocortical activity in the α, β and the high γ band located in the anterior cingulate, posterior parietal, left and right sensorimotor cortex. In summary, the literature describes two major alterations of EEG oscillations during gait. First, neuronal oscillations in the

μ and β band are suppressed (ERD) during movement when compared to a rest, non-movement condition. Second, their amplitudes are modulated locked to the gait cycle phase during walking.

The previously mentioned studies relied heavily on independent component analysis (ICA) and dipole analysis for spatial location identification. While this methodology has many benefits, the location of specific independent components is not necessarily consistent with the location of certain brain activity patterns, e.g., ERD/ERS. The aim of this work was to directly localize μ and β ERD activities as well as gait phase modulated oscillations. To meet this objective, we introduced a measure that quantifies the gait cycle related amplitude modulation of a certain oscillation. These activity measures were mapped on the cortex using EEG source imaging (Baillet et al., 2001; Michel et al., 2004) based on individual anatomy reconstructed from magnetic resonance imaging (MRI) scans. Furthermore, we discuss the coexistence and superposition of sustained μ and β ERD and gait phase modulated oscillations in terms of cortical location and frequency of appearance, since these phenomena have thus far only been discussed separately.

MATERIALS AND METHODS

EXPERIMENT

Ten healthy volunteers (S1–S10, five female, five male, 25.6 ± 3.5 years) participated in this study. The experimental procedure was approved by the ethical committee of the Medical University Graz. Each subject gave informed consent before the experiment. Participants completed 4 runs (6 min each) of active walking and 3 runs of upright standing (3 min each) in a robotic gait orthosis (Lokomat, Hocoma, Switzerland). Walking speed was constant and adjusted to the participants' leg length ranging from 1.8 to 2.2 km per hour. Body weight support was adjusted with the help of experienced physical therapists to less than 30% in every participant. The Lokomat was operated with 100% guidance force. This set-up was chosen to ensure a well-controlled and steady gait pattern during the experiment. Participants were trained to walk in a natural way in the Lokomat and were asked look straight ahead and to blink normally to avoid eye artifacts during the experiment.

RECORDINGS

120 EEG channels were recorded by combining four 32-channel amplifiers (BrainAmp, Brainproducts, Munich, Germany). To determine the electrode positions and anatomical landmarks (nasion, vertex, left- and right pre-auricular points) for each subject, we used a 3D localizer (Zebris Elpos system, USA). Structural T1 MRI scans were recorded in a post-screening session using a 3.0 Tesla (Tim Trio/Skyra, Siemens, Erlangen, Germany) scanner. EEG was sampled to 2.5 kHz, high pass filtered at 0.1 Hz and low pass filtered at 1 kHz. The electrode montage was in accordance with the 5% international 10/20 EEG system (EasyCap, Germany; Oostenveld and Praamstra, 2001). Reference and ground electrodes were placed on the left and right mastoids respectively. Electrode impedances were <10 kΩ. Foot contact was measured by electro-mechanical switches placed over the calcaneus bone at the heel of both feet. We defined one gait cycle as the interval between two right leg heel contacts. More detailed information about the experimental set-up and procedure can be found in Wagner et al. (2012).

DATA ANALYSIS

Preprocessing and artifact correction

The EEG recordings were high pass filtered at 1 Hz [zerophase FIR filter order 7500] and low pass filtered at 200 Hz [zerophase FIR filter order 36]. To reduce computation time and required memory for time-frequency (TF) analysis, the data was down sampled to 250 Hz. EEG data from the active walking (gait) condition was epoched and time warped according to the mean gait cycle duration for every subject individually (group mean 2.13 ± 0.17 s). EEG data from the upright standing (rest) condition was sliced into non-overlapping segments with the length of the mean gait cycle duration. An EEG channel was not used if its variance was >2 times the median variance of all channels or if its kurtosis was >5 resulting in 99.28 ± 7.36 retained channels. An entire trial was rejected if more than half of the electrodes were excluded based on the previously mentioned criteria. Finally, an average of 219.3 (range 89–484) gait trials and 231.6 (range 130–301) rest segments were used for analysis. EEG was re-referenced according to the common average and the trials were corrected for direct current (DC) offsets.

EEG source modeling

To enable neuroimaging during the gait paradigm, we applied inverse mapping to high-density EEG recordings using a distributed source model based on individual anatomy. Source imaging of high-density EEG data (Baillet et al., 2001; Darvas et al., 2004; Michel et al., 2004) is increasingly evolving into a capable brain imaging method (Michel and Murray, 2012) due to advances in signal processing and the availability of computational power. The capability of high-density EEG source imaging based on sophisticated head models using individual anatomy has been demonstrated by Brodbeck et al. (2011) in a large-scale clinical study. Thus, we computed realistic head models as boundary element model (BEM) consisting of four surface layers (brain, inner skull, outer skull, head surface) that were reconstructed from individual structural T1 MRI scans. Cortical reconstruction and volumetric segmentation was performed with the Freesurfer image analysis suite (Dale et al., 1999; Fischl, 2012)[1]. The BEM model and EEG electrode positions were co-registered using four anatomical landmarks (nasion, vertex, left- and right pre-auricular points). The bioelectric forward problem was formulated as distributed source model using OpenMEEG (Kybic et al., 2005; Gramfort et al., 2010), in which 15000 sources were oriented perpendicular to the reconstructed gray matter cortical surface. This number of sources was necessary to model the folded brain surface and to take into account the individual gyri and sulci of each individual. To solve the ill-posed inverse problem, we used the sLORETA approach (Pascual-Marqui, 2002). The noise covariance matrix was calculated from the rest EEG segments and was used for

[1] http://surfer.nmr.mgh.harvard.edu/

whitening the lead field matrix. These analyses were performed with the Brainstorm toolbox (Tadel et al., 2011)[2].

Time-frequency decomposition of EEG sources

To enable the computation of functional topographies that can describe the dynamics of different brain rhythms during the gait cycle, we analyzed the EEG sources in the TF domain preserving the high temporal resolution of the EEG. Based on previously demonstrated utility in EEG analysis (Tallon-Baudry and Bertrand, 1999), we used Morlet et al. (1982) wavelets for TF decomposition. To design the mother wavelet, we set the full width half maximum value to 3 s for the Gaussian kernel at a center frequency of 1 Hz. Because TF decomposition is linear, we performed it in the sensor space before applying the linear inverse method to reduce computational cost. TF magnitudes were then calculated in the source space. This analysis results in brain topographies for each center frequency (4–50 Hz, 2 Hz steps) and every time sample. To enhance the signal to noise ratio (SNR) of the topographies, we averaged the TF magnitudes for the gait and rest condition segments respectively.

μ *and* β *ERD source imaging*

Logarithmic (natural logarithm) amplitude ratios of the gait and rest condition were computed in the EEG source space. These topographies illustrated relative amplitude changes between the gait and rest condition for a specific frequency. We applied a logarithmic function to give an activity scale that was centered at 0 and avoid the strong effect effect of outliers on power spectrum values induced by squaring. In noisy data squaring has the effect to amplify outliers relative to the signal of interest. Although logarithmic amplitude ratio is distinct from the classically defined ERD/ERS, it describes the same phenomena namely a relative spectral change between a defined task and reference period, in our case walking relative to upright standing. Because the terms ERD/ERS are well established in EEG analysis community, we continue using these terms.

To show general, sustained ERD/ERS activity over the whole gait cycle we calculated temporal mean ERD/ERS topographies for every frequency. The individual μ (8–13 Hz) and β (13–30 Hz) center frequencies were identified from local extreme ERD values for these bands. These ERD extremes were obtained from a global, spatially independent spectrum calculated from the population mean of the 150 source vertices (1% of the source space vertices) in the whole source space that showed most ERD. We used this approach to assure the identification of sensorimotor rhythms (μ and β) was fully data driven, without any *a priori* spatial region of interest (ROI). For the resulting μ and β center frequencies, we obtained ERD/ERS topographies, which showed significant ERD in the sensorimotor cortex. We clustered these significant vertices in sensorimotor cortex to identify an individual brain ROI in every subject. This cluster was reduced to the 150 sources (1% of the source space vertices) where ERD was greatest to obtain the same ROI size for each subject.

[2]http://neuroimage.usc.edu/brainstorm

Gait phase modulated oscillatory amplitudes

To analyze the modulation of oscillatory amplitudes relative to the gait cycle, we calculated logarithmic magnitude ratios for each time point relative to the mean TF magnitude of the whole gait cycle. These activities therefore express relative spectral changes across the gait cycle, not changes relative to the rest condition. To identify and localize the EEG frequency components with amplitude modulations most strongly locked to the gait cycle, we introduce the gait phase modulation (GPM) measure. To do so, we calculated a modified version of the modulation index that has previously been used to quantify the phase amplitude coupling (Canolty et al., 2006) of slow to fast neuronal oscillations. Here, we generated a phase signal according to the gait cycle, assuming a two periods pattern.

$$GPM(f) = \frac{2}{\sqrt{2} \cdot \sigma_{A(f)}} \cdot \sum_{n=0}^{N-1} A(n,f) \cdot e^{-2\pi i \cdot \frac{2 \cdot n}{N}}$$

In this formula, A denotes the TF magnitude at a certain frequency f and sample point n. N is the total number of samples per gait cycle. $\sigma_{A(f)}$ is the standard deviation of A and was multiplied with $\frac{2}{\sqrt{2}}$ to normalize the modulation measure. The GPM is a complex number which has a magnitude of 1 if A is modulated sinusoidally with the step frequency. The angle of A expresses the reconstructed phase of the modulation. This formulation is equivalent to the scaled discrete Fourier transform (DFT) component of the TF magnitude at the step frequency, and therefore can be back-transformed using the inverse DFT. This would result in a representation as a sinusoid with the step frequency having the magnitude and phase of the GPM. **Figure 1** shows an exemplary low γ amplitude modulation and the reconstructed GPM. This measure was calculated for multiple frequencies (4–50 Hz, 2 Hz

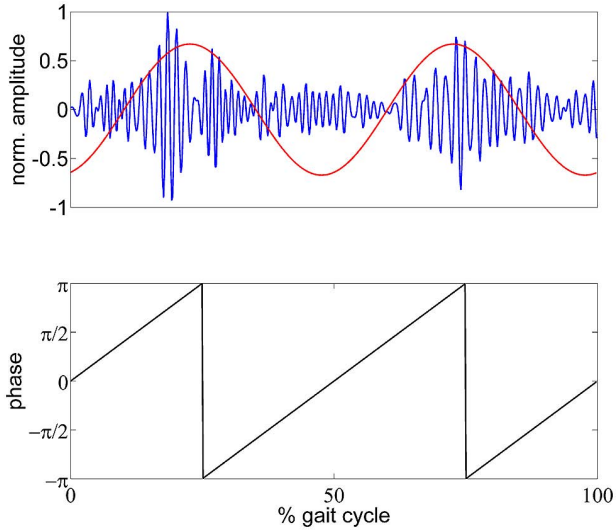

FIGURE 1 | Schematic illustration of the GPM measure. Top panel: exemplary (single trial) gait phase modulated low γ oscillation in blue and reconstructed GPM as time course. Bottom panel: generated gait phase assuming a two period pattern per gait cycle.

steps) and every vertex in the source space. The resulting functional topographies show the actual cortical origin of the GPM. Additionally, we can evaluate whether the GPM are caused by EMG activities, since EMG artifacts occur as superposition in EEG recordings. Considering electrical volume conduction it is likely that EMG sources get mapped to regions close to the muscle locations, especially at sites near the neck muscles. If the GPM were caused by EMG activities these modulations would be larger in brain regions near the muscles than in central sensorimotor cortical areas.

Statistical non-parametric mapping (SnPM)

In statistical analysis of functional brain topographies, it is important to control for Type I errors due to the multiple comparison problem inherent to a large number of vertices or sources in a model. The family-wise error rate (FWER) was controlled by applying SnPM using permutation tests (Nichols and Holmes, 2001; Maris and Oostenveld, 2007). We pooled the single trial topographies from the gait and rest condition. From this pooled data two random subsets were drawn with permuted labels from the gait and rest condition. The logarithmic ratio of the two random subset means was computed, resulting in random ERD/ERS topographies calculated from the actual data with permuted condition labels. This procedure was performed for 10^4 permutations. Activity was indicated as significant if its value was larger than the 95% of the maximum activity values from 10^4 random topographies, resulting in FWER < 0.05. To evaluate GPM chance levels, we destroyed the temporal order between the trials. To this end, we shifted the TF magnitudes in time using randomly (uniform distribution) drawn time lags between 0 and the mean gait cycle period. We calculated the mean over these temporally shifted trials, resulting in topographies. Again, we performed 10^4 permutations and set thresholds of 5% for the topographies. We ranked clustered activity according to the cluster size. Activity was deemed significant if a cluster was larger than 95% of the largest clusters from 10^4 permutations.

To evaluate the chance level of the GPM in the central sensorimotor ROI for different rhythms we performed the same time shift procedure as described above. Here we calculated the mean GPM in the ROI, ranked the randomly observed GPM values, and deemed the GPM significant if its magnitude was greater than 95% of the values from 10^4 permutations.

RESULTS

μ AND β ERD SOURCE IMAGES

Event-related desynchronization and synchronization topographies showed significant ERD in sensorimotor areas for the μ and β rhythm. Significant β ERD was visible focused in central sensorimotor areas (**Figure 2A**) in 8/10 Subjects. S6 showed weak, but still significant activity in central sensorimotor areas, while S10 showed a different pattern in the sensorimotor area. We also observed significant μ ERD for most of the subjects (**Figure 2B**), which were spatially less consistent across subjects than the β activity patterns. S6 and S8 showed fewer than 150 sources with significant activity in the sensorimotor cortex for the β topography. So, we used a smaller cluster of 69 sources for S8. The focal μ cluster in the central sensorimotor areas was downsized to a size of 150 sources and used as ROI for S6. Activities in **Figure 2** illustrated in red are likely to be caused by EMG artifacts and not by ERS brain activities.

GAIT PHASE MODULATED AMPLITUDES

Amplitude changes were found in central sensorimotor ROI, both from walking to standing and across the gait cycle (**Figure 3**). ERD/ERS activities during the gait cycle show sustained μ and β ERD during the entire gait cycle (**Figure 3A**). There were pronounced amplitude modulations relative to the mean gait cycle activity at 25–40 Hz with similar temporal dynamics locked to the gait cycle in 9/10 Subjects (**Figure 3C**). Subject 10, who already showed unusual μ and β brain topographies, also featured different TF patterns. A comparison of the temporal dynamics of TF magnitudes at μ and β frequencies compared to GPM center frequencies revealed that the GPM magnitudes were significantly higher (Wilcoxon signed rank) at the GPM peak frequency than at the μ ($p = 0.0049$) and the β ($p = 0.002$) center frequencies (**Table 1**; **Figure 3D**). While sustained ERD is by definition maximal at β center frequencies, the temporal amplitude modulation is bigger at the peak GPM frequencies (**Figures 3A,D**). Moreover, the GPM frequencies were significantly different (Wilcoxon signed rank) from the μ ($p = 0.002$) and β ($p = 0.0137$) center frequencies (**Figure 3B**). This indicates that sustained μ and β ERD and GPM occur in different neuronal rhythms. The GPM activities were localized to the central sensorimotor areas for 8/10 Subjects.

DISCUSSION

We directly localized μ and β ERD and gait phase modulated amplitudes during upright walking in humans using EEG source imaging. To investigate and quantify the cortical origin and frequency spectrum of gait phase modulated oscillations, we introduced the GPM measure.

Upper μ (10–12 Hz) and β (18–30 Hz) rhythms were suppressed (ERD) during the whole gait cycle, while low γ (25–40 Hz) oscillations were dynamically modulated related to the gait cycle phase. β ERD and low γ GPM were both localized in central sensorimotor areas. Interestingly, ERD and GPM center frequencies were identified to be different. They may therefore be caused by different neuronal rhythms.

μ AND β ERD SOURCE IMAGES

The ERD/ERS brain topographies showed β ERD patterns in central sensorimotor areas. These spatial patterns are consistent with the classical somatotopic location of lower extremities in the human motor cortex (Jasper and Penfield, 1949). Furthermore, these patterns coincide with results for invasive electrocorticographic (ECoG) recording studies that showed β spectral power decreased in central sensorimotor areas during isolated leg movements (Crone et al., 1998; Miller et al., 2007). The variability of functional somatotopy across individuals has been reported before (Crone et al., 1998; Miller et al., 2007). Yet, the inter-subject consistent β ERD pattern located in central sensorimotor areas was a robust feature of our study. ERD/ERS topographies illustrate general, conditional spectral changes between

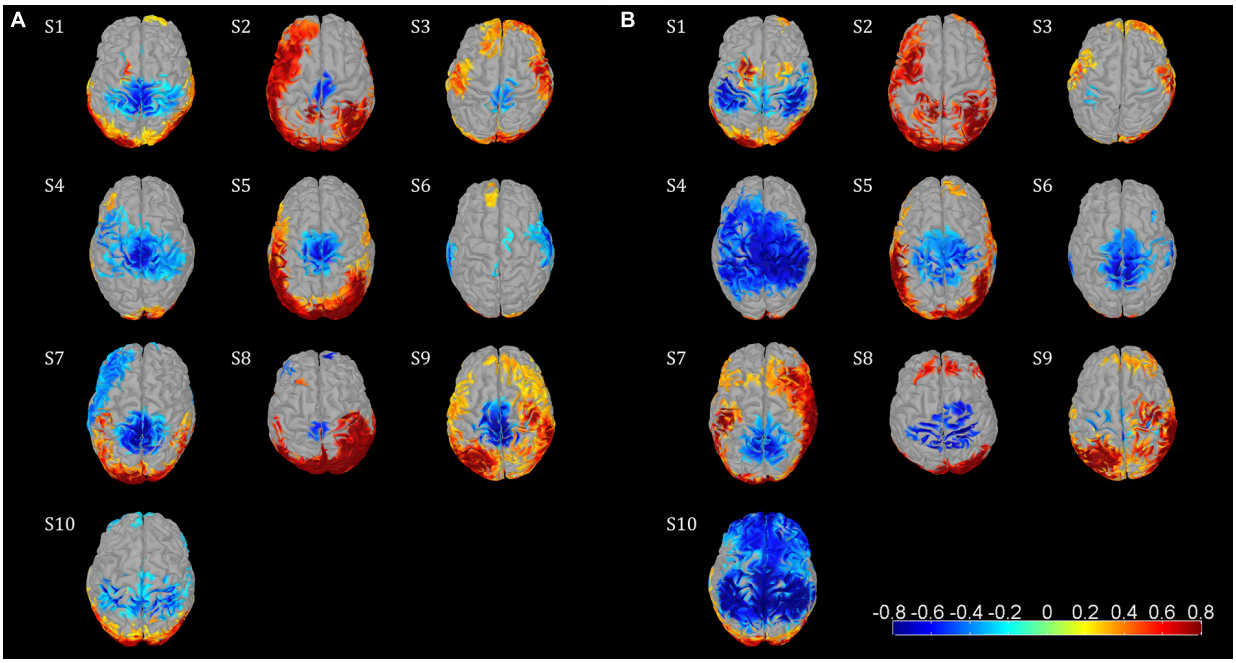

FIGURE 2 | Functional topographies of the 10 subjects illustrating significant μ and β ERD in the sensorimotor cortex during the active walking compared to the upright standing. (A) β rhythm topographies, activity in log spectral magnitude ratios. Significant (non-parametric permutation tests, corrected $p < 0.05$) spectral decrease (ERD) is illustrated in blue, spectral increase in red. **(B)** μ rhythm topographies, figure setting as in **(A)**. Individual center frequencies were used for the μ and β rhythm in every subject which showed most ERD, whereas all μ peaks were identified at 10–12 Hz and all β peaks were between 18–30 Hz; the specific frequencies are listed in **Table 1**. Based on these functional topographies the central sensorimotor ROI was identified individually for every subject.

active walking and upright standing, since there was no temporal information considered in this measure. ERD in the μ and β rhythm consequently describe general state changes for these oscillations during walking relative to a non-movement condition. ERD was interpreted as an electrophysiological correlate of activated cortical areas that are involved in sensory or cognitive processing, or in the production of motor behavior (Pfurtscheller and Lopes da Silva, 1999). Following this theory the sustained ERD reflects an active state of the sensorimotor areas during walking.

SUPERPOSITION OF SUSTAINED ERD AND GAIT PHASE MODULATED AMPLITUDES

In addition to sustained μ and β ERD, during the whole gait cycle, oscillatory amplitudes are modulated relative to the gait phase in the low γ band. These two phenomena occur simultaneously during walking and are superimposed, both in spatial location and frequency range. The GPM values are significantly larger in the low γ than at μ and β center frequencies (**Figure 3**, **Table 1**). This finding shows that GPM values, which are largest for frequencies between 28 and 36 Hz, cannot be explained exclusively by modulations of the μ and β rhythm. These modulations in the low γ are strongly linked to the gait cycle phase (**Figure 3C**, **Table 1**). The GPM maxima are clustered and located isolated in central sensorimotor areas (**Figure 4**). This localization suggests that the GPM are caused by brain signals and not by EMG activities, considering the location of head muscles and electrical volume conduction. Moreover, large GPM is present in a limited frequency band (24–40 Hz), not as broadband activity, which was reported to be associated with motion or muscular artifacts during walking (Castermans et al., 2014). The gait phase related rhythm in the low γ band was previously reported by our group (Wagner et al., 2012) using ICA and dipole reconstruction for localization. Again, the location of particular independent components is not necessarily congruent with the location of ERD/ERS activity or the GPM measures we introduced in the present work. Here, we directly localized μ and β ERD and low γ GPM using inverse modeling in a distributed source model. Moreover, our results show that μ and β ERD occur at different frequencies than the GPM, which are driven by a different rhythm in the low γ range.

The superposition of μ and β ERD and GPM is shown in **Figure 3**, where the overlay of these two phenomena can be determined to be dependent upon the frequency overlap (**Figure 3B**, **Table 1**) of the β ERD and the GPM center frequencies. In some subjects, the β ERD "covers" the GPM in these plots. The isolated gait phase related modulations are illustrated in **Figure 3C**. Because gait cycle mean activities were used as a reference, sustained ERD/ERS activities disappear in these plots. The time courses in **Figure 3D** additionally outline the coexistence of sustained ERD and GPM. Depending on the difference of the β and GPM center frequencies, these time courses differs in terms of their offset (ERD/ERS) or their temporal modulation (related to GPM).

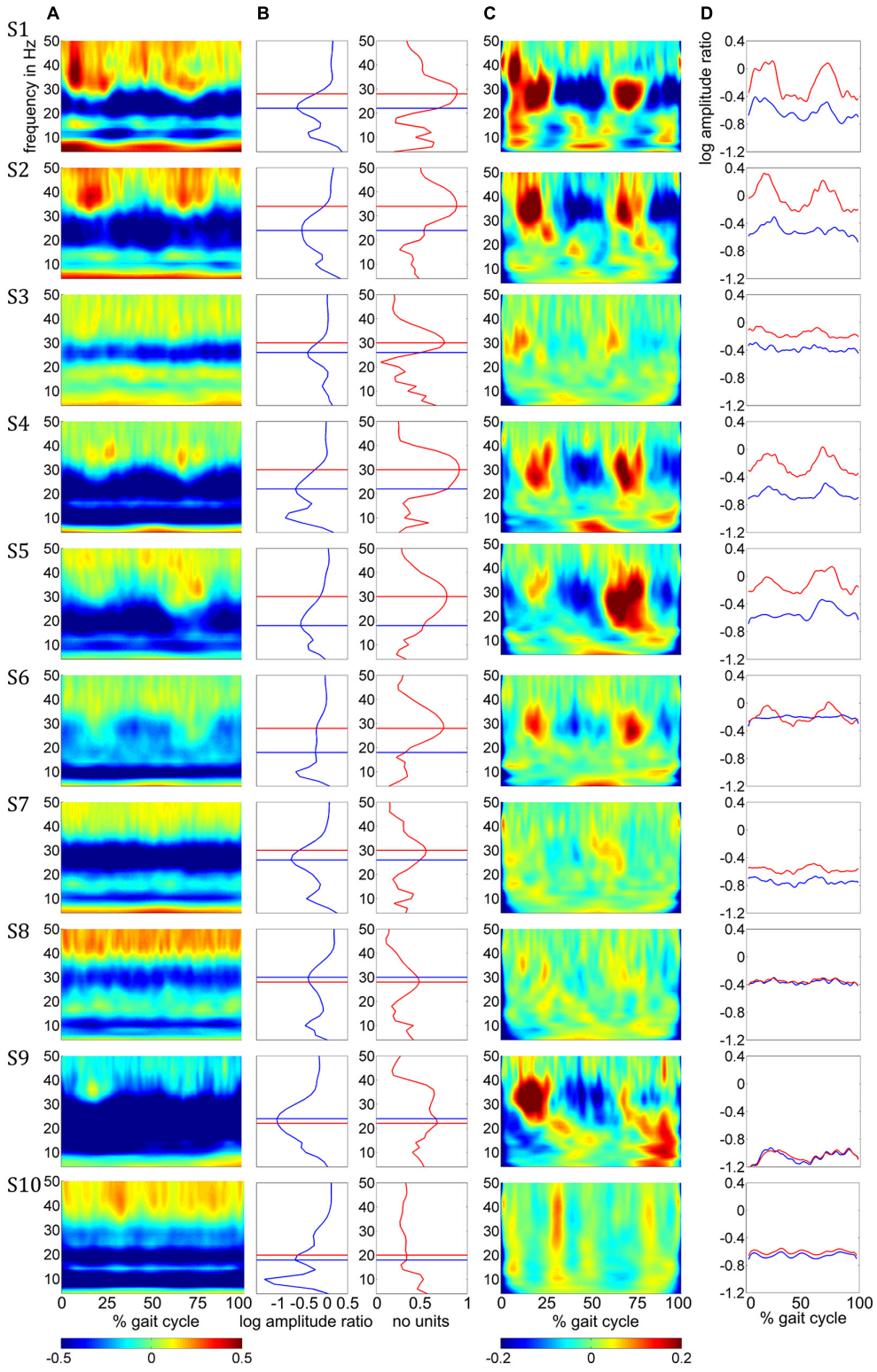

FIGURE 3 | (A) Time-frequency ERD/ERS plots from the 10 subjects illustrating spectral changes between active walking and upright standing. Activity in log spectral ratios, spectral de/increase in blue/red **(B)** ERD (blue) and GPM (red) as a function of frequency. **(C)** TF plots illustrating amplitude modulations relative to the gait cycle mean activities. **(D)** Time courses for the β rhythm (blue) and GPM (red) center frequency. The negative offsets in these plots represent sustained ERD while the temporal modulation indicates the GPM. All plots in this figure show mean activity in the individual central sensorimotor ROI for each subject.

Table 1 | μ, β rhythm and modulation center frequencies (f) in Hz with the corresponding GPM values.

	f_{μ}	f_{β}	f_{mod}	GPM_{μ}	GPM_{β}	GPM_{mod}	p_{mod}
S1	12	22	28	0.603	0.679	0.887	0.0001
S2	10	24	34	0.384	0.522	0.884	0.0001
S3	12	26	30	0.440	0.492	0.753	0.0001
S4	10	22	30	0.312	0.781	0.914	0.0001
S5	10	18	30	0.355	0.515	0.777	0.0001
S6	10	18	28	0.333	0.318	0.741	0.0001
S7	10	26	30	0.386	0.478	0.549	0.0001
S8	10	30	28	0.408	0.456	0.475	0.0015
S9	12	24	22	0.475	0.657	0.673	0.0001
S10	10	18	20	0.517	0.334	0.333	0.0120
Median	10	23	29	0.397	0.503	0.747	0.0001

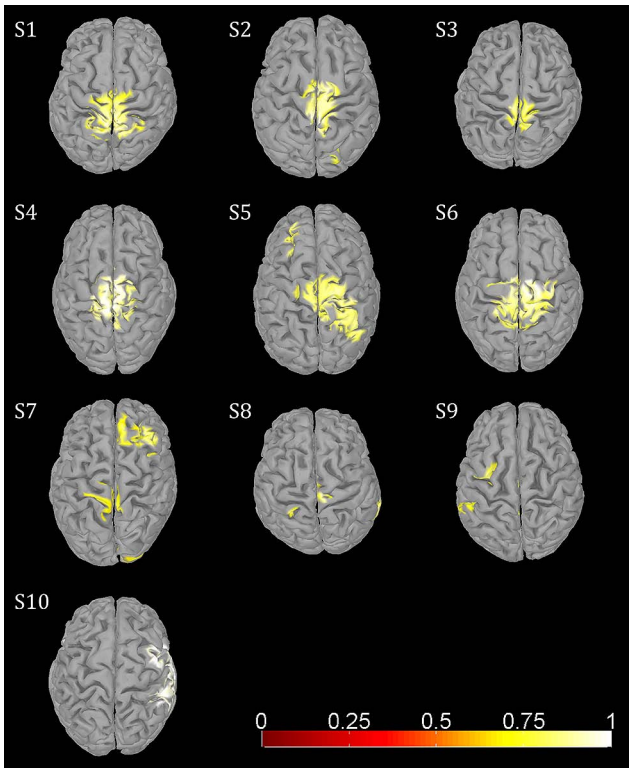

FIGURE 4 | Functional topographies of significant (non-parametric permutation tests, corrected FWER < 0.05) gait phase modulated oscillations (GPM) at individual GPM center frequencies (Table 1).

POTENTIAL LIMITATIONS OF THE CURRENT STUDY AND FUTURE WORK

We investigated robot-assisted walking in the Lokomat for several reasons. First, the robotic gait orthosis ensures a very steady gait pattern during the experiment. Second, the participants' trunk can be stabilized to some extent using body weight support, which reduces movement artifacts. Third, we plan to study electrophysiology during stroke rehabilitation in future studies using the Lokomat. Nonetheless, Lokomat walking is similar but still different from treadmill walking (Hidler and Wall, 2005; Hidler et al., 2008). The generalizability of our findings therefore has to be investigated for everyday walking tasks in the future. However, our findings may be helpful both for analysis of EEG data in more naturalistic human walking tasks on one hand as well as ultimately for clinical research on the other hand.

Lower extremities are both represented close to the midline in the human motor cortex (Jasper and Penfield, 1949). Due to this cortical location and the low spatial resolution of the EEG, we are limited to reporting summed activity from both feet. In this study, it is not possible to discuss EEG activity in relation to the movement of a particular foot. For example, increased amplitudes during 10–30% of the gait cycle could be related ether to the initial and midswing phases (10–37%) of the left foot or to the mid stance phase (10–30%) of the right foot. We are therefore careful in discussing TF activity in relation to certain phases of a particular foot.

FUNCTIONAL MEANING OF β ERD AND LOW γ MODULATION

In this section, we discuss our findings in relation to previous studies in terms of frequency ranges of the gait modulated oscillations and their cortical origin. The frequency ranges we report in this study for sustained β ERD (18–30 Hz) and the GPM (24–40 Hz) are very similar to corticomuscular coherence (CMC) peak frequencies from a recent study. In Petersen et al. (2012), the synchrony of EEG and EMG signals were investigated during treadmill walking. The authors reported CMC peaks located at the vertex (at the Cz electrode) for frequencies at 15–30 Hz for static contraction of the anterior tibial muscle, but for frequencies of 24–40 Hz for slow and normal walking. The drift of CMC peak frequencies from the β range during isometric movement tasks toward the low γ range during phasic movements has been previously discussed for upper limbs (Marsden et al., 2000; Omlor et al., 2007) and lower limbs (Gwin and Ferris, 2012). Considering these findings and assuming that different neuronal oscillations reflect different functional networks (Buzsáki and Draguhn, 2004; Schnitzler and Gross, 2005), the CMC peak drift from β frequencies during isometric movement toward low γ frequencies during phasic movements could be explained by different cerebral networks associated with the β rhythm and the low γ we identified and distinguished in this work.

The presence of β oscillations is related to maintenance of the current motor set (Engel and Fries, 2010) and promotes tonic activity at the expense of voluntary movement (Gilbertson et al., 2005; Brown, 2007; Pogosyan et al., 2009; Jenkinson and Brown, 2011). Thus, β ERD may reflect the suppression of an inhibitory network and signifies a neuronal state during walking that enables voluntary movement. We argue that β ERD during walking reflects a sustained active, movement related neuronal state, which is present during the whole gait cycle.

The most recent work from our group investigated different interactive virtual environment (VE) tasks during robot-assisted walking (Wagner et al., 2014). The authors reported low γ (23–40 Hz) gait cycle related modulations in the premotor cortex to be dependent on the VE task. This dependence was greatest

during 10–30 and 60–80% of the gait cycle and was suggested to represent processes involved in motor planning. In local field potential (LFP) recordings, low γ frequencies at 25–40 Hz have been shown to modulate the firing rate of macaque primary motor neurons during a center-out brain-machine interface task (Canolty et al., 2010). γ synchronization is a fundamental process in cortical computation (Fries et al., 2007; Fries, 2009) and facilitates the coordination of distributed functional cell assemblies (Canolty et al., 2010). Consequently, the gait phase modulated low γ oscillations we report could be involved in gait phase dependent local synchronization of neuronal populations linked to sensorimotor processing or integration. The particular involvement of low γ oscillations in motor control will be investigated in future work.

μ and β ERD and gait phase related amplitude modulations are simultaneously present during walking. Following the view that neuronal oscillations at different frequencies are involved in different cortical networks (Buzsáki and Draguhn, 2004; Schnitzler and Gross, 2005; Siegel et al., 2012), our findings suggest that the sustained μ and β ERD reflect altered states of the associated networks during walking. Furthermore, another network related to the low γ rhythm may be modulated dynamically locked to the gait cycle phase. Gait phase related low γ amplitude modulation and sustained μ and β suppression may therefore be organized in different neuronal networks.

ACKNOWLEDGMENTS

This work was supported by the European Union research project BETTER, BioTechMed and the Land Steiermark project BCI4REHAB.

REFERENCES

Baillet, S., Mosher, J. C., and Leahy, R. M. (2001). Electromagnetic brain mapping. *IEEE Signal Process. Mag.* 18, 14–30. doi: 10.1109/79.962275

Brodbeck, V., Spinelli, L., Lascano, A. M., Wissmeier, M., Vargas, M. I., Vulliemoz, S., et al. (2011). Electroencephalographic source imaging: a prospective study of 152 operated epileptic patients. *Brain* 134, 2887–2897. doi: 10.1093/brain/awr243

Brown, P. (2007). Abnormal oscillatory synchronisation in the motor system leads to impaired movement. *Curr. Opin. Neurobiol.* 17, 656–664. doi: 10.1016/j.conb.2007.12.001

Buzsáki, G., and Draguhn, A. (2004). Neuronal oscillations in cortical networks. *Science* 304, 1926–1929. doi: 10.1126/science.1099745

Canolty, R. T., Edwards, E., Dalal, S. S., Soltani, M., Nagarajan, S. S., Kirsch, H. E., et al. (2006). High gamma power is phase-locked to theta oscillations in human neocortex. *Science* 313, 1626–1628. doi: 10.1126/science.1128115

Canolty, R. T., Ganguly, K., Kennerley, S. W., Cadieu, C. F., Koepsell, K., Wallis, J. D., et al. (2010). Oscillatory phase coupling coordinates anatomically dispersed functional cell assemblies. *Proc. Natl. Acad. Sci. U.S.A.* 107, 17356–17361. doi: 10.1073/pnas.1008306107

Castermans, T., Duvinage, M., Cheron, G., and Dutoit, T. (2014). About the cortical origin of the low-delta and high-gamma rhythms observed in EEG signals during treadmill walking. *Neurosci. Lett.* 561, 166–170. doi: 10.1016/j.neulet.2013.12.059

Crone, N. E., Miglioretti, D. L., Gordon, B., Sieracki, J. M., Wilson, M. T., Uematsu, S., et al. (1998). Functional mapping of human sensorimotor cortex with electrocorticographic spectral analysis. I. Alpha and beta event-related desynchronization. *Brain* 121, 2271–2299. doi: 10.1093/brain/121.12.2301

Dale, A., Fischl, B., and Sereno, M. I. (1999). Cortical surface-based analysis. I. Segmentation and surface reconstruction. *Neuroimage* 9, 179–194. doi: 10.1006/nimg.1998.0395

Darvas, F., Pantazis, D., Kucukaltun-Yildirim, E., and Leahy, R. M. (2004). Mapping human brain function with MEG and EEG: methods and validation. *Neuroimage* 23, 289–299. doi: 10.1016/j.neuroimage.2004.07.014

Engel, A. K., and Fries, P. (2010). Beta-band oscillations: signalling the status quo? *Curr. Opin. Neurobiol.* 20, 156–165. doi: 10.1016/j.conb.2010.02.015

Fischl, B. (2012). FreeSurfer. *Neuroimage* 62, 774–781. doi: 10.1016/j.neuroimage.2012.01.021

Fries, P. (2009). Neuronal gamma-band synchronization as a fundamental process in cortical computation. *Annu. Rev. Neurosci.* 32, 209–224. doi: 10.1146/annurev.neuro.051508.135603

Fries, P., Nikolic, D., and Singer, W. (2007). The gamma cycle. *Trends Neurosci.* 30, 309–316. doi: 10.1016/j.tins.2007.05.005

Gilbertson, T., Lalo, E., Doyle, L., Di Lazzaro, V., Cioni, B., and Brown, P. (2005). Existing motor state is favored at the expense of new movement during 13–35 Hz oscillatory synchrony in the human corticospinal system. *J. Neurosci.* 25, 7771–7779. doi: 10.1523/JNEUROSCI.1762-05.2005

Gramfort, A., Papadopoulo, T., Olivi, E., and Clerc, M. (2010). OpenMEEG: open-source software for quasistatic bioelectromagnetics. *Biomed. Eng. Online* 45, 1–20. doi: 10.1186/1475-925X-9-45

Gwin, J. T., and Ferris, D. P. (2012). Beta- and gamma-range human lower limb corticomuscular coherence. *Front. Hum. Neurosci.* 6:258. doi: 10.3389/fnhum.2012.00258

Gwin, J. T., Gramann, K., Makeig, S., and Ferris, D. P. (2011). Electrocortical activity is coupled to gait cycle phase during treadmill walking. *Neuroimage* 54, 1289–1296. doi: 10.1016/j.neuroimage.2010.08.066

Hidler, J. M., and Wall, A. E. (2005). Alterations in muscle activation patterns during robotic-assisted walking. *Clin. Biomech.* 20, 184–193. doi: 10.1016/j.clinbiomech.2004.09.016

Hidler, J. M., Wisman, W., and Neckel, N. (2008). Kinematic trajectories while walking within the Lokomat robotic gait-orthosis. *Clin. Biomech.* 23, 1251–1259. doi: 10.1016/j.clinbiomech.2008.08.004

Jasper, H., and Penfield, W. (1949). Electrocorticograms in man: effect of voluntary movement upon the electrical activity of the precentral gyrus. *Eur. Arch. Psychiatry Clin. Neurol.* 183, 163–174.

Jenkinson, N., and Brown, P. (2011). New insights into the relationship between dopamine, beta oscillations and motor function. *Trends Neurosci.* 34, 611–618. doi: 10.1016/j.tins.2011.09.003

Kybic, J., Clerc, M., Abboud, T., Faugeras, O., Keriven, R., and Papadopoulo, T. (2005). A common formalism for the integral formulations of the forward EEG problem. *IEEE Trans. Med. Imaging* 24, 12–28. doi: 10.1109/TMI.2004.837363

Maris, E., and Oostenveld, R. (2007). Nonparametric statistical testing of EEG and MEG-data. *J. Neurosci. Methods* 164, 177–190. doi: 10.1016/j.jneumeth.2007.03.024

Marsden, J. F., Werhahn, K. J., Ashby, P., Rothwell, J., Noachtar, S., and Brown, P. (2000). Organization of cortical activities related to movement in humans. *J. Neurosci.* 20, 2307–2314.

Michel, C. M., and Murray, M. M. (2012). Towards the utilization of EEG as a brain imaging tool. *Neuroimage* 61, 371–385. doi: 10.1016/j.neuroimage.2011.12.039

Michel, C. M., Murray, M. M., Lantz, G., Gonzalez, S., Spinelli, L., and Grave de Peralta, R. (2004). EEG source imaging. *Clin. Neurophysiol.* 115, 2195–2222. doi: 10.1016/j.clinph.2004.06.001

Miller, K. J., Leuthardt, E. C., Schalk, G., Rao, R. P. N., Anderson, N. R., Moran, D. W., et al. (2007). Spectral changes in cortical surface potentials during motor movement. *J. Neurosci.* 27, 2424–2432. doi: 10.1523/JNEUROSCI.3886-06.2007

Morlet, J., Arens, G., Fourgenau, E., and Glard, D. (1982). Wave propagation and sampling theory—Part I: complex signal and scattering in multilayered media. *Geophysics* 47, 222–236. doi: 10.1190/1.1441328

Müller-Putz, G. R., Zimmermann, D., Grainmann, B., Nestinger, K., Korisek, G., and Pfurtscheller, G. (2007). Event-related beta EEG-changes during passive and attempted foot movements in paraplegic patients. *Brain Res.* 1137, 84–91. doi: 10.1016/j.brainres.2006.12.052

Nichols, T. E., and Holmes, A. P. (2001). Nonparametric permutation tests for functional neuroimaging: a primer with examples. *Hum. Brain Mapp.* 15, 1–25. doi: 10.1002/hbm.1058

Omlor, W., Patino, L., Hepp-Reymond, M. C., and Kristeva, R. (2007). Gamma-range corticomuscular coherence during dynamic force output. *Neuroimage* 34, 1191–1198. doi: 10.1016/j.neuroimage.2006.10.018

Oostenveld, R., and Praamstra, P. (2001). The five percent electrode system for high-resolution EEG and ERP measurements. *Clin. Neurophysiol.* 112, 713–719. doi: 10.1016/S1388-2457(00)00527-7

Pascual-Marqui, R. D. (2002). Standardized low resolution brain electromagnetic tomography (sLORETA): technical details. *Methods Find. Exp. Clin. Pharmacol.* 24(Suppl. D), 5–12.

Petersen, T. H., Willerslev-Olsen, M., Conway, B. A., and Nielsen, J. B. (2012). The motor cortex drives the muscles during walking in human subjects. *J. Physiol.* 590, 2443–2452. doi: 10.1113/jphysiol.2012.227397

Pfurtscheller, G., and Aranibar, A. (1977). Event-related cortical desynchronization detected by power measurements of scalp EEG. *Electroencephalogr. Clin. Neurophysiol.* 42, 817–826. doi: 10.1016/0013-4694(77)90235-8

Pfurtscheller, G., and Lopes da Silva, F. H. (1999). Event-related EEG/MEG synchronization and desynchronization: basic principles. *Clin. Neurophysiol.* 110, 1842–1857. doi: 10.1016/S1388-2457(99)00141-8

Pfurtscheller, G., and Neuper, C. (1997). Motor imagery activates primary sensorimotor area in humans. *Neurosci. Lett.* 239, 65–68. doi: 10.1016/S0304-3940(97)00889-6

Pfurtscheller, G., Neuper, C., Andrew, C., and Edlinger, G. (1997). Foot and hand area mu rhythms. *Int. J. Psychophysiol.* 26, 121–135. doi: 10.1016/S0167-8760(97)00760-5

Pfurtscheller, G., Stancák, A. Jr., and Neuper, C. (1996). Post-movement beta synchronization. A correlate of an idling motor area? *Electroencephalogr. Clin. Neurophysiol.* 98, 281–293. doi: 10.1016/0013-4694(95)00258-8

Pogosyan, A., Gaynor, L. D., Eusebio, A., and Brown, P. (2009). Boosting cortical activity at beta-band frequencies slows movement in humans. *Curr. Biol.* 19, 1637–1641. doi: 10.1016/j.cub.2009.07.074

Severens, M., Nienhuis, B., Desain, P., and Duysens, J. (2012). Feasibility of measuring event related desynchronization with electroencephalography during walking. *Conf. Proc. IEEE Eng. Med. Biol. Soc.* 2012, 2764–2767. doi: 10.1109/EMBC.2012.6346537

Schnitzler, A., and Gross, J. (2005). Normal and pathological oiscillatory communication in the brain. *Nat. Rev. Neurosci.* 6, 285–296. doi: 10.1038/nrn1650

Siegel, M., Donner, T. H., and Engel, A. K. (2012). Spectral fingerprints of large-scale neuronal interactions. *Nat. Rev. Neurosci.* 13, 121–134. doi: 10.1038/nrn3137

Solis-Escalante, T., Müller-Putz, G. R., Pfurtscheller, P., and Neuper, C. (2012). Cue-induced beta rebound during withholding of overt and covert foot movement. *Clin. Neurophysiol.* 123, 1182–1190. doi: 10.1016/j.clinph.2012.01.013

Tadel, F., Baillet, S., Mosher, J. C., Pantazis, D., and Leahy, R. M. (2011). Brainstorm: a user-friendly application for MEG/EEG analysis. *Comput. Intell. Neurosci.* 2011:879716. doi: 10.1155/2011/879716

Tallon-Baudry, C., and Bertrand, O. (1999). Oscillatory gamma activity in humans and its role in object representation. *Trends Cogn. Sci.* 3, 151–162. doi: 10.1016/S1364-6613(99)01299-1

Wagner, J., Solis-Escalante, T., Grieshofer, P., Neuper, C., Müller-Putz, G. R., and Scherer, R. (2012). Level of participation in robotic-assisted treadmill walking modulates midline sensorimotor EEG rhythms in able-bodied subjects. *Neuroimage* 63, 1203–1211. doi: 10.1016/j.neuroimage.2012.08.019

Wagner, J., Solis-Escalante, T., Scherer, R., Neuper, C., and Müller-Putz, G. R. (2014). It's how you get there: walking down a virtual alley activates premotor and parietal areas. *Front. Hum. Neurosci.* 8:93. doi: 10.3389/fnhum.2014.00093

Conflict of Interest Statement: The authors declare that the research was conducted in the absence of any commercial or financial relationships that could be construed as a potential conflict of interest.

Received: 03 April 2014; accepted: 16 June 2014; published online: 08 July 2014.
Citation: Seeber M, Scherer R, Wagner J, Solis-Escalante T and Müller-Putz GR (2014) EEG beta suppression and low gamma modulation are different elements of human upright walking. Front. Hum. Neurosci. ***8****:485. doi: 10.3389/fnhum.2014.00485*
This article was submitted to the journal Frontiers in Human Neuroscience.

frontiers in Human Neuroscience

GENERAL COMMENTARY
published: 02 October 2015
doi: 10.3389/fnhum.2015.00542

Corrigendum: EEG beta suppression and low gamma modulation are different elements of human upright walking

Martin Seeber[1,2]*, *Reinhold Scherer*[1,2,3], *Johanna Wagner*[1,2], *Teodoro Solis-Escalante*[1,2,4] *and Gernot R. Müller-Putz*[1,2]

[1] Laboratory of Brain–Computer Interfaces, Institute for Knowledge Discovery, Graz University of Technology, Graz, Austria, [2] BioTechMed-Graz, Graz, Austria, [3] Rehabilitation Clinic Judendorf-Strassengel, Judendorf-Strassengel, Austria, [4] Department of Biomechanical Engineering, Delft University of Technology, Delft, Netherlands

Keywords: electroencephalography (EEG), gait, brain mapping, motor cortex, magnetic resonance imaging

A corrigendum on

EEG beta suppression and low gamma modulation are different elements of human upright walking

by Seeber, M., Scherer, R., Wagner, J., Solis-Escalante, T., and Müller-Putz, G. R. (2014) Front. Hum. Neurosci. 8:485. doi: 10.3389/fnhum.2014.00485

OPEN ACCESS

Edited and reviewed by:
Sophie Molholm, Albert Einstein College of Medicine, USA

***Correspondence:**
Martin Seeber
seeber@tugraz.at

Received: *13 August 2015*
Accepted: *15 September 2015*
Published: *02 October 2015*

Citation:
Seeber M, Scherer R, Wagner J, Solis-Escalante T and Müller-Putz GR (2015) Corrigendum: EEG beta suppression and low gamma modulation are different elements of human upright walking. Front. Hum. Neurosci. 9:542. doi: 10.3389/fnhum.2015.00542

In the Original Research Article there is a missing normalization by "N" in the formula on page 3. This formula describes the gait phase modulation (GPM) measure. The corrected formula is written below.

$$GPM(f) = \frac{2}{\sqrt{2} \cdot \sigma_{A(f)} \cdot N} \cdot \sum_{n=0}^{N-1} A\left(n, f\right) \cdot e^{-2\pi i \cdot \frac{2 \cdot n}{N}}$$

In our original article, the description of the GPM formula as well as the reported results are correct. As properly stated in the commentary from Trenado (2015) to our original article, the normalization by N is necessary to scale the *GPM* magnitude in an interval from 0 to 1. In our calculations this normalization was already applied what is represented in the GPM values we reported in Table 1 and Figure 4 in the original publication.

In contrast to Trenado (2015) we suggest to use the GPM measure as complex number, not only it's magnitude. The GPM magnitude expresses it's strength, while the GPM angle represents the phase lag between behavior and amplitude envelop at a given carrier frequency and location in the brain. In our opinion it is a benefit of the GPM measure not only to describe the correlation between amplitude envelops of brain oscillations and behavior, i.e., walking patterns, but also to provide their phase relation.

Acknowledgments

This work was supported by the European Union research project BETTER (ICT-2009.7.2-247935) (www.car.upm-csic.es/bioingenieria/better/), BioTechMed Graz and the Land Steiermark projects BCI4REHAB (bci.tugraz.at/bci4rehab) and rE(EG)map! (bci.tugraz.at/reegmap).

References

Trenado, C. (2015). Commentary: EEG beta suppression and low gamma modulation are different elements of human upright walking. *Front. Hum. Neurosci.* 9:380. doi: 10.3389/fnhum.2015.00380

Conflict of Interest Statement: The authors declare that the research was conducted in the absence of any commercial or financial relationships that could be construed as a potential conflict of interest.

NeuroImage 112 (2015) 318–326

Contents lists available at ScienceDirect

NeuroImage

journal homepage: www.elsevier.com/locate/ynimg

High and low gamma EEG oscillations in central sensorimotor areas are conversely modulated during the human gait cycle

Martin Seeber [a,b], Reinhold Scherer [a,b,c], Johanna Wagner [a,b], Teodoro Solis-Escalante [a,b,d], Gernot R. Müller-Putz [a,b,*]

[a] Graz University of Technology, Institute for Knowledge Discovery, Laboratory of Brain–Computer Interfaces, Graz, Austria
[b] BioTechMed-Graz, Graz, Austria
[c] Rehabilitation Clinic Judendorf-Strassengel, Judendorf-Strassengel, Austria
[d] Department of Biomechanical Engineering, Delft University of Technology, Delft, The Netherlands

ARTICLE INFO

Article history:
Received 12 November 2014
Accepted 16 March 2015
Available online 24 March 2015

Keywords:
Electroencephalography (EEG) source imaging
Human gait
High gamma oscillations
Sensorimotor system
Robotic gait training

ABSTRACT

Investigating human brain function is essential to develop models of cortical involvement during walking. Such models could advance the analysis of motor impairments following brain injuries (e.g., stroke) and may lead to novel rehabilitation approaches. In this work, we applied high-density EEG source imaging based on individual anatomy to enable neuroimaging during walking. To minimize the impact of muscular influence on EEG recordings we introduce a novel artifact correction method based on spectral decomposition.

High γ oscillations (>60 Hz) were previously reported to play an important role in motor control. Here, we investigate high γ amplitudes while focusing on two different aspects of a walking experiment, namely the fact that a person walks and the rhythmicity of walking. We found that high γ amplitudes (60–80 Hz), located focally in central sensorimotor areas, were significantly increased during walking compared to standing. Moreover, high γ (70–90 Hz) amplitudes in the same areas are modulated in relation to the gait cycle. Since the spectral peaks of high γ amplitude increase and modulation do not match, it is plausible that these two high γ elements represent different frequency-specific network interactions. Interestingly, we found high γ (70–90 Hz) amplitudes to be coupled to low γ (24–40 Hz) amplitudes, which both are modulated in relation to the gait cycle but conversely to each other. In summary, our work is a further step towards modeling cortical involvement during human upright walking.

Introduction

The ability to walk safely and independently is important for humans. Cortical injuries (e.g., stroke) can cause motor impairment and lead to limitations in the execution of daily life activities. Thus, great effort is put into restoring walking in people with motor impairments. To get a deeper understanding of cortical involvement during walking it is necessary to develop models, which are capable of describing cortical activities in relation to human walking patterns. Such models could facilitate the development of novel rehabilitation strategies in the future.

Neuroimaging studies using functional magnet resonance imaging (fMRI) restrict subjects to a lying position with fixated heads. Therefore, such setups are not well-suited for studying human brain function during walking. To overcome these methodical limitations electroencephalographic (EEG) source imaging (Baillet et al., 2001; Michel et al., 2004, 2004) can be used. Despite its low spatial resolution (centimeters), sophisticated analysis of the EEG offers several advantages. First, the temporal resolution of EEG signals in milliseconds allows analyzing cortical processes in relation to walking patterns. Second, analysis in the frequency domain opens possibilities to investigate different elements of cortical activity (Buzsáki and Draguhn, 2004; Siegel et al., 2012). Third and most important for investigating cortical involvement during walking, EEG source imaging can be done in ambulatory conditions (i.e., mobile brain imaging).

In recent years, several studies have investigated brain activity during walking (Gwin et al., 2011; Gramann et al., 2010; Presacco et al., 2011; Severens et al., 2012; Petersen et al., 2012; Wagner et al., 2012, 2014; De Sanctis et al., 2014; Ehinger et al., 2014; Lau et al., 2014; Seeber et al., 2014). In agreement with earlier studies of isolated foot movement (Pfurtscheller et al., 1997; Crone et al., 1998; Miller et al., 2007; Müller-Putz et al., 2007), β oscillations in central sensorimotor areas were found to be suppressed (event-related desynchronization, ERD) during walking relative to a non-movement reference (Wagner et al., 2012; Severens et al., 2012; Seeber et al., 2014). Additionally, low γ (25–40 Hz) amplitudes were found to be modulated locked to

* Corresponding author at: Graz University of Technology, Inffeldgasse 13, 8010 Graz, Austria. Fax: +43 316 873 30702.
E-mail address: gernot.mueller@tugraz.at (G.R. Müller-Putz).

http://dx.doi.org/10.1016/j.neuroimage.2015.03.045
1053-8119/

the gait cycle (Wagner et al., 2012, 2014; Seeber et al., 2014). The same frequency range was reported by Petersen et al. (2012) for significant coherence between EEG recordings over leg motor areas and the anterior tibialis muscle.

Sustained β suppression and low γ modulation were found to be simultaneously present and superimposed in the frequency domain and in spatial location during walking. Nevertheless, the different spectral peaks of β suppression and low γ modulation suggest that these phenomena are different elements of EEG activity during walking. We proposed that altered levels of β suppression during walking signify enhanced cortical excitability in central sensorimotor areas. Furthermore, gait cycle related modulation of low γ amplitudes may reflect sensorimotor processing linked to the motion sequences (Seeber et al., 2014).

In this work, we further develop the electrophysiological model of walking, including data from higher frequency oscillations (>50 Hz). Previous studies showed high γ oscillations (60–90 Hz) to play an important role in motor execution (Crone et al., 1998; Pfurtscheller et al., 2003; Miller et al., 2007; Cheyne et al., 2008; Ball et al., 2008; Donner et al., 2009; Muthukumaraswamy, 2010; Darvas et al., 2010; Joundi et al., 2012). High γ power increase in electrocorticographic (ECoG) recordings correspond spatially well to fMRI activity (Hermes et al., 2012a) and its superior focal distribution enables the decoding of single finger movement (Kubánek et al., 2009; Miller et al., 2009; Scherer et al., 2009; Hermes et al., 2012b). The feasibility of detecting high γ activity in the motor system from non-invasive recordings was reported for magnetoencephalography (MEG) (Cheyne et al., 2008; Dalal et al., 2008; Donner et al., 2009; Muthukumaraswamy, 2010) and EEG (Ball et al., 2008; Darvas et al., 2010) during isolated limb movements. However, due to muscular [electromyographic (EMG)] and movement artifacts, it is very challenging to detect high γ activity from EEG recordings during walking. EMG artifacts during body movements affect EEG recordings in a wide range of frequencies (~20–300 Hz) (Muthukumaraswamy, 2013; Castermans et al., 2014).

Extending the previous findings of our group (Wagner et al., 2012; Seeber et al., 2014) we focus on two different aspects of the walking experiment: the fact that a person walks and the rhythmicity of walking movements. Therefore, we first investigate differences of the amplitude spectra between conditions walking and standing. In these analyses we introduce a novel artifact correction method based on spectral decomposition to minimize the impact of muscular influence on EEG source images. This correction method enables us to analyze high γ activity during walking. Second, we examine amplitude modulations in relation to gait phases reflecting the rhythmicity of walking movements.

Methods

Experiment and recordings

Data were taken from a previous study of our group (Wagner et al., 2012). Ten healthy volunteers (5 female, 5 male, 25.6 ± 3.5 years) completed four runs (6 min each) of active walking and three runs of upright standing (3 min each) in a robotic gait orthosis (Lokomat, Hocoma, Switzerland). Walking speed was constant and adjusted for each participant individually ranging from 1.8 to 2.2 km per hour. The Lokomat was operated with 100% guidance force and body weight support was less than 30% in every participant. This set-up was chosen to ensure a well-controlled and steady gait pattern during the experiment. Participants were trained to walk in a natural way, in accord with the movement pattern of the Lokomat.

Multichannel EEG (120 channels) was recorded by combining four 32-channel amplifiers (BrainAmp, Brainproducts, Germany). A 3D localizer (Zebris Elpos system, USA) was used to determine electrode positions and anatomical landmarks (nasion, vertex, left- and right pre-auricular points) for each subject. Structural T1 magnetic resonance imaging (MRI) scans were recorded in a post screening session using a 3.0 T (Tim Trio/Skyra, Siemens, Erlangen, Germany) scanner. EEG sampling rate was set to 2.5 kHz and the band pass filter to 0.1 Hz and 1 kHz. Electrodes were mounted in accord with the 5% international 10/20 EEG system (EasyCap, Germany) (Oostenveld and Praamstra, 2001). Reference and ground electrodes were placed on the left and right mastoids, respectively. Electrode impedances were lower than 10 kΩ. Foot contact was measured by electro-mechanical switches placed over the calcaneus bone at the heel of both feet. We defined one gait cycle as the interval between two right leg heel contacts. More detailed information about the experimental set-up and procedure can be found in Wagner et al., 2012.

Preprocessing

The EEG recordings were band pass filtered between 1 and 200 Hz, notch filtered at the line frequency (50 Hz) and its integer multiples (i.e., 100, 150, and 200 Hz). EEG data during walking was segmented into gait cycle periods corresponding to the measured foot triggers. EEG data from upright standing was separated into non-overlapping segments with the length of the mean gait cycle duration of every subject. EEG channels were not used if their variance was greater than 2 times the median variance of all channels or exceeded a threshold of ± 1 mV resulting in 98.9 ± 7.5 retained channels. A segment was excluded from analysis if any channel exceeded a threshold of ± 200 μV. This resulted in 404 walking and 231 standing segments (99.2% of all segments) that were analyzed on average for each subject. EEG was re-referenced according to the common average and the trials were corrected for direct current (DC) offsets.

EEG source imaging

High-density EEG source imaging (Baillet et al., 2001; Darvas et al., 2004; Michel et al., 2004; Michel and Murray, 2012) was applied based on distributed source models using realistic head models. Forward models were computed using OpenMEEG (Kybic et al., 2005; Gramfort et al., 2010) as boundary element models (BEM) consisting of four layers (brain, inner skull, outer skull, head surface) which were reconstructed from individual structural T1 MRI scans. Cortical reconstruction and volumetric segmentation were performed with the FreeSurfer image analysis suite (Dale et al., 1999; Fischl, 2012) (http://surfer.nmr.mgh.harvard.edu/). BEM model and EEG electrode positions were co-registered using four anatomical landmarks (nasion, vertex, left- and right pre-auricular points). 15,002 brain sources were modeled with perpendicular orientation to gray matter surface. This number of sources was necessary to take into account the individual gyri and sulci of each folded brain surface. sLORETA (Pascual-Marqui, 2002) was used to solve the ill-posed inverse problem. For whitening the lead field matrix, we used the noise covariance matrix calculated from the standing EEG segments. Analyses were performed in Matlab (Mathworks, Natick, USA) using custom scripts and the Brainstorm toolbox (Tadel et al., 2011) (http://neuroimage.usc.edu/brainstorm).

Time–frequency analysis

Time–frequency (TF) decomposition was used to investigate temporal dynamics of EEG oscillations in the source space. These analyses contained the following 6 stages:

(1) TF decomposition was applied to walking and standing segments. We used Morlet wavelets (Morlet et al., 1982) for TF analyses (2–200 Hz, 2 Hz steps). Mother wavelet parameters were set to full width half maximum value of 3 s for the Gaussian kernel at a center frequency of 1 Hz. The magnitudes of TF decomposed signals were calculated in the source space and

time warped to match the mean gait cycle duration. This data was then averaged for the walking and standing segments, respectively.

(2) We calculated relative amplitude changes (in decibel, dB) between the walking and standing condition for every frequency denoted above. These TF matrices (sources × time × frequencies) were used in each individual for muscular artifact correction as described in the next section.

(3) We investigated gait cycle related amplitude modulations representing the rhythmicity of walking movements. Therefore, we computed the amplitude ratio (in dB) of every time point in the gait cycle to the temporal mean amplitude at a certain frequency to obtain zero-mean amplitude modulations. From these data we calculated the gait phase related amplitude modulation (GPM) measures as normalized Fourier transform component of TF source magnitudes corresponding to the step frequency (Seeber et al., 2014). The magnitude of this measure expresses the correlation of the amplitude envelope at a certain carrier frequency and a sinusoid of the modulation, in our case, the step frequency. The benefit of the GPM measure is, due to its Fourier-based origin the capability to evaluate the phase lag of the amplitude modulation and the heel strike. This property is not provided by the common correlation coefficient.

(4) TF plots were calculated in the central sensorimotor region of interest (ROI). This ROI was defined as the cortical region in which low γ (24–40 Hz) GPM was significant (see section Group statistical analysis). The pattern, frequency range, and location of the low γ GPM were previously reported from this data set (Wagner et al., 2012; Seeber et al., 2014).

(5) Specific frequencies of interest were selected for further analysis based on frequency spectra in the central sensorimotor ROI. Peaks in the relative amplitude spectrum indicate maximal differences between walking and standing. Accordingly, peaks in the GPM spectrum indicate maximal gait phase related amplitude modulations at this frequency. Source images at the selected frequencies were subsequently tested for significant activity.

(6) Cross-frequency coupling (CFC) was analyzed in the central sensorimotor ROI as correlation of the amplitude envelopes for every frequency combination. Again, peaks in the GPM spectra were used to select frequency ranges to test for significant CFC.

Muscular artifact correction

Previous EEG studies on walking mostly focused on independent component analysis (ICA) (Gwin et al., 2011; Petersen et al., 2012; Wagner et al., 2012) to correct for artifacts. In this work, we use a different approach based on frequency spectral decomposition. Instead of decomposing the EEG signals in time domain into independent components our intention was to decompose the frequency spectra into orthogonal spectral components using principal component analysis (Jolliffe, 2002). Muscular activity (EMG) is present in a wide range of frequencies (~20–300 Hz) (Muthukumaraswamy, 2013; Castermans et al., 2014) and spreads spatially to many EEG channels during walking, especially to ones which are close to neck muscles (Gramann et al., 2010; Gwin et al., 2011; Seeber et al., 2014). In contrast, amplitudes of cortical oscillations decrease in narrow frequency ranges in the upper μ (10–12 Hz) and β (18–30 Hz) range during isolated foot movements (Pfurtscheller et al., 1997; Crone et al., 1998; Miller et al., 2007; Müller-Putz et al., 2007) and walking (Wagner et al., 2012; Severens et al., 2012; Seeber et al., 2014). High gamma amplitudes increase in an approximately 20 Hz wide range centered between 60–100 Hz and were located to contralateral hand/feet representation areas in the motor cortex during finger (Ball et al., 2008; Cheyne et al., 2008; Donner et al., 2009; Muthukumaraswamy, 2010; Darvas et al., 2010) and foot movements (Cheyne et al., 2008) respectively. Because of these spatial and spectral differences between muscular activity and cortical signals, the assumption of the proposed approach is that these two sources are separable. Therefore, our objective was to decompose the mixed spectral profiles we are recording as EEG into muscular artifacts and actual cortical activities. The spectral profile of muscular artifacts then is identified and the corresponding principal spectral component (PSC) ignored in the back projection. The utility of spectral decomposition approaches in EEG analysis for different purposes was shown previously (Miller et al., 2009; Onton and Makeig, 2009).

Commonly, temporal information is used to calculate the covariance matrix for PCA or ICA in EEG analysis to decompose the channels. Here, we used the spatial information of EEG sources to calculate the covariance matrix to decompose the frequency spectra.

$$C = X^T \cdot X$$

$$C \cdot V = V \cdot D$$

$$W = X \cdot V$$

$$U = V^{-1}$$

$$Y_{PSC\ n} = W_{1:N,n} \cdot U_{n,1:N}$$

e.g.

$$Y_{PSC\ 1} = W_{1:N,1} \cdot U_{1,1:N}$$

$$Y_{PSC\ 2:M} = W_{1:N,\ 2:M} \cdot U_{2:M,\ 1:N}$$

Where X is a matrix of the dimension $N \times M$ (sources × frequencies) containing the amplitude ratios between walking (at a specific time point) and standing. C is the covariance matrix of the size $M \times M$. V is a matrix containing the eigenvectors and D is a diagonal matrix containing the eigenvalues. Eigenvalues were sorted in descending order and columns in V were rearranged accordingly. W is a matrix containing the images projected on the eigenvectors, i.e., the images of the orthogonal spectral components. $Y_{PSC\ n}$ is a $N \times M$ matrix of the back-projected principal spectral component n. Each PSC has a static brain topography ($W_{1:N,n}$) scaled by its frequency profile ($U_{n,1:N}$). The frequency spectra of the PSCs' are orthogonal due to the decomposition criteria. In sum, each PSC is therefore identified by a static topographic pattern and its frequency spectrum. This decomposition was calculated for every time sample in the gait cycle, individually for every subject.

Group statistical analysis

Results are reported on the group level statistics in this work. To enable group analysis it is necessary to project the individual EEG source images on a common space. Here, we used the Colin 27 (Montreal Neurological Institute, http://imaging.mrc-cbu.cam.ac.uk/imaging/MniTalairach) surface. Each hemisphere of individuals' cortices was inflated to a sphere. This sphere then was warped to align the individual gyri and sulci to the Colin 27 surface. The result of this spatial aligning process is a projection matrix, which can be used to project EEG source images from one cortical surface to another. This spatial aligning procedure (Fischl et al., 1999) was performed using the FreeSurfer image analysis suite (Dale et al., 1999; Fischl, 2012) (http://surfer.nmr.mgh.harvard.edu/). Gait cycle durations were different for each subject. Therefore, we time warped the TF data according to the grand average gait cycle duration to enable group analysis.

Significant EEG source activity was identified based on nonparametric permutation tests (Nichols and Holmes, 2001; Maris and Oostenveld, 2007). We selected specific frequency ranges for each measure respectively. First, for analyzing amplitude differences between walking and

standing we selected μ (10–12 Hz), β (18–30 Hz) and high γ (60–80 Hz) ranges. Second, for the GPM measure we focused on low γ (24–40 Hz) and high γ (70–90 Hz) ranges. These frequency ranges were selected based on peaks in the frequency spectra in the central sensorimotor ROI. Afterwards, we tested for significant activity in source images of these five selected features. To correct for the multiple comparisons inherent to the large number of sources (15,002) we applied suprathreshold cluster size tests (Nichols and Holmes, 2001; Maris and Oostenveld, 2007). The primary threshold was set to the 95% quantile of activities in an actual image which was calculated with unpermuted labels. We pooled the source images from the walking and standing condition. Therefore, the pooled data set contained 20 source images (ten individuals × two conditions). From these pooled data sets ten images were drawn randomly and used to calculate the group average. This procedure was performed for 10^4 permutations. The primary threshold was applied in every image resulting from the permutations. A cluster in the actual images was then defined as significant if its size was larger than 95% of the maximal cluster sizes from the randomly observed 10^4 images.

Spearman's rank correlation coefficient was calculated to determine the coupling of high γ (70–90 Hz) and low γ (24–40 Hz) amplitude envelopes. We tested for significant correlation using a permutation test similar to the one described above. Here, we pooled amplitude envelopes from central sensorimotor ROI for the subjects and the walking and standing condition. We intentionally tested high γ and low γ correlation to be larger during walking compared to standing and not only to be significantly larger than zero. By this means, we are able to preclude that this correlation is a result of the TF analysis itself or the artifact correction method, because we used identical analysis pipelines for walking and standing data for these statistical tests.

Results

Muscular artifact correction

The spatial map of the first PSC (with the largest eigenvalue) showed activity located in lateral and dorsal regions close to the location of head and neck muscles (Figs. 1a, 2c). The eigenvalue of the first PSC was 5–10 times bigger than the eigenvalue of the 2nd one in every subject (Fig. 2b). Moreover, the spectral profile of this component increases from 2–20 Hz and remains at a certain level for higher frequencies (Figs. 1b/c, 2a/c, S1). The spatial location and spectral profile of the first PSC suggests this component to reflect muscular activity rather than cortical oscillations. Thus, this component was excluded from further analysis.

The first PSC resembled the spectral profile at dorsolateral sites (Fig. 2c) where after artifact correction (omitting this component) the spectral amplitudes were close to the reference level (standing, 0 dB). Similarly, spectral amplitudes in central sensorimotor areas were lowered in a wide frequency range in accord with the first PSC spectrum. In contrast, narrow band μ and β amplitude decrease as well as high γ increase at 60–80 Hz (Figs. 1a/b, 2c) remain in central sensorimotor areas after applying the correction method. GPM magnitudes were decreased in the high γ range in left and right dorsolateral regions after applying the artifact correction method, but were increased in

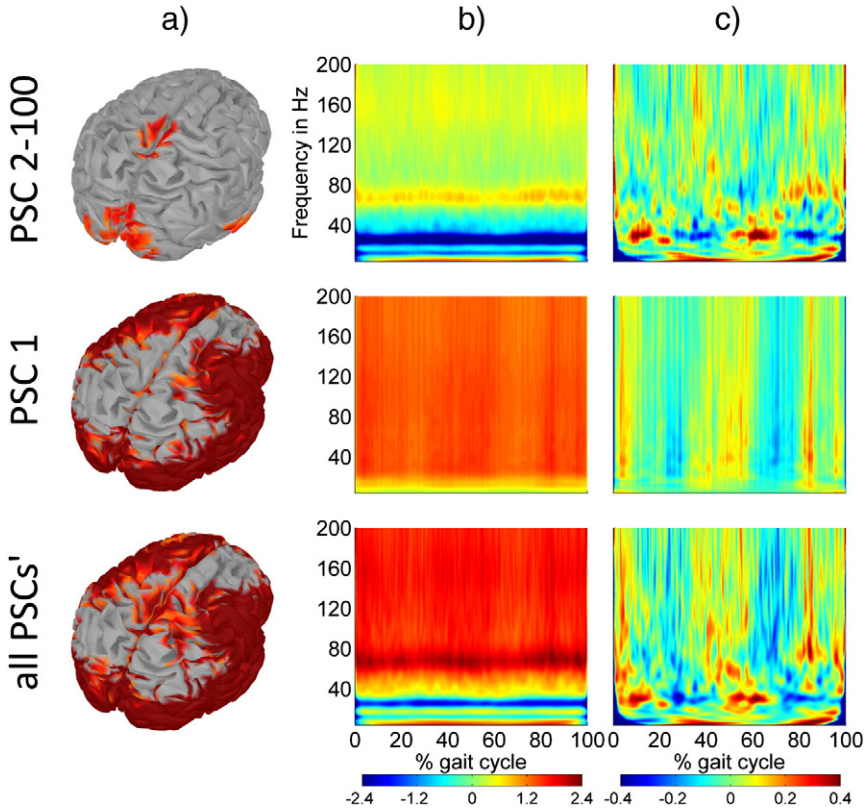

Fig. 1. Artifact correction method. The rows in a–c) show the corrected (PSC 2-100), removed (PSC 1) and uncorrected (all PSC's) patterns of a representative subject. a) Amplitude increase at 68 Hz (reference: standing). Note the focal activity in central sensorimotor areas in the corrected image, the prominent activities at dorsal and lateral sites of the removed component and the summation of these patterns in the uncorrected image. b) TF plots in central sensorimotor ROI (reference: standing). The corrected TF plot shows well-known amplitude decrease for μ and β frequencies (blue) and high γ increase (red) in dB. TF plot of the removed component illustrates broadband activities, which spectral profile is quite similar over the gait cycle. c) TF plots in central sensorimotor ROI (reference: walking). The corrected TF plot reveals narrow band modulations in the high γ and low γ frequency range, broadband activity in the removed component and the summation of all components in the uncorrected TF plot.

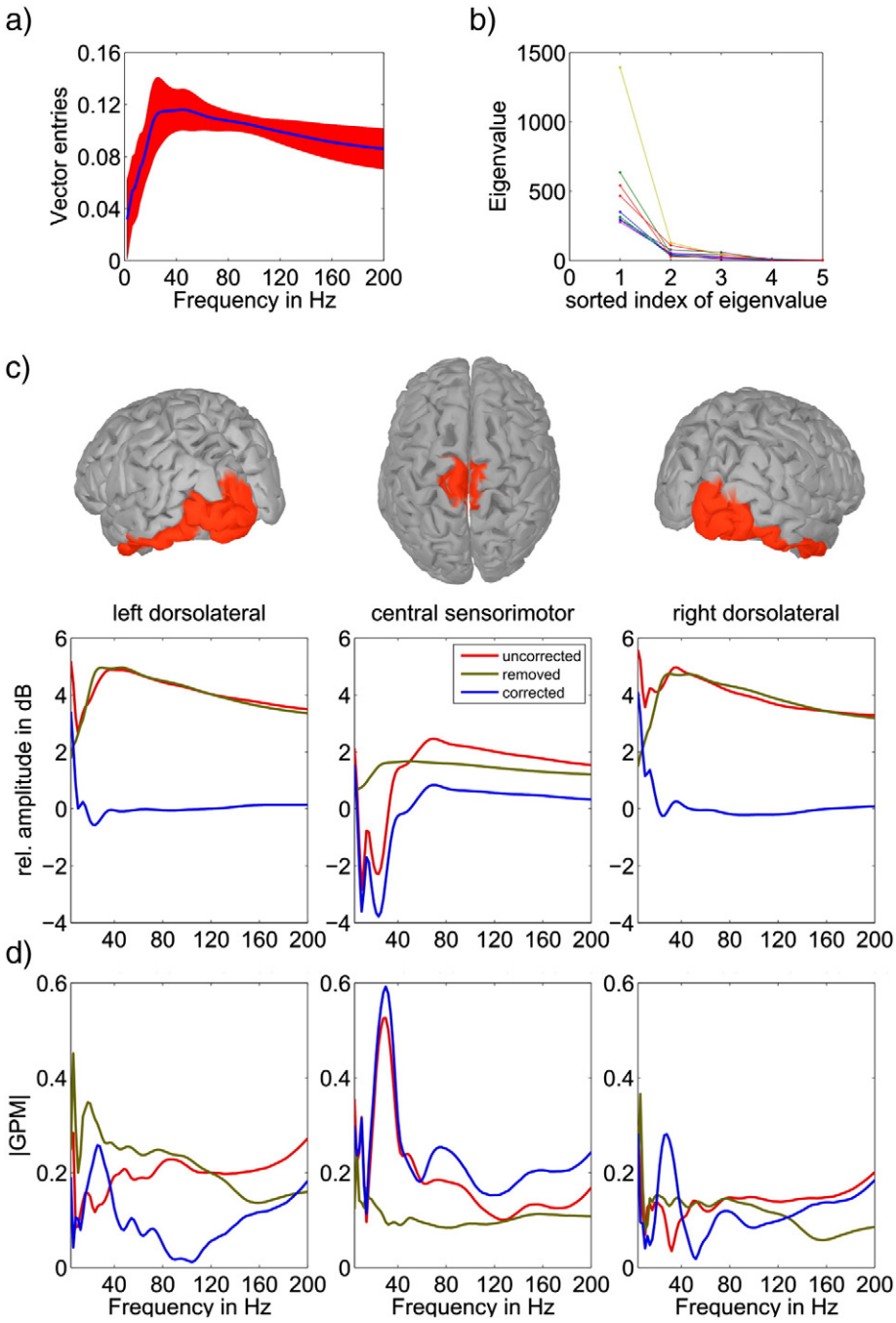

Fig. 2. Characteristics of the artifact correction method. a) First eigenvector entries (subjects' mean ± std) show the spectral profile of this component b) Eigenvalues 1–5 for each subject, where the first (largest) eigenvalue is 5–10 times larger than the second eigenvalue and therefore can robustly be identified. c) Relative amplitude spectra (subjects' mean) during walking in left dorsolateral, central sensorimotor and right dorsolateral areas (ROIs indicated on top). The uncorrected frequency spectra are illustrated in red, the removed component in green and the resulting, corrected spectra in blue. d) Frequency spectra of GPM magnitudes, areas and colors as in c.

central sensorimotor areas at the low γ and high γ 'bump' in the spectrum (Fig. 2d).

High γ amplitudes during walking

High γ (60–80 Hz) amplitudes were increased during walking relative to standing. Significant high γ amplitude increase was located to central sensorimotor areas (Figs. 3, S2). Furthermore, high γ (70–90 Hz) amplitudes were significantly modulated in relation to the gait cycle. Interestingly, the spectral peaks of the high γ amplitude increase (70 Hz) and the carrier frequency (76 Hz) of the high γ modulation do not match (Figs. 3, S2). We also reanalyzed earlier findings showing significant μ (Fig. S3) and β suppression as well as low γ GPM in central sensorimotor areas (Figs. 3, S2).

TF results are illustrated in twofold fashion with different references. First, the TF plot in the right panel of Fig. 3 shows amplitudes during walking relative to standing. Amplitudes during *standing* were averaged over time and used as reference in this TF plot. The frequency spectrum in the right panel of Fig. 3 shows the temporal mean of this TF plot. That is the spectral profile of relative amplitude differences between walking and standing. Second, the TF plot in the left panel of Fig. 3 shows amplitudes during walking relative to the mean amplitudes during walking. Here, amplitudes during *walking* were averaged over time and used as reference. The spectrum in the left panel of Fig. 3 shows the spectral

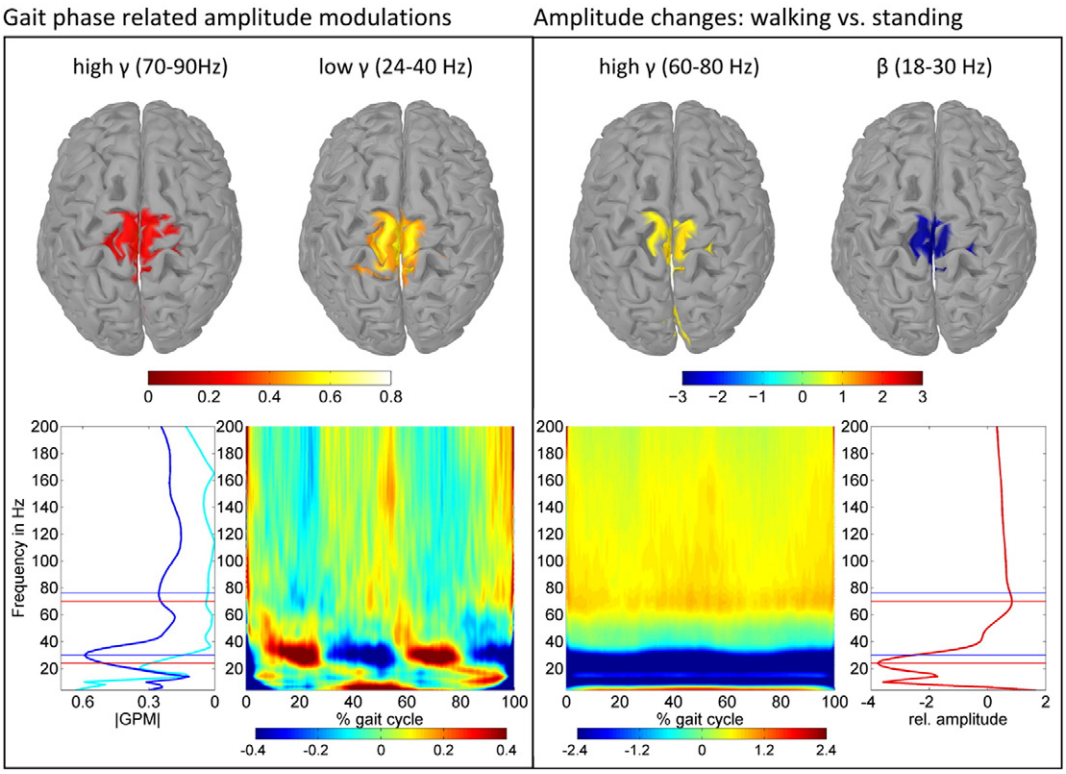

Fig. 3. Left panel: Gait phase related amplitude modulations (GPM). EEG source images show significant high γ and low γ GPM (grand average) located focally in central sensorimotor areas. The temporal modulation of high γ and low γ amplitudes in the gait cycle is illustrated in the TF plot (reference: walking) below. The spectrum of GPM magnitudes (walking in blue, standing in cyan) indicates amplitude modulation in relation to the gait cycle as a function of frequency. Right panel: Relative amplitude changes between walking and standing. Significant high γ increase and β decrease (grand average) occurred in central sensorimotor areas. The sustained high γ increase and μ and β decrease during the gait cycle is shown in the TF plot (reference: standing). The temporal mean of the relative amplitude changes (walking vs. standing) are illustrated as frequency spectrum (red). Spectra and TF plots were calculated in the central sensorimotor ROI, all amplitude changes in dB. Spectral peaks of high γ (76 Hz) and low γ (30 Hz) GPM are marked with blue lines, while the spectral peaks of high γ increase (70 Hz) and β decrease (24 Hz) are marked with red lines.

profile of the GPM magnitude, which quantifies the amplitude modulation in relation to the gait cycle.

High γ and low γ amplitudes are conversely modulated during walking

High γ (70–90 Hz) and low γ (24–40 Hz) amplitudes were both modulated with the step frequency (Fig. 4a). Notably, high γ and low γ amplitude envelopes are negatively correlated ($\rho = -0.847$, $p = 0.0014$) (Figs. 4b, 3 left TF plot). We also investigated amplitude modulation at different modulation frequencies from the step frequency. As shown in Fig. 4a, high γ and low γ amplitudes are modulated with the step frequency, but not with other modulation frequencies. The cross-frequency amplitude correlation plot in Fig. 4b additionally underpins the negative coupling of high γ and low γ amplitudes. Moreover, it

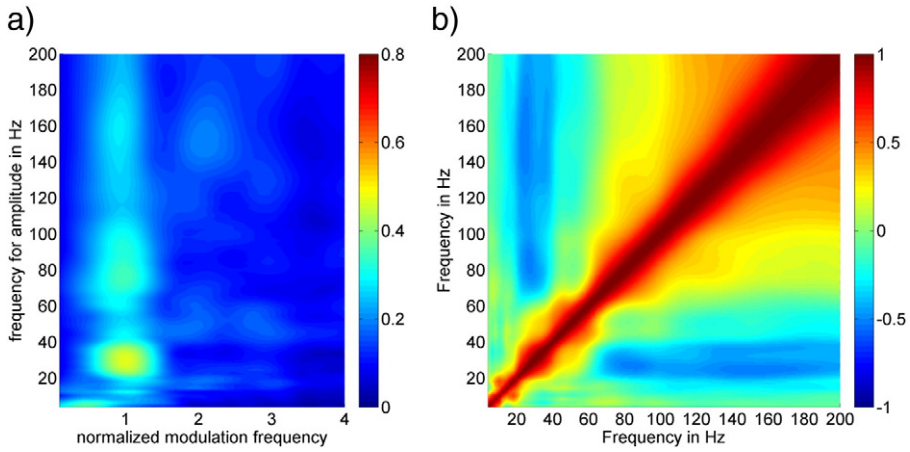

Fig. 4. a) GPM magnitudes as a function of carrier and modulation frequency. High γ (70–90 Hz) and low γ (24–40 Hz) amplitudes are modulated with the step frequency. Modulation frequencies were normalized by the step frequency. b) Cross-frequency amplitude correlation plot (pos./neg. correlation in red/blue) illustrates that high γ and low γ amplitudes are negatively correlated.

provides more general results of the amplitude envelope correlation for various frequencies. Note that the high γ and low γ amplitude correlation is the most prominent one.

Discussion

Muscular artifact correction

The spatial location and the frequency spectrum of the first principal spectral component (Figs. 1a–c) suggest this component to represent muscular artifacts. The first PSC can be robustly identified by its eigenvalue, because its magnitude is 5 to 10 times larger than the eigenvalue of the 2nd PSC in every subject (Fig. 2b). Spatially widespread activity and such with high amplitudes lead to large eigenvalues in our approach. Both criteria are given for muscular activities and therefore explain the dominant first component. Although the first PSC was identified in every subject (Figs. 2a, S2) to reflect artifacts in this work, it is not necessarily given that this is the case for every walking paradigm. More work is needed to generalize this finding on various walking experiments. Hence, it is mandatory to take great care in the selection of components which are omitted during artifact correction.

The reduction of spectral power in dorsolateral areas to approximately baseline levels (Fig. 2c) suggests that the correction method is able to minimize the influence of muscular artifacts during walking. Furthermore, high γ increase at 60–80 Hz was larger in central sensorimotor than in dorsolateral areas (Figs. 2c, 3 right panel). Similarly, gait cycle related amplitude modulation in the high γ range at 70–90 Hz was larger in central sensorimotor than in dorsolateral areas (Figs. 2d, 3 left panel). Because electric potentials decrease monotonically with the distance to its source, these results show the cortical origin of both high γ phenomena that we report in this work.

GPM magnitudes describe the proportion of gait cycle related amplitude modulation to the standard deviation of amplitude envelopes at a given frequency. Therefore, the increase of GPM magnitudes after artifact correction at the low γ and high γ spectral 'bump' in central sensorimotor areas, but its decrease at dorsolateral sites (Fig. 2d) additionally suggests an improved signal to noise ratio of gait cycle related cortical signals to muscular noise.

Taken together, the proposed artifact method was capable of robustly identifying and rejecting patterns, which are likely to represent muscular artifacts.

The first PSC in the present study must not be confused with the first PSC described in Miller et al. (2009, 2014). In these works the spectral decomposition was applied on single ECoG electrodes and the first PSC was used as a marker of asynchronous local population firing.

High γ amplitudes during walking

We report increased high γ (60–80 Hz) amplitudes during walking compared to standing, which were located focally in central sensorimotor areas. The frequency range of high γ increase is in agreement with previous reports of isolated limb movements (Crone et al., 1998; Pfurtscheller et al., 2003; Miller et al., 2007; Cheyne et al., 2008; Ball et al., 2008; Donner et al., 2009; Darvas et al., 2010). The spatial location of high γ increase in central sensorimotor area is consistent with results from studies of isolated foot movements using invasive ECoG (Crone et al., 1998; Miller et al., 2007) and noninvasive MEG (Cheyne et al., 2008) recordings. This localization to central sensorimotor areas is anatomically meaningful considering the foot representation areas in the somatotopic organization of the motor cortex (Jasper and Penfield, 1949). To our knowledge, this is the first study that provides evidence of significantly increased high γ amplitudes located central sensorimotor area during human upright walking. High γ (60–80 Hz) amplitudes were constantly increased during the whole gait cycle (Fig. 3 right panel). Previous studies suggested high γ oscillations to facilitate movements (Brown, 2003) in individuals suffering from Parkinson's disease. Moreover, Joundi et al. (2012) provided first evidence for mechanistic relationship of high γ oscillations and motor performance. The authors reported enhanced motor performance when high γ oscillations are artificially increased using transcranial alternating current stimulation (tACS). Thus, the increase in high γ amplitudes during walking may represent a state of enhanced cortical excitability in central sensorimotor areas which facilitates motor processing.

We also found high γ (70–90 Hz) amplitudes to be modulated in relation to the gait cycle (Fig. 3, left TF plot). Previous studies showed that high γ power envelopes are related to the motor output during repeated finger movements (Miller et al., 2007; Darvas et al., 2010; Muthukumaraswamy, 2010; Hermes et al., 2012b). Our finding that high γ amplitude modulation is related to the motor output is in accord with these studies.

A recent study by Gwin et al., 2011 investigated electrocortical activity during treadmill walking based on ICA. The authors reported that spectral power in wide-range of frequencies including the high γ range are coupled to the gait cycle phase. The corresponding independent components were localized in left/right sensorimotor, posterior parietal and anterior cingulate regions. These results are controversially discussed in Castermans et al., 2014. In our work we directly addressed and corrected for activities occurring in a wide frequency range and at dorsal and lateral cortical sites. The gait phase related amplitude high γ modulation we report here is in contrast to results from Gwin et al., 2011 in many respects. First, high γ gait related amplitude modulation was localized in central sensorimotor areas in our study. Second, we report that high γ and low γ amplitudes are conversely modulated in relation to the gait cycle. Third, because we directly corrected for broad band activities our results showed that high γ modulation was strongest for a limited frequency range between 70 and 90 Hz (GPM spectrum in Fig. 3).

High γ increase and modulation — signatures of different networks?

In this work we report high γ amplitude increase (60–80 Hz) and modulation (70–90 Hz) during walking relative to standing. These phenomena can be separated by their time course (static increase vs. gait phase related modulation) and frequency spectra. A narrow-band peak in the EEG frequency spectrum was proposed to reflect increased synchrony of underlying neuronal populations (Elul, 1972; Singer, 1993; Pfurtscheller and Lopes da Silva, 1999; Buzsáki et al., 2012). Neuronal oscillations arise from frequency-specific neuronal network interactions (Buzsáki and Draguhn, 2004; Donner and Siegel, 2011; Siegel et al., 2012; Womelsdorf et al., 2014). Therefore, EEG amplitude changes at a specific frequency can be interpreted as altered synchrony levels of large neuronal populations in the same frequency-specific neuronal network. Thus, the static increase of high γ amplitudes (60–80 Hz) during walking relative to standing may reflect an altered synchrony state of the associated network. Furthermore, the dynamic, gait phase related amplitude modulations at 70–90 Hz could be a signature of gait phase dependent interactions in another frequency-specific neuronal network.

High γ and low γ amplitudes are conversely modulated during walking

We report high γ (70–90 Hz) low γ (24–40 Hz) amplitudes are both modulated in relation to the gait cycle (Fig. 3, left TF plot), but conversely to each other (Fig. 3 left panel, Fig. 4). This is an interesting finding, since γ oscillations are classically discussed for frequencies >30 Hz. Because of the negative coupling of high and low γ amplitudes it is necessary to distinguish these two modulations in walking experiments. Cross-frequency amplitude envelope correlation was observed previously but its functional role remains unclear (Canolty and Knight, 2010). Unfortunately, we are not able to relate the time course of the amplitude modulations to a particular foot movement for two reasons. First, both feet are simultaneously involved in walking. Second, the

cortical areas representing the left and right foot area are spatially too close to each other to separate them with EEG source localization for now. Thus, we are not able to separate the temporally and spatially summed activity of both feet. Further studies are needed to explain why high γ and low γ amplitudes are negatively correlated during robot-assisted walking.

However, the previously reported prokinetic role of high γ and antikinetic role of β oscillations (reviewed in Brown, 2003; Hutchison et al., 2004; Engel and Fries, 2010; Jenkinson and Brown, 2011) may be relevant. We recently reported that β suppression and low γ modulation are different elements of human walking, which are superimposed in their frequency range and cortical location (Seeber et al., 2014). These results are emphasized in this work. Analogous to these findings we found that spectral peaks of high γ amplitude increase (70 Hz) and modulation (76 Hz) are different (Figs. 3, S2). This suggests that underlying neuronal networks which drive these phenomena are different. In contrast to high γ, enhanced β oscillations in the human motor cortex promote tonic motor sets (Brown, 2003; Joundi et al., 2012).

Basically, the superposition of high γ increase and modulation could be caused by the summation of two independent phenomena in overlapping frequency ranges and cortical areas due to volume conduction. Because these phenomena can be identified by their peak frequency and time course to be different, the key question is whether high γ increase and modulation are functionally coupled at the intersection of their frequency ranges. The same applies to β suppression and low γ modulation.

Notably, tACS enhancement of β oscillations slows voluntary movements (Pogosyan et al., 2009), but enhancement of high γ oscillations facilitate such (Joundi et al., 2012). Thus, total β and high γ amplitude levels seem to play a role in motor performance. The sustained lowered level of β and raised level of high γ amplitudes that we report may both reflect altered states of increased cortical excitability during walking. It would be plausible that gait phase related high γ and low γ amplitudes dynamically modulate these states. From this perspective the negative correlation of high γ and low γ amplitudes we report here (Fig. 3 left panel, Fig. 4) would contribute to causing the modulation of cortical excitability.

Acknowledgments

This work was supported by the European Union research project BETTER (ICT-2009.7.2-247935) (www.car.upm-csic.es/bioingenieria/better/), BioTechMed Graz and the Land Steiermark projects BCI4REHAB (bci.tugraz.at/bci4rehab) and rE(EG)map! (bci.tugraz.at/reegmap). This is the sole opinion of the authors and funding agencies are not liable for any use that may be made of the information contained herein.

Appendix A. Supplementary data

Supplementary data to this article can be found online at http://dx.doi.org/10.1016/j.neuroimage.2015.03.045.

References

Baillet, S., Mosher, J.C., Leahy, R.M., 2001. Electromagnetic brain mapping. IEEE Signal Process. Mag. 18 (6), 14–30.
Ball, T., Demandt, E., Mutschler, I., Neitzel, E., Mehring, C., Vogt, K., Aertsen, A., Schulze-Bonhage, A., 2008. Movement related activity in the high gamma range of the human EEG. Neuroimage 42 (2), 302–310.
Brown, P., 2003. Oscillatory nature of human basal ganglia activity: relationship to the pathophysiology of Parkinson's disease. Mov. Disord. 18 (4), 357–363.
Buzsáki, G., Draguhn, A., 2004. Neuronal oscillations in cortical networks. Science 304, 1926–1929.
Buzsáki, G., Anastassiou, C.A., Koch, C., 2012. The origin of extracellular fields and currents—EEG, ECoG, LFP and spikes. Nat. Rev. Neurosci. 13 (6), 407–420.
Canolty, R.T., Knight, R.T., 2010. The functional role of cross-frequency coupling. Trends Cogn Sci. 14 (11), 506–515.
Castermans, T., Duvinage, M., Cheron, G., Dutoit, T., 2014. About the cortical origin of the low-delta and high-gamma rhythms observed in EEG signals during treadmill walking. Neurosci. Lett. 561, 166–170.
Cheyne, D., Bells, S., Ferrari, P., Gaetz, W., Bostan, A.C., 2008. Self-paced movements induce high-frequency gamma oscillations in primary motor cortex. Neuroimage 42 (1), 332–342.
Crone, N.E., Miglioretti, D.L., Gordon, B., Sieracki, J.M., Wilson, M.T., Uematsu, S., Lesser, R.P., 1998. Functional mapping of human sensorimotor cortex with electrocorticographic spectral analysis. I. Alpha and beta event-related desynchronization. Brain 121 (12), 2271–2299.
Dalal, S.S., Guggisberg, A.G., Edwards, E., Sekihara, K., Findlay, A.M., Canolty, R.T., Berger, M.S., Knight, R.T., Barbaro, N.M., Kirsch, H.E., Nagarajan, S.S., 2008. Five-dimensional neuroimaging: localization of the time–frequency dynamics of cortical activity. 40 (4), 1686–1700.
Dale, A., Fischl, B., Sereno, M.I., 1999. Cortical surface-based analysis. I. Segmentation and surface reconstruction. Neuroimage 9 (2), 179–194.
Darvas, F., Pantazis, D., Kucukaltun-Yildirim, E., Leahy, R.M., 2004. Mapping human brain function with MEG and EEG: methods and validation. Neuroimage 23, 289–299.
Darvas, F., Scherer, R., Ojemann, J.G., Rao, R.P., Miller, K.J., Sorensen, L.B., 2010. High gamma mapping using EEG. Neuroimage 49 (1), 930–938.
De Sanctis, P., Butler, J.S., Malcolm, B.R., Foxe, J.J., 2014. Recalibration of inhibitory control systems during walking-related dual-task interference: a Mobile Brain-Body Imaging (MOBI) study. Neuroimage 94 (1), 55–64.
Donner, T.H., Siegel, M., 2011. A framework for local cortical oscillation patterns. Trends Cogn. Sci. 15 (5), 191–199.
Donner, T.H., Siegel, M., Fries, P., Engel, A.K., 2009. Buildup of choice-predictive activity in human motor cortex during perceptual decision making. Curr. Biol. 19 (18), 1581–1585.
Ehinger, B.V., Fischer, P., Gert, A.L., Kaufhold, L., Weber, F., Pipa, G., König, P., 2014. Kinesthetic and vestibular information modulate alpha activity during spatial navigation: a mobile EEG study. Front. Hum. Neurosci. 8 (71).
Elul, R., 1972. The genesis of the EEG. Int. Rev. Neurobiol. 15, 227–272.
Engel, A.K., Fries, P., 2010. Beta-band oscillations: signalling the status quo? Curr. Opin. Neurobiol. 20, 156–165.
Fischl, B., 2012. FreeSurfer. Neuroimage 62 (2), 774–781.
Fischl, B., Sereno, M.I., Tootell, R.B.H., Dale, A.M., 1999. High-resolution intersubject averaging and a coordinate system for the cortical surface. Hum. Brain Mapp. 8, 272–284.
Gramann, K., Gwin, J.T., Bigdely-Shamlo, N., Ferris, D.P., Makeig, S., 2010. Visual evoked responses during standing and walking. Front. Hum. Neurosci. 4, 202.
Gramfort, A., Papadopoulo, T., Olivi, E., Clerc, M., 2010. OpenMEEG: opensource software for quasistatic bioelectromagnetics. BioMed. Eng. Online 45 (9), 1–20.
Gwin, J.T., Gramann, K., Makeig, S., Ferris, D.P., 2011. Electrocortical activity is coupled to gait cycle phase during treadmill walking. Neuroimage 54 (2), 1289–1296.
Hermes, D., Miller, K.J., Vansteensel, M.J., Aarnoutse, E.J., Leijten, F.S., Ramsey, N.F., 2012a. Neurophysiologic correlates of fMRI in human motor cortex. Hum. Brain Mapp. 33 (7), 1689–1699.
Hermes, D., Siero, J.C., Aarnoutse, E.J., Leijten, F.S., Petridou, N., Ramsey, N.F., 2012b. Dissociation between neuronal activity in sensorimotor cortex and hand movement revealed as a function of movement rate. J. Neurosci. 32 (28), 9736–9744.
Hutchison, W.D., Dostrovsky, J.O., Walters, J.R., Courtemanche, R., Boraud, T., Goldberg, J., Brown, P., 2004. Neuronal oscillations in the basal ganglia and movement disorders: evidence from whole animal and human recordings. J. Neurosci. 24 (42), 9240–9243.
Jasper, H., Penfield, W., 1949. Electrocorticograms in man: effect of voluntary movement upon the electrical activity of the precentral gyrus. Eur. Arch. Psychiatry Clin. Neurol. 183, 163–174.
Jenkinson, N., Brown, P., 2011. New insights into the relationship between dopamine, beta oscillations and motor function. Trends Neurosci. 34 (12), 611–618.
Jolliffe, I., 2002. Principal Component Analysis. Encyclopedia of Statistics in Behavioral Science.
Joundi, R.A., Jenkinson, N., Brittain, J.S., Aziz, T.Z., Brown, P., 2012. Driving oscillatory activity in the human cortex enhances motor performance. Curr. Biol. 22 (5), 403–407.
Kubánek, J., Miller, K.J., Ojemann, J.G., Wolpaw, J.R., Schalk, G., 2009. Decoding flexion of individual fingers using electrocorticographic signals in humans. J. Neural Eng. 6 (6), 1–14.
Kybic, J., Clerc, M., Abboud, T., Faugeras, O., Keriven, R., Papadopoulo, T., 2005. A common formalism for the integral formulations of the forward EEG problem. IEEE Trans. Med. Imaging 24, 12–28.
Lau, T.M., Gwin, J.T., Ferris, D.P., 2014. Walking reduces sensorimotor network connectivity compared to standing. J. Neuroeng. Rehabil. 11 (14).
Maris, E., Oostenveld, R., 2007. Nonparametric statistical testing of EEG and MEG-data. J. Neurosci. Methods 164, 177–190.
Michel, C.M., Murray, M.M., 2012. Towards the utilization of EEG as a brain imaging tool. Neuroimage 61 (2), 371–385.
Michel, C.M., Murray, M.M., Lantz, G., Gonzalez, S., Spinelli, L., Grave de Peralta, R., 2004. EEG source imaging. Clin. Neurophysiol. 115, 2195–2222.
Miller, K.J., Leuthardt, E.C., Schalk, G., Rao, R.P.N., Anderson, N.R., Moran, D.W., Miller, J.W., Ojemann, J.G., 2007. Spectral changes in cortical surface potentials during motor movement. J. Neurosci. 27 (9), 2424–2432.
Miller, K.J., Zanos, S., Fetz, E.E., den Nijs, M., Ojemann, J.G., 2009. Decoupling the cortical power spectrum reveals real-time representation of individual finger movements in humans. J. Neurosci. 29 (10), 3132–3137.
Miller, K.J., Honey, C.J., Hermes, D., Rao, R.P., denNijs, M., Ojemann, J.G., 2014. Broadband changes in the cortical surface potential track activation of functionally diverse neuronal populations. Neuroimage 85 (2), 711–720.
Morlet, J., Arens, G., Fourgenau, E., Glard, D., 1982. Wave propagation and sampling theory—part I: complex signal and scattering in multilayered media. Geophysics 47 (2), 222–236.

Müller-Putz, G.R., Zimmermann, D., Grainmann, B., Nestinger, K., Korisek, G., Pfurtscheller, G., 2007. Event-related beta EEG-changes during passive and attempted foot movements in paraplegic patients. Brain Res. 1137, 84–91.
Muthukumaraswamy, S.D., 2010. Functional properties of human primary motor cortex gamma oscillations. J. Neurophysiol. 104 (5), 2873–2885.
Muthukumaraswamy, S.D., 2013. High-frequency brain activity and muscle artifacts in MEG/EEG: a review and recommendations. Front. Hum. Neurosci. 7 (138).
Nichols, T.E., Holmes, A.P., 2001. Nonparametric permutation tests for functional neuroimaging: a primer with examples. Hum. Brain Mapp. 15, 1–25.
Onton, J., Makeig, S., 2009. High-frequency broadband modulations of electroencephalographic spectra. Front. Hum. Neurosci. 3 (61).
Oostenveld, R., Praamstra, P., 2001. The five percent electrode system for high-resolution EEG and ERP measurements. Clin. Neurophysiol. 112 (4), 713–719.
Pascual-Marqui, R.D., 2002. Standardized low resolution brain electromagnetic tomography (sLORETA): technical details. Methods Find. Exp. Clin. Pharmacol. 24D, 5–12.
Petersen, T.H., Willerslev-Olsen, M., Conway, B.A., Nielsen, J.B., 2012. The motor cortex drives the muscles during walking in human subjects. J. Physiol. 590 (10), 2443–2452.
Pfurtscheller, G., Lopes da Silva, F.H., 1999. Event-related EEG/MEG synchronization and desynchronization: basic principles. Clin. Neurophysiol. 110, 1842–1857.
Pfurtscheller, G., Neuper, C., Andrew, C., Edlinger, G., 1997. Foot and hand area mu rhythms. Int. J. Psychophysiol. 26, 121–135.
Pfurtscheller, G., Graimann, B., Huggins, J.E., Levine, S.P., Schuh, L.A., 2003. Spatiotemporal patterns of beta desynchronization and gamma synchronization in corticographic data during self-paced movement. Clin. Neurophysiol. 114 (7), 1226–1236.
Pogosyan, A., Gaynor, L.D., Eusebio, A., Brown, P., 2009. Boosting cortical activity at beta-band frequencies slows movement in humans. Curr. Biol. 19 (19), 1637–1641.
Presacco, A., Goodman, R., Forrester, L., Contreras-Vidal, J.L., 2011. J. Neurophysiol. 106 (4), 1875–1887.
Scherer, R., Zanos, S.P., Miller, K.J., Rao, R.P., Ojemann, J.G., 2009. Classification of contralateral and ipsilateral finger movements for electrocorticographic brain–computer interfaces. Neurosurg. Focus. 27 (1), E12.
Seeber, M., Scherer, R., Wagner, J., Solis-Escalante, T., Müller-Putz, G.R., 2014. EEG beta suppression and low gamma modulation are different elements of human upright walking. Front. Hum. Neurosci. 8 (485).
Severens, M., Nienhuis, B., Desain, P., Duysens, J., 2012. Feasibility of measuring event related desynchronization with electroencephalography during walking. Conf. Proc. IEEE Eng. Med. Biol. Soc. 2012, 2764–2767.
Siegel, M., Donner, T.H., Engel, A.K., 2012. Spectral fingerprints of large-scale neuronal interactions. Nat. Rev. Neurosci. 13, 121–134.
Singer, W., 1993. Synchronization of cortical activity and its putative role in information processing and learning. Annu. Rev. Physiol. 1993 (55), 349–374.
Tadel, F., Baillet, S., Mosher, J.C., Pantazis, D., Leahy, R.M., 2011. Brainstorm: a user-friendly application for MEG/EEG analysis. Comput. Intell. Neurosci. 2011.
Wagner, J., Solis-Escalante, T., Grieshofer, P., Neuper, C., Müller-Putz, G.R., Scherer, R., 2012. Level of participation in robotic-assisted treadmill walking modulates midline sensorimotor EEG rhythms in able-bodied subjects. Neuroimage 63 (3), 1203–1211.
Wagner, J., Solis-Escalante, T., Scherer, R., Neuper, C., Müller-Putz, G.R., 2014. It's how you get there: walking down a virtual alley activates premotor and parietal areas. Front. Hum. Neurosci. 8 (93).
Womelsdorf, T., Valiante, T.A., Sahin, N.T., Miller, K.J., Tiesinga, P., 2014. Dynamic circuit motifs underlying rhythmic gain control, gating and integration. Nat. Neurosci. 17 (8), 1031–1039.

Behavioral/Cognitive

EEG Oscillations Are Modulated in Different Behavior-Related Networks during Rhythmic Finger Movements

Martin Seeber, Reinhold Scherer, and Gernot R. Müller-Putz
Graz University of Technology, Institute of Neural Engineering, Laboratory of Brain- Computer Interfaces Graz, and BioTechMed-Graz, Graz 8010, Austria

Sequencing and timing of body movements are essential to perform motoric tasks. In this study, we investigate the temporal relation between cortical oscillations and human motor behavior (i.e., rhythmic finger movements). High-density EEG recordings were used for source imaging based on individual anatomy. We separated sustained and movement phase-related EEG source amplitudes based on the actual finger movements recorded by a data glove. Sustained amplitude modulations in the contralateral hand area show decrease for α (10–12 Hz) and β (18–24 Hz), but increase for high γ (60–80 Hz) frequencies during the entire movement period. Additionally, we found movement phase-related amplitudes, which resembled the flexion and extension sequence of the fingers. Especially for faster movement cadences, movement phase-related amplitudes included high β (24–30 Hz) frequencies in prefrontal areas. Interestingly, the spectral profiles and source patterns of movement phase-related amplitudes differed from sustained activities, suggesting that they represent different frequency-specific large-scale networks. First, networks were signified by the sustained element, which statically modulate their synchrony levels during continuous movements. These networks may upregulate neuronal excitability in brain regions specific to the limb, in this study the right hand area. Second, movement phase-related networks, which modulate their synchrony in relation to the movement sequence. We suggest that these frequency-specific networks are associated with distinct functions, including top-down control, sensorimotor prediction, and integration. The separation of different large-scale networks, we applied in this work, improves the interpretation of EEG sources in relation to human motor behavior.

Key words: EEG source imaging; finger movements; large-scale networks; neural oscillations; sensorimotor system; spectral profiles

Significance Statement

EEG recordings provide high temporal resolution suitable to relate cortical oscillations to actual movements. Investigating EEG sources during rhythmic finger movements, we distinguish sustained from movement phase-related amplitude modulations. We separate these two EEG source elements motivated by our previous findings in gait. Here, we found two types of large-scale networks, representing the right fingers in distinction from the time sequence of the movements. These findings suggest that EEG source amplitudes reconstructed in a cortical patch are the superposition of these simultaneously present network activities. Separating these frequency-specific networks is relevant for studying function and possible dysfunction of the cortical sensorimotor system in humans as well as to provide more advanced features for brain-computer interfaces.

Introduction

Generation of motoric actions for interacting appropriately with the environment is one of the key functions of the human brain. Sequencing of our body movements is essential for performing motoric tasks. Significant progress was achieved in studying relationships between brain activity and rhythmic motor behavior in humans (Gerloff et al., 1998; Toma et al., 2002; Pollok et al., 2005; Miller et al., 2009; Houweling et al., 2010; Hermes et al., 2012). Yet, the temporal relation between cortical activities in different brain areas and human motor behavior is not fully understood. In this study, we investigate EEG source oscillations in various brain regions during rhythmic finger movements. Because of the high temporal resolution of EEG source reconstructed signals (Baillet et al., 2001; Michel et al., 2004), it is possible to investigate the temporal relation of cortical activities to movement sequences.

During movements, α and β oscillations are suppressed in sensorimotor areas, but high γ amplitudes are increased compared with a premovement reference period (Pfurtscheller and Aranibar, 1977; Pfurtscheller et al., 1997; Crone et al., 1998a, b; Müller et al., 2003; Miller et al., 2007; Scherer et al., 2009; Hermes

Received May 30, 2016; revised July 28, 2016; accepted Sept. 10, 2016.
Author contributions: M.S., R.S., and G.R.M.-P. designed research; M.S. performed research; M.S. contributed unpublished reagents/analytic tools; M.S. analyzed data; M.S., R.S., and G.R.M.-P. wrote the paper.
This work was supported by the Land Steiermark project rE(EG)map! and BioTechMed Graz.
The authors declare no competing financial interests.
Correspondence should be addressed to either Dr. Martin Seeber or Dr. Gernot R. Müller Putz, Graz University of Technology, Stremayrgasse 16, Graz 8010, Austria. E-mail: seeber@tugraz.at or gernot.mueller@tugraz.at.
DOI:10.1523/JNEUROSCI.1739-16.2016
 0270-6474/16/3611671-11$15.00/0

et al., 2012). These relative amplitude decreases and increases were suggested to represent altered synchrony states (event-related (de)synchronization [ERD/ERS]) of underlying neuronal populations (for review, see Pfurtscheller and Lopes da Silva, 1999; Neuper and Pfurtscheller, 2001). Especially, β oscillations were discussed to play a prominent role in motor function (for review, see Engel and Fries, 2010; Jenkinson and Brown, 2011). For faster movement rates, β ERD becomes stronger (Houweling et al., 2010; Yuan et al., 2010), and its amplitude does not return to premovement levels anymore during finger tapping (Yuan et al., 2010; Hermes et al., 2012). Additionally, β amplitudes were found to decrease prior movement onset and increase afterward, forming a comodulated pattern with the time sequence of rhythmic finger movements (Toma et al., 2002; Houweling et al., 2010). In sensorimotor regions, β ERD was suggested to represent an increased excitability state of neuronal populations, whereas β ERS was interpreted as active inhibition of neuronal circuitry (for review, see Neuper and Pfurtscheller, 2001). In contrast to β oscillations, high γ amplitudes increase prior movement onsets, and its time course resembles the movement sequence during finger tapping (Miller et al., 2009; Hermes et al., 2012).

In recent walking experiments of our group (Wagner et al., 2012, 2014; Seeber et al., 2014, 2015), we report two different EEG source elements. First, sustained β ERD along with high γ increase, which are present during the entire gait cycle. We interpreted this pattern as altered synchrony states in respective central sensorimotor networks. Second, we found gait cycle-related amplitude modulations in the high β/low γ and high γ frequency range, which were conversely modulated to each other. Interestingly, the spectral profiles of sustained ERD/ERS did not match those of gait cycle-related amplitude modulations (Seeber et al., 2014, 2015). Different spectral profiles were suggested to represent different large-scale neuronal network interactions (Donner et al., 2011; Siegel et al., 2012). Therefore, we hypothesize that, during continuous rhythmic movements, one type of large-scale networks (up)regulate the neuronal excitability state in specific cortical regions, but other networks represent the temporal structure of the movement sequence. In this work, we test this viewpoint for rhythmic finger movements to derive principles, which may unify findings from both extremities. In contrast to foot movements, the fingers are represented laterally in the somatotopic arrangement of the motor cortex (Jasper and Penfield, 1949). Because of the low spatial resolution of the EEG, it was not possible to unambiguously separate supplementary motor area (SMA) from central motor areas in the walking studies. Because of the lateral representation of the fingers, we further hypothesize in this work that sustained ERD/ERS and movement phase-related sources are different in both respect, their spectral profile, and, additionally, in their spatial patterns during rhythmic finger movements.

Materials and Methods

Experiment and recordings. We recorded EEG from 18 right-handed healthy volunteers (24 ± 4 years, 9 female) during rhythmic right finger movements. Each participant gave informed consent to the study, which was performed in accordance to the Declaration of Helsinki. During the experiments, subjects were seated in a comfortable chair in an electrical shielded room with their right hand supinated on an armrest. A blue dot was shown in the center of a computer screen and was blinking three times, indicating either 0.67 or 1.5 Hz finger movement cadences (see Fig. 1*a*). Participants were asked to rhythmically open and close their right hand continuously, imitating the previously displayed blinking cadence of the dot. Subjects initiated their movements after the dot stopped blinking. Importantly, no external stimuli were present during the movement period. Because we aimed to study the cortical motor system, we minimized the impact from other sensory modalities. A movement trial ended when the dot disappeared from screen. In total, one trial lasted 13 s and was followed by a 1–2 s random break with a black screen. Ninety trials were completed for both movement cadences, respectively. Participants were asked to fixate the dot with their eyes, not to count during the movements and avoid any additional movement as good as possible. At the beginning of each trial, a red arrow was additionally displayed. It was pointing down to indicate finger movements without the thumb or pointing toward left for thumb movements only. The movement experiment was recorded in three blocks. Before and after each movement block, we recorded EEG during a resting period lasting 3 min each. During the resting period, the blue dot was constantly shown on the screen for gaze fixation. We pooled finger and thumb movement data for each tapping cadence because we investigate temporal patterns of movement sequences in this work, not which fingers were moved.

EEG was recorded combining five 16 channel amplifiers (g.USBamp, g.tec) sampled to 512 Hz and bandpass filtered between 0.1 Hz and 200 Hz. A notch filter was set to suppress 50 Hz line noise. Passive Ag/AgCl electrodes were mounted at selected 72 positions (see Fig. 1*d*) of the 5% international 10/20 EEG system (Oostenveld and Praamstra, 2001). Reference and ground electrodes were placed on the left and right mastoid, respectively. Electrode impedances were kept $<5\ \mathrm{k}\Omega$. Electrode positions were measured using a 3D localizer (Elpos, Zebris). Finger movements were digitalized using a data glove (5DT Data Glove 14 Utra, 5DT). Structural MRI T1 scans (TE = 2.07 ms, TR = 1560 ms, voxel size = 1 × 1 × 1 mm, 3 tesla Skyra, Siemens) were acquired in a post-screening session for each individual brain.

EEG preprocessing. EEG was visually inspected for prominent artifacts, and related time intervals were excluded from further analysis (94.1% were kept). Subsequent independent component analysis (ICA) (Hyvärinen, 1999) (FastICA, https://research.ics.aalto.fi/ica/fastica/) was used to identify noncortical components. Artifact stereotypical ICs were selected based on their time course, power spectra, and topographies and were rejected ranging from 3 to 7 ICs per subject. After ICA correction, signal periods exceeding amplitudes of $\pm 200\ \mu\mathrm{V}$ were detected and ignored for subsequent analysis. Considering the previously excluded time periods, 88.3% of the raw data points remained in total for further analysis. Subsequently, EEG recordings were rereferenced to common average reference.

EEG source imaging. EEG source imaging (Baillet et al., 2001; Darvas et al., 2004; Michel et al., 2004; Michel and Murray, 2012) was applied based on realistic head models using individual MRI scans. To describe the propagation of electrical fields from the cortical surface to the scalp, a forward model was formulated as boundary element model (BEM) for each subject using OpenMEEG (Kybic et al., 2005; Gramfort et al., 2010). The BEM consisted of four surface layers (brain, inner skull, outer skull, head surface), which were reconstructed from individual T1 MRI scans. Cortical reconstruction and volumetric segmentation were performed with the FreeSurfer image analysis suite (Dale et al., 1999; Fischl, 2012) (http://surfer.nmr.mgh.harvard.edu/). BEM and electrode positions were coregistered, matching four anatomical landmarks (nasion, vertex, left and right preauricular points). EEG sources were modeled perpendicular to individual gray matter surfaces and consisted of 5000 vertices. Resting EEG periods were used to calculate the noise covariance matrix for whitening the lead field matrix. For solving the inverse problem, sLORETA (Pascual-Marqui, 2002) implemented in the Brainstorm toolbox (Tadel et al., 2011) (http://neuroimage.usc.edu/brainstorm) was applied. sLORETA is a standardized variant of the minimum norm inverse solution (Hämäläinen and Ilmoniemi, 1994). To prevent overfitting, no EEG data of the movement trials and no frequency-specific information was used to calculate the inverse Kernel.

EEG source amplitude envelope (AE) analysis and glove data alignment. AEs were computed in the EEG source space using complex Morlet wavelet (Morlet et al., 1982) for time-frequency (TF) decomposition (2–100 Hz, 2 Hz steps). Parameters for the mother wavelet were set to FWHM of 3 s for the Gaussian kernel at a center frequency of 1 Hz.

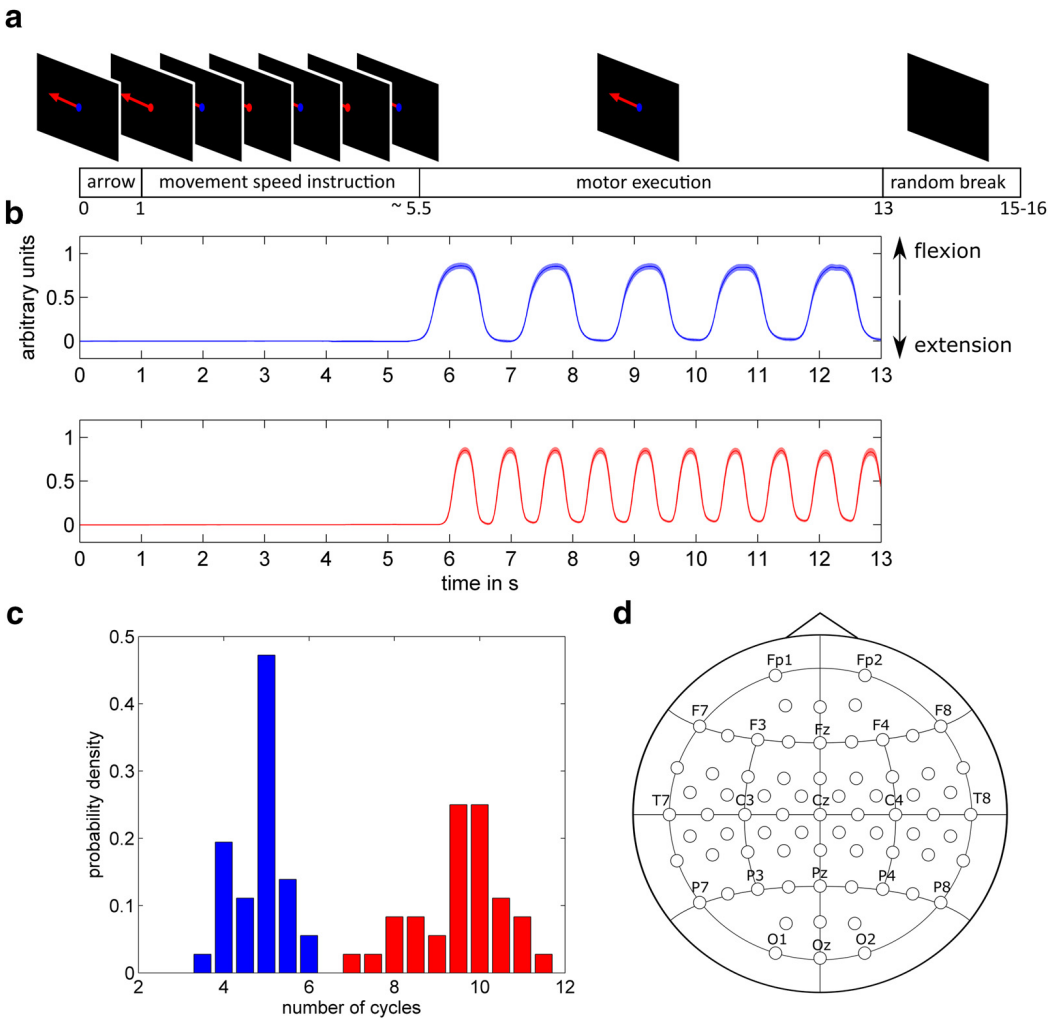

Figure 1. Task, behavior, and EEG montage. ***a***, Time line of the movement task instruction displayed on the computer screen. ***b***, Glove data (mean ± SEM) after alignment of trials for the slow (blue) and fast (red) tapping cadence. ***c***, Histogram of performed movement cycles. ***d***, EEG montage. Circles represent electrodes.

Magnitudes of TF decomposed signals were calculated to obtain EEG source amplitude envelopes.

Glove data were used to align and warp the EEG source AE. The first principal component (Jolliffe, 2002) of the glove sensors was calculated to get a single curve describing the finger movements. Movement cycles were quantized in quarters, which were determined by the turning points and zeniths of this movement curve for each trial. Subsequently, the glove data were stretched and bended to match these sampling points and the average movement cycle quantity for all trials of the two different movement cadences, respectively. The glove data were equally used to realign and time warp the EEG source AE on a single-trial basis.

EEG source amplitudes were normalized relative to a nonmovement reference period (second 2–4 of the trial) in decibels (dB) for each subject. To improve signal quality for higher frequencies (>30 Hz), we suppressed broadband source space activity, which we consider to reflect electromuscular activity during movement tasks, using a spectral decomposition approach (Seeber et al., 2015). These AEs then were low and high pass filtered at 0.3 Hz, respectively, to separate sustained and dynamic AEs (see Fig. 2). This frequency is a trade-off between capturing sustained effects precisely without affecting modulations in the movement frequency range. Sustained AE in our analysis corresponds to sustained ERD/ERS (Pfurtscheller and Lopes da Silva, 1999) measures using a logarithmic scale in dB. To assess movement phase-related amplitudes (MPAs), we investigated the dynamic AE in relation to the movement cycle phase from the glove data. To do so, we quantized the movement cycle phase into 4° ($\pi/45$) steps. TF source amplitude values were averaged for each phase step to determine amplitude curves as function of the phase in the movement cycle. To quantify this relationship, we computed the modulation (analytical) amplitude of the resulting MPA curves using Hilbert transform.

These calculations were processed for every source vertex and analyzed frequency resulting in source images for both, sustained and MPA.

In this work, we present time courses, frequency spectra, and TF plots in a left and right ROI. These ROIs were determined based on the centers of the well-known β (18–24 Hz) ERD patterns and were subsequently normalized to the same spatial size. Frequency ranges for the topographical analysis were chosen based on peaks in the frequency spectra. We also investigated amplitude comodulation between cortical areas using the ROIs as seed regions. Amplitude comodulation was investigated because it was previously shown to reveal similar connectivity patterns as fMRI networks (Brookes et al., 2011; Engel et at., 2013). To ignore volume conduction effects, we computed the imaginary part of coherence (Nolte et al., 2004) between AEs.

Group analyses were enabled by aligning and projecting individual cortices to match the ICBM 152 surface (Fischl et al., 1999; Tadel et al., 2011). Significant clusters in EEG source images were determined and corrected for multiple comparisons using nonparametric permutation tests (Nichols and Holmes, 2002; Maris and Oostenveld, 2007). In detail, EEG source amplitudes of randomly selected halves (9 of 18) subjects were sign flipped and averaged to obtain a random distribution. We performed 10^4 permutations for each source topography. From these analysis, we applied a primary threshold of $p = 1e\text{-}3$ for the ERD/ERS and MPA images, except for high γ MPA images. For these images, $p = 0.01$ was used due to the lower signal-to-noise ratio for higher frequencies.

After applying the primary thresholds, the resulting clusters were compared with maximum clusters sizes from again 10^4 permutations. We chose the same significance levels as described above for these cluster-level statistics. Significant amplitude comodulations were determined using the same procedure for the AE coherence.

Results

Behavioral data

Glove data showed that subjects performed 5 and 9.75 movement cycles on average for the slow and fast movement cadence, respectively (Fig. 1*b*,*c*). These data also show that the aligning and warping procedure was successful due to the small standard error of the mean (SEM). Considering the movement duration, the performed movement cadences were 0.66 and 1.37 Hz. The visual instruction (i.e., dot blinking frequency) were 0.67 Hz and 1.5 Hz, so the movement frequency for the faster movement was not exactly as instructed. However, the histogram of performed movements shows two clear, nonoverlapping groups for the slow and fast cadence (Fig. 1*c*).

Sustained and movement phase-related AE

We separated source AE in two elements: a sustained and a dynamic one. The latter, we hypothesized to represent the movement phases. These two elements are significantly present in sensorimotor areas for both movement cadences (Figs. 2, 3*b–d*, 4*b–d*). First, for the sustained AE element, amplitudes decrease in the α (10–12 Hz) and β1 (18–24 Hz), but increase in the high γ (60–80 Hz) frequency range during movements. This amplitude de/increase starts 2.5 s and 2.6 s before the slow and fast movement, respectively, peaks at its onset, and remains at a sustained level during the entire movement duration (Figs. 2, 3*c*, 4*c*). Second, the dynamic AE element shows a clear relationship to the movement phase in the β1 (18–24 Hz) and β2 (24–30 Hz) frequency range and resembled the glove data (Figs. 2, 3*b*,*f*, 4*b*,*f*). Movement phase-related β2 amplitudes peak at the start of a movement cycle (phase: −3.00 rad and −2.93 rad) and are lowest preceding maximal finger flexion at −0.97 rad and −0.63 rad during slow and fast movement cadences, respectively. For the slow movement cadence, a second peak is present at 0.70 rad (Figs. 3*f*, 4*f*). We also found that AE of different frequencies showed a similar temporal structure locked to the movement cycle but shifted to each other. β2 precedes α amplitudes in the movement cycle. This delay was tested for significance ($\chi^2_{(1,17)} = 21.33$, $p = 3.9\text{e-}6$) using a Friedman's test with factors frequency range ($n = 2$) and experimental condition ($n = 2$) in the right ROI, where β2 and α MPA spatially overlap. Further, β2 amplitudes are conversely modulated to high γ amplitudes in a movement cycle. These amplitudes are negatively correlated to each other for slow (permutation test, $r = -0.90$, $p = 1\text{e-}4$) and fast movements (permutation test, $r = -0.78$, $p = 2\text{e-}4$).

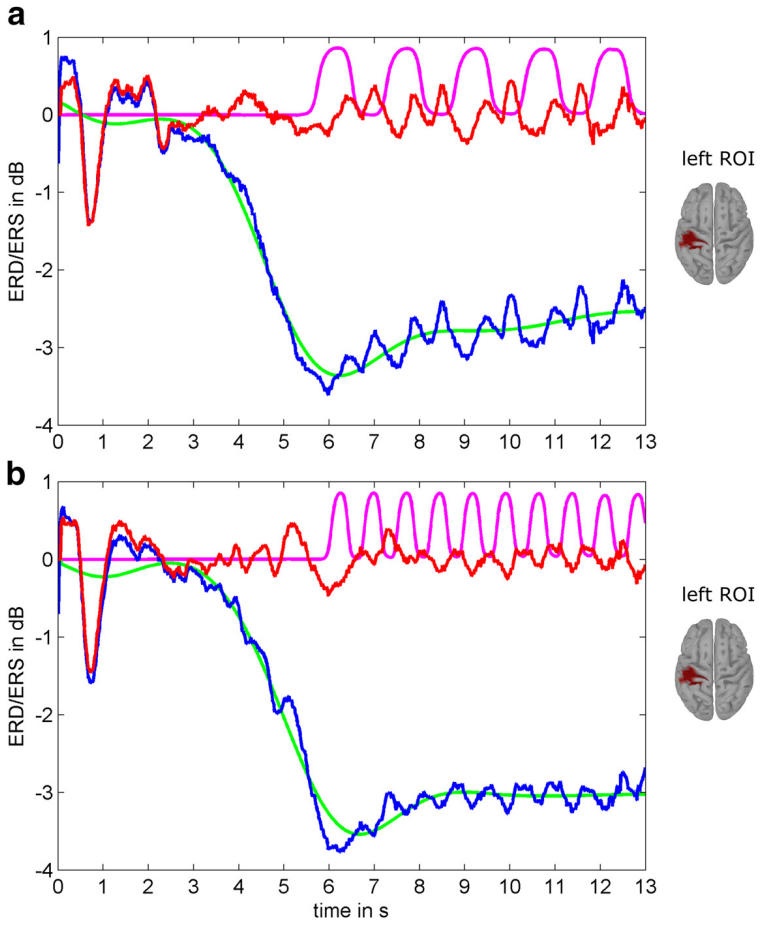

Figure 2. Separating sustained from dynamic AE. ***a***, Amplitude time course for β1 (18–24 Hz) frequencies during the slow movement cadence (0.66 Hz) in the left ROI. Blue represents original AE. Green represents low pass filtered "sustained AE." Red represents high pass filtered "dynamic AE." Magenta represents glove data, shown for comparison with dynamic AE, which are related to the movement phase. ***b***, Same illustration as in ***a***, but for faster movement (1.37 Hz).

Interestingly, the MPA frequency spectra does not fully match with the spectra of sustained amplitude decreases/increases. Spectral β peaks for the sustained decrease are at 20 Hz for both movement cadences. MPAs are additionally present in the β2 frequency range, especially for the faster movement cadences (Figs. 3*g*, 4*g*). Selecting these specific frequency ranges, we further analyzed the spatial patterns of both modalities.

EEG source images

The sources of the sustained AE element (Figs. 5*a*, 6*a*) show a well-known left hemisphere lateralized pattern in the right hand representation area of the sensorimotor cortex for β1 desynchronization and high γ increase. Apart from this contralateral hand area, we also located significant clusters in the homologous right sensorimotor area and paracentral regions for these frequency ranges. Sustained α amplitudes decrease less specific in bilateral sensorimotor areas. Friedman's test with factors frequency range ($n = 2$) and experimental condition ($n = 2$) determined a higher lateralization for β1 compared with α desynchronization ($\chi^2_{(1,17)} = 8.53$, $p = 0.0035$). Comparing fast with slow movement cadences, sustained β1 ERD in the left cluster is significantly stronger during fast movements (Wilcoxon signed rank, $p = 0.0073$). No significant difference in β1 lateralization (Wilcoxon signed rank, $p = 0.71$) was found.

In contrast to the well-known ERD/ERS patterns during movement, MPA sources revealed different sources (Figs. 5, 6).

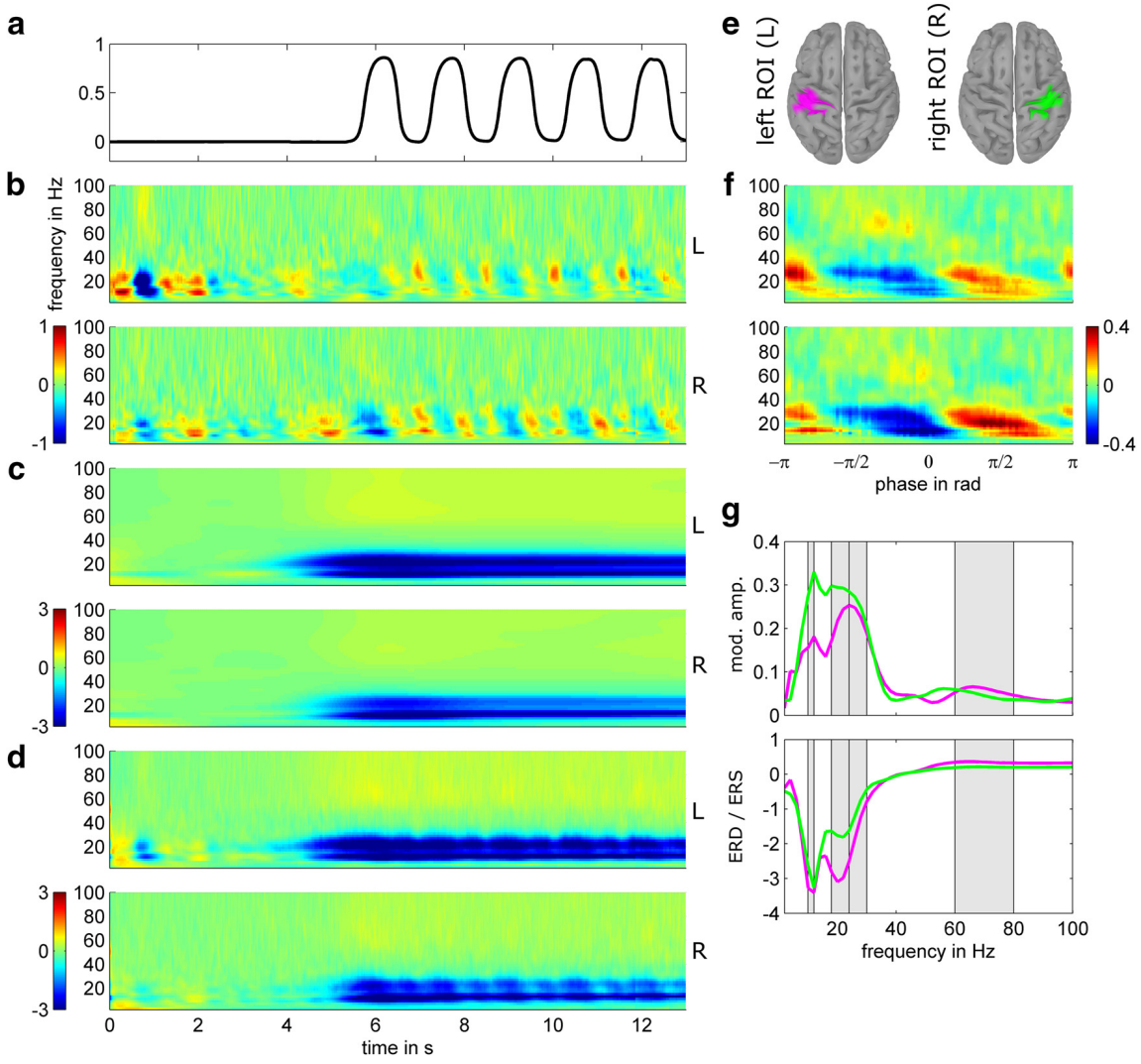

Figure 3. Dynamic and sustained AE in the right and left ROI during the slow movement cadence. ***a***, Glove data. ***b–d***, TF plot of dynamic (high pass filtered), sustained (low pass filtered), and original (unfiltered) source AE. ***e***, Right and left ROI. ***f***, Relation of dynamic AE to the movement phase, centered (0 rad) at peak displacement of the fingers. ***g***, Frequency spectra for sustained (bottom) and MPA (top) for the left/right ROI in magenta/green. Selected frequency ranges marked in gray shaded regions. Amplitudes in dB.

Because of the different spectral profiles we found in the sensorimotor regions, we pooled β frequencies to compare the spatial patterns of both modalities in terms of lateralization. Friedman's test with factors modality (sustained ERD/ERS and MPA, $n = 2$) and experimental condition ($n = 2$) identified different lateralization for β frequencies ($\chi^2_{(1,17)} = 22.53$, $p = 2.1\text{e-}6$). β MPA sources were localized to bilateral sensorimotor and paracentral regions. These activities are significantly lower (Wilcoxon signed rank, $p = 2\text{e-}4$) during fast compared with slow movements. For the faster movement cadence, we additionally found MPA located in the right prefrontal cortex at $\beta 2$ frequencies (Fig. 6*b*). High γ MPA sources were localized to the contralateral hand area and left paracentral region during slow movements. For fast movements, the paracentral cluster exclusively reached significance. α MPA sources showed a widespread pattern, which was strongest in right sensorimotor areas, but also covered bilateral superior parietal and paracentral regions (Figs. 5, 6).

Amplitude comodulation between cortical areas

We also observed well-pronounced amplitude modulations during the visual instruction strongest for α frequencies in the left ROI (Figs. 3*b*, 4*b*). In this time interval, of course, there was no movement executed. To further investigate this modulation, we computed amplitude comodulation between the left ROI (seed region) to every other site of the cortex using α as carrier frequency. This analysis showed significant comodulation in visual areas for both movement conditions, which precede the left seed region (Fig. 7, left).

Furthermore, we focused on the analysis of $\beta 2$ MPA in the right ROI to test for significant comodulation with other cortical sites. During slow movements, subcortical areas are significantly comodulated with the right seed region and precedes in the movement cycle. For the fast cadence, prefrontal areas are significantly comodulated and are leading the right sensorimotor seed cluster (Fig. 7, right).

To provide further information about the temporal relation of $\beta 2$ MPA sources in different cortical areas, we rendered videos for both movement cadences showing $\beta 2$ amplitudes in dependence of the movement cycle phase (Movies 1, 2). During slow movements, we observe two peaks during a movement cycle. The first peak occurs at the movement cycle onset at $-\pi/\pi$ and shows a pattern in bilaterally in sensorimotor hand areas. Subsequently, $\beta 2$ amplitudes decrease, reaching its minimum preceding the maximal displacement of the fingers (at 0 rad). Then a second

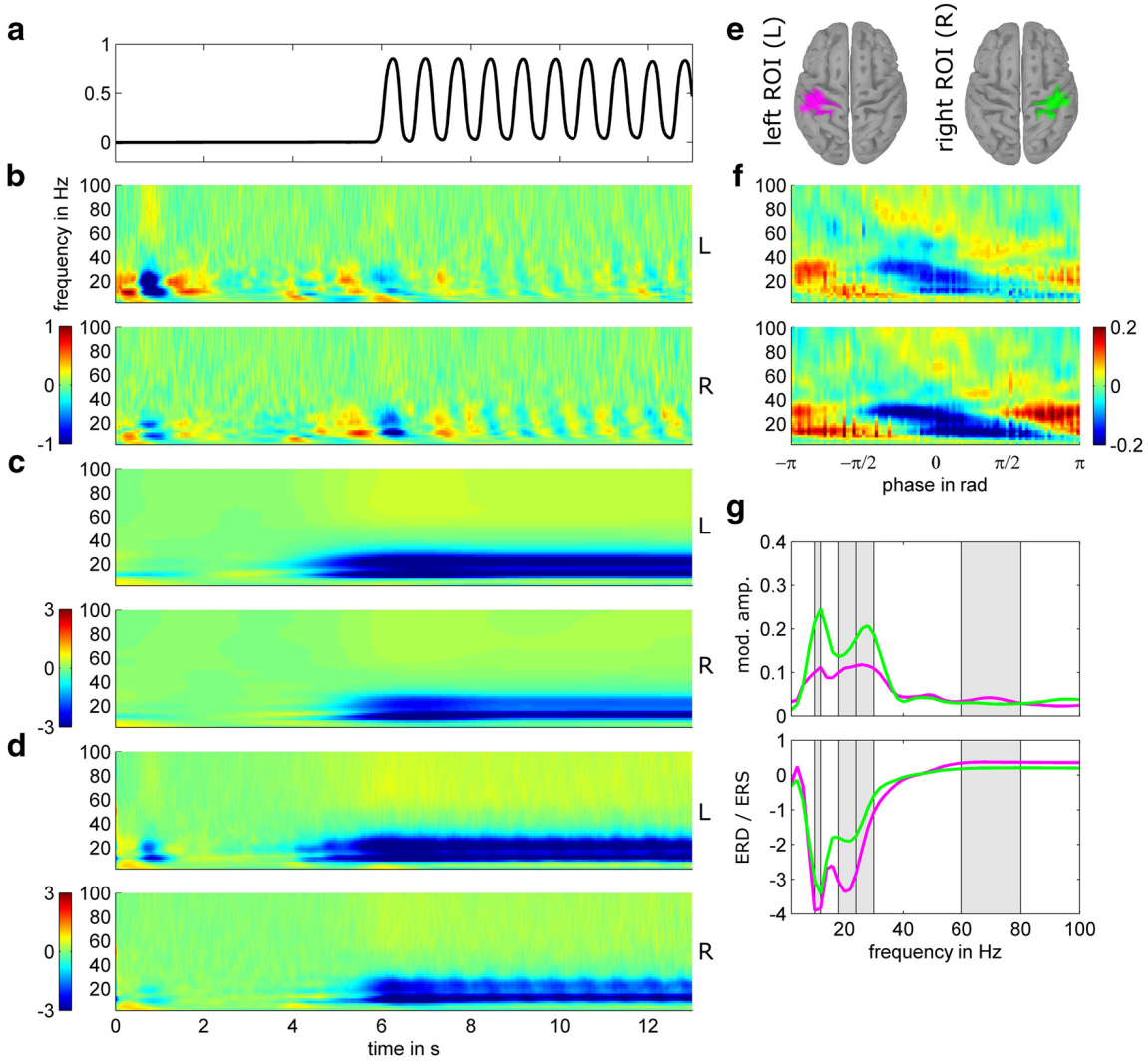

Figure 4. Dynamic and sustained AE in the right and left ROI during the fast movement cadence. ***a***, Glove data. ***b–d***, TF plot of dynamic (high pass filtered), sustained (low pass filtered), and original (unfiltered) source AE. ***e***, Right and left ROI. ***f***, Relation of dynamic AE to the movement phase, centered (0 rad) at peak displacement of the fingers. ***g***, Frequency spectra for sustained (bottom) and MPA (top) for the left/right ROI in magenta/green. Selected frequency ranges marked in gray shaded regions. Amplitudes in dB.

peak evolves, which is, compared with the first peak, rather associated with superior sensorimotor and central regions. During the fast movement cadence, the temporal sequence of $\beta 2$ amplitudes shares two characteristics with the slow movement cadence: that is, (1) the peak at the movement cycle onset, and (2) the $\beta 2$ minimum before the finger displacement maximum. Additionally, amplitudes in prefrontal areas are modulated in relation to the movement cycle. These prefrontal modulations show a different phase relation to the movement cycle, preceding amplitude envelopes in sensorimotor regions. In summary, one can observe that amplitudes start decrease and increase in frontal areas, which then spreads toward parietal areas while additional amplitude modulations in the sensorimotor network occur.

Discussion

In this study, we investigated EEG sources during rhythmic finger movements in humans. Analyzing these source we distinguish between sustained (de-)synchronization (ERD/ERS) and MPA modulations. We found that the sources of these two electrocortical elements are different, confirming our hypothesis.

The sustained ERD/ERS element replicated previous works showing α and β desynchronization accompanied with high γ increase in contralateral areas representing right finger movements (Pfurtscheller et al., 1997; Crone et al., 1998b; Miller et al., 2007). Further, the temporal properties of these features, evolving at ~2 s before the movement are also in line with these studies. As well as that, α are less spatially specific than β ERD sources (Crone et al., 1998a). Further, consistent with previous reports, we found sustained β desynchronization (Hermes et al., 2012), which is getting stronger during faster rhythmic movements (Yuan et al., 2010).

α and β desynchronization along with high γ increase may signify a state of enhanced cortical excitability in associated areas, which facilitates motor processing. Previous studies indeed provide evidence for causal relationship of cortical oscillations and motor performance. These studies showed that transcranial alternating current stimulation at β frequencies slows voluntary movements (Pogosyan et al., 2009), but stimulation at high γ facilitates motor processing (Joundi et al., 2012). Consequently, β and high γ oscillations were found to possess opposing roles in the motor cortex, the former to inhibit, the latter to facilitate, dynamic motor actions during its preparation and performance.

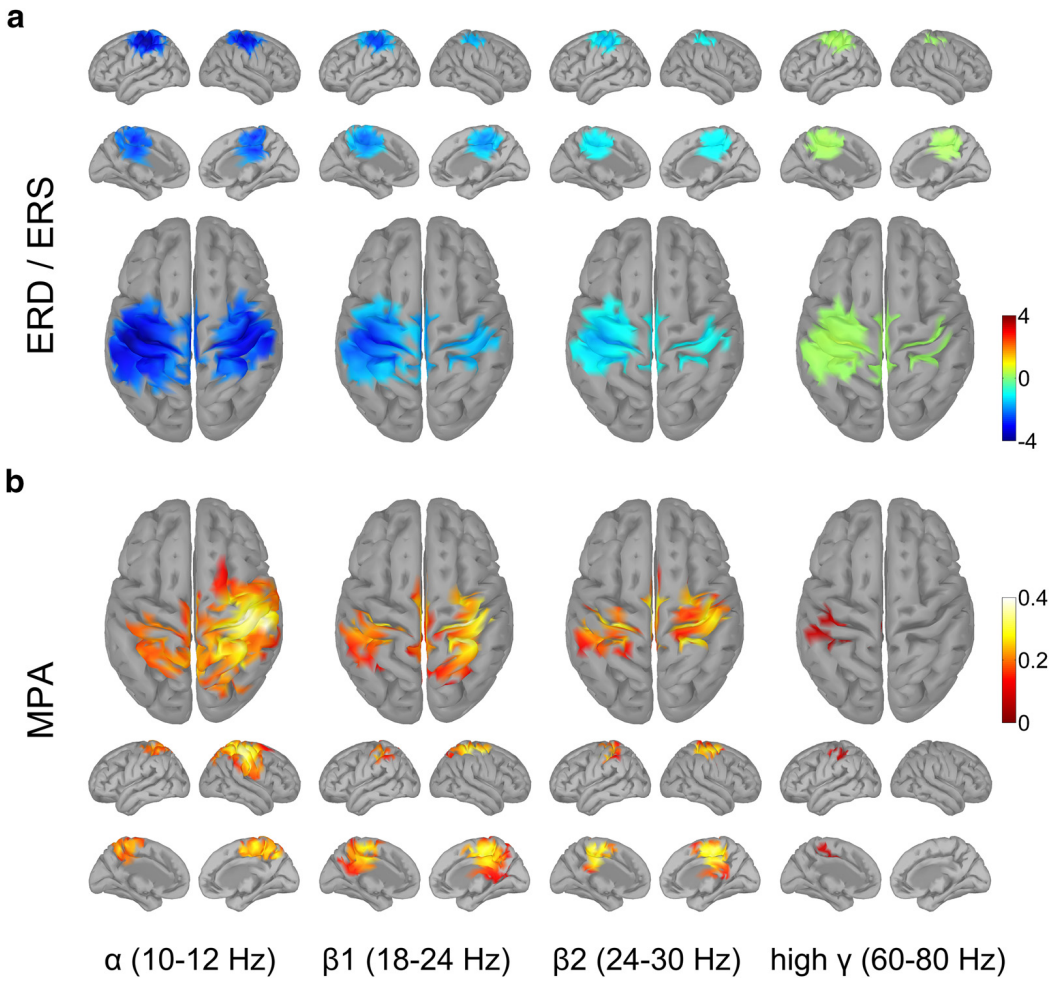

Figure 5. EEG source images of the slow movement cadence in selected frequency ranges (left to right column). ***a***, EEG sources of sustained ERD/ERS during movements are illustrated in blue/yellow-red. ***b***, EEG sources of movement MPAs are illustrated as modulation magnitude in red to white. Amplitudes in dB.

We found the MPA sources to be different from the well-known ERD/ERS patterns during movement. EEG source imaging revealed different spatial patterns for these two elements (Figs. 5, 6). Further, the spectral profiles we investigated in left and right sensorimotor areas did not match. For instance, we found different β peaks for the sustained ERD and MPA feature. Narrow-band peaks in the EEG frequency spectra reflect the summation of neuronal oscillations on a larger spatial scale. Neuronal oscillations mediate synchrony in neuronal populations forming frequency-specific networks (Buzsáki, 2006; Siegel et al., 2012). Because of spatiotemporal integration inherent in large-scale recordings as EEG, the amplitudes of these signals are markers of underlying network synchrony (Elul, 1971; Pfurtscheller and Lopes da Silva, 1999; Donner et al., 2011; Buzsáki et al., 2012). Amplitude modulation at a certain frequency, therefore, is a signature of modulated synchrony in a frequency-specific neuronal network. Based on this, we interpret sustained ERD/ERS and MPA to represent two different types of large-scale networks, due to the different spectral profiles and spatial patterns we report in this study.

First, networks represented by sustained ERD/ERS, which statically modulate their synchrony level during continuous movements. These patterns may upregulate neuronal excitability during motor preparation and performance specific to the limb, in this work the right hand area.

Second, MPAs are generated by other frequency-specific networks, which dynamically adapts their synchrony levels dependent on the phase in a movement cycle. Therefore, these networks provide information about the movement sequence timing. We found MPAs are well pronounced at β frequencies in sensorimotor regions and SMA. This spatial pattern resembles the sensorimotor resting state network (Raichle, 2010). Notably, β MPAs are significantly stronger during slow compared with fast movements, which was also reported previously (Toma et al., 2002; Houweling et al., 2010; Hermes et al., 2012). These studies further described β amplitude modulations associated with different movements to merge at faster movements ($\geq$2 Hz). We did not find this phenomenon probably because of the comparably lower movement cadences we studied. To build up neural synchrony, increasing time is needed for larger cortical populations (Buzsáki, 2006). This relationship could explain the larger MPA during the slower movement cadences, where longer time periods are available in movement cycle to build up synchronized networks.

Movement phase-related β synchrony peaked at the start of a movement cycle, that is, at the initial position of the fingers, and it was diminished preceding the maximal fingers flexion (Fig. 4*f*). Because of the bilateral sensorimotor regions we found for β MPA, it would be plausible that they also mediate sensorimotor processing between the hemispheres. The time course of β modulation in the motor system was previously reported to be associated with predictive timing of upcoming external rhythmic visual (Saleh et al., 2010)

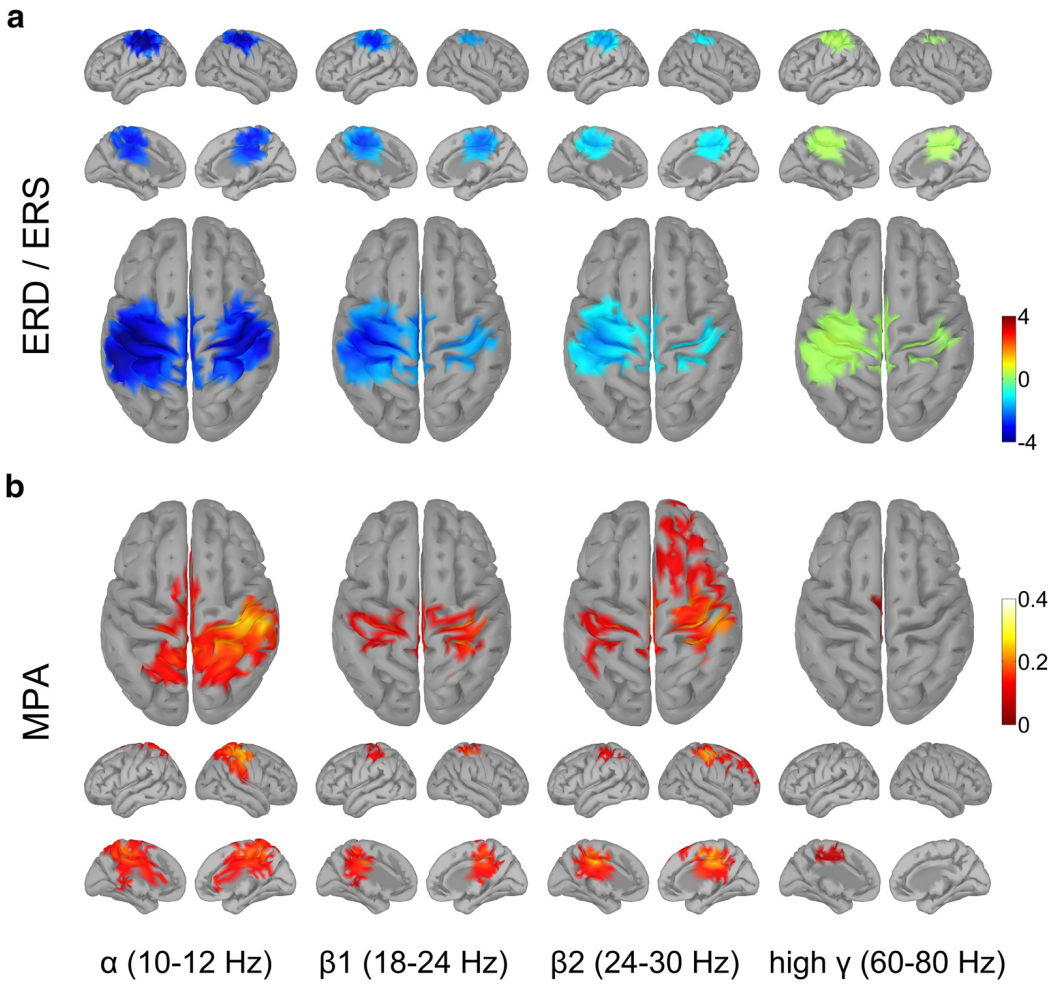

Figure 6. EEG source images of the fast movement cadence in selected frequency ranges (left to right column). ***a***, EEG sources of sustained ERD/ERS during movements are illustrated in blue/yellow-red. ***b***, EEG sources of movement MPAs are illustrated as modulation magnitude in red to white. Amplitudes in dB.

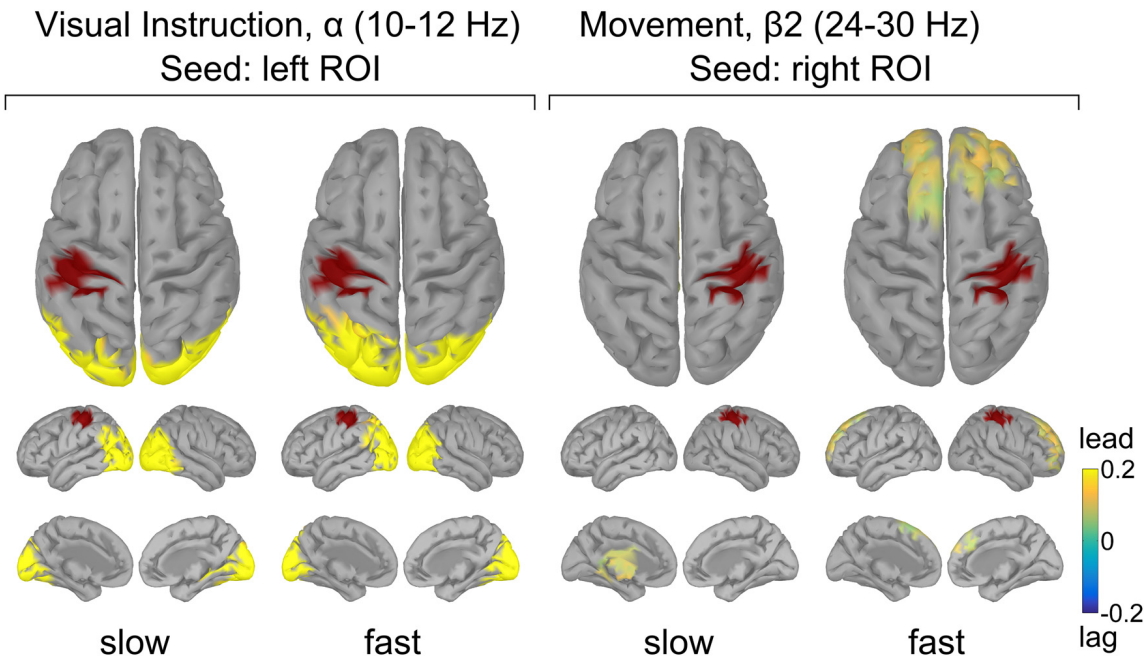

Figure 7. Amplitude comodulation between cortical areas. Left, Visual areas are comodulated with the left sensorimotor area (seed region in red) during visual instruction. Right, Subcortical regions are comodulated with the right sensorimotor area (seed region in red) during slow, but prefrontal areas during fast movement cadences.

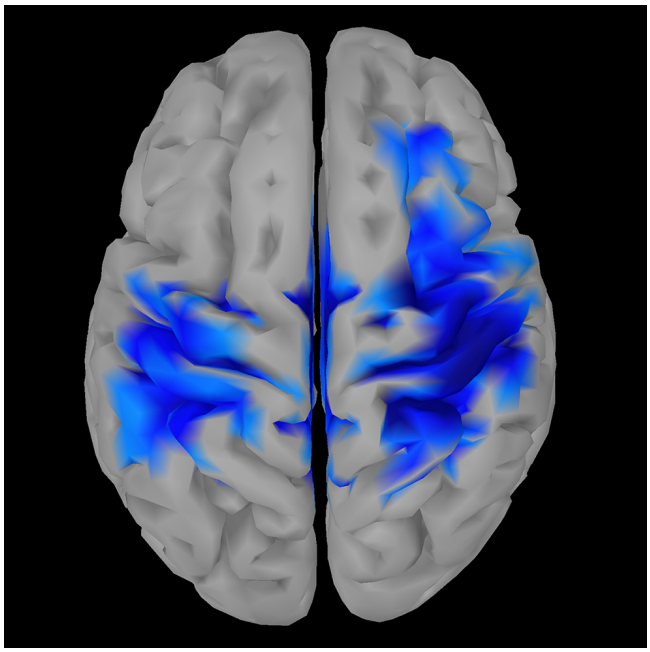

Movie 1. EEG source amplitudes for high β (24–30 Hz) frequencies during the slow movement cadence as function of the phase in a movement cycle. Phase axis in radian, ranging from $-\pi$ to π, is centered (0) at the maximal flexion of the fingers. Relative amplitude decreases/increases are illustrated in blue/red. EEG source amplitude threshold was set to 50% of the color scale maximum; the minimum cluster size was set to 20 vertices.

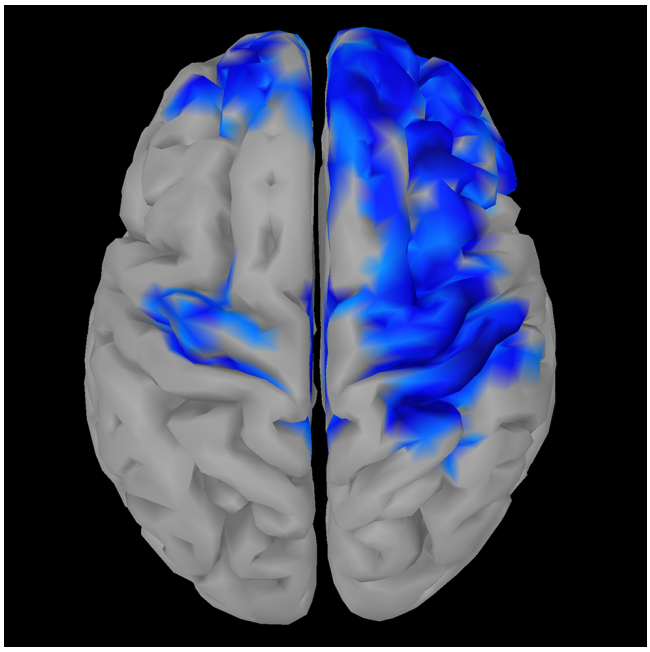

Movie 2. EEG source amplitudes for high β (24–30 Hz) frequencies during the fast movement cadence as function of the phase in a movement cycle. Phase axis in radian, ranging from $-\pi$ to π, is centered (0) at the maximal flexion of the fingers. Relative amplitude decreases/increases are illustrated in blue/red. EEG source amplitude threshold was set to 50% of the color scale maximum; the minimum cluster size was set to 20 vertices.

and auditory (Fujioka et al., 2012) stimuli in absence of actual movements. In this study, we investigated the opposite scenario, where no external stimuli were provided during rhythmic movement execution. Naturally, sensory inputs of the fingers are present during movements. Consequently, β MPA we report may represent processes related to the prediction and integration of this information. Saleh et al. (2010) observed β synchrony in the primary motor cortex only for behaviorally relevant, anticipated cues that required attention. Indeed, high β synchronization in prefrontal areas was found to be involved in top-down attention and control (Buschman and Miller, 2007; Buschman et al., 2012). Therefore, we interpret the prefrontal MPA cluster we found for $\beta 2$ frequencies (Fig. 6b) to reflect additional top-down control during the faster movement cadence. Moreover, analyzing amplitude comodulation between cortical areas showed that prefrontal $\beta 2$ MPA precedes those in the right sensorimotor seed (Fig. 7). This relationship is also visible in Movie 2 where $\beta 2$ MPAs travel from frontal toward sensorimotor and parietal areas, contributing to the modulation in these regions. For the slow movement cadence, we found two β peaks in a movement cycle in sensorimotor regions (Fig. 3*f*). Based on Movie 1, we suggest that these two peaks are related to two different processing streams. The first involves sensorimotor processing in bilateral hand regions; the second one is more related to central sensorimotor regions and SMA. In contrast to prefrontal $\beta 2$ MPA during fast movements, subcortical regions are leading sensorimotor seed cluster modulations during the slow movement cadence. This may be explained by the basal ganglia and thalamus being involved in top-down control during simple tasks but prefrontal regions during more complex behaviors (Buschman and Miller, 2014). However, precise localization of deep sources based on EEG recordings is challenging. More work is needed to further disentangle β MPA and investigate their specific functions. We observed this β modulation pattern simultaneously with the much stronger sustained β desynchronization we suggest to represent another network. Therefore, the MPA cannot be explained by postmovement β synchronization effects. Further, in contrast to the bilateral β MPA we report in this work, postmovement β synchronization was localized focally to contralateral areas (for review, see Neuper and Pfurtscheller, 2001; Cheyne, 2013).

We also found significant MPA at α and high γ frequencies. Their time courses resembled the β MPA in sensorimotor areas, but they were temporally shifted in the movement cycle and showed different spatial source patterns. α temporally lagged $\beta 2$ MPA in sensorimotor areas. We localized α MPA to bilateral sensorimotor, SMA, and parietal areas, which were stronger in the right hemisphere. Alpha oscillations in these cortical areas are related to working memory during retention of previously shown items (Jensen et al., 2002). Because our paradigm included remembering the movement speed instruction, it would be plausible that the α MPA we found here represents short-term working memory processes.

We found high γ MPA in the contralateral hand region, which is in agreement with invasive studies showing a close relation of high γ amplitudes to movement sequences (Miller et al., 2009; Hermes et al., 2012). An interesting finding is that only the SMA cluster reached significance during the faster movement cadence (Fig. 6b). In these clusters, high γ amplitudes were conversely modulated to the high β MPA. This relationship could be explained by the opposing roles of β and high γ oscillations we discussed above. Moreover, we similarly found amplitudes in the high β/low γ range to be conversely modulated to high γ amplitudes in a gait cycle during walking in humans (Seeber et al., 2015). Further, we previously reported sustained α and β ERD along with high γ increase during walking (Wagner et al., 2012; Seeber et al., 2014, 2015). Together, these findings suggest

shared electrophysiological principles of rhythmic finger tapping and walking.

In conclusion, we showed two different types of networks during rhythmic finger movements in this work. First, sustained α and β desynchronization may be associated with release of inhibition during movement. Together with high γ enhancement, these networks may upregulate excitability in regions specific to the body parts that are prepared to be, or actually are, moved (Pfurtscheller and Lopes da Silva, 1999; Miller et al., 2007). Second, movement phase-related networks, which modulate their synchrony in relation to the flexion and extension sequence of the fingers. We suggest frequency-specific MPA to signify distinct large-scale networks associated with specific functions, including top-down control, sensorimotor prediction, and integration. Our findings suggest that EEG source amplitudes reconstructed in a cortical patch are the summation of simultaneous present overlapping networks. Separating these two types of behavior-related large scale networks we distinguished in this work improves the interpretability of EEG sources and advances to relate them to human motor behavior.

References

Baillet S, Mosher JC, Leahy RM (2001) Electromagnetic brain mapping. IEEE Signal Processing Magazine 18:14–30. CrossRef

Brookes MJ, Woolrich M, Luckhoo H, Price D, Hale JR, Stephenson MC, Barnes GR, Smith SM, Morris PG (2011) Investigating the electrophysiological basis of resting state networks using magnetoencephalography. Proc Natl Acad Sci U S A 108:16783–16788. CrossRef Medline

Buschman TJ, Miller EK (2007) Top-down versus bottom-up control of attention in the prefrontal and posterior parietal cortices. Science 315: 1860–1862. CrossRef Medline

Buschman TJ, Miller EK (2014) Goal-direction and top-down control. Philos Trans R Soc Lond B Biol Sci. 369:20130471. CrossRef Medline

Buschman TJ, Denovellis EL, Diogo C, Bullock D, Miller EK (2012) Synchronous oscillatory neural ensembles for rules in the prefrontal cortex. Neuron 76:838–846. CrossRef Medline

Buzsáki, G (2006) Rhythms of the brain. Oxford: Oxford UP

Buzsáki G, Anastassiou CA, Koch C (2012) The origin of extracellular fields and currents: EEG, ECoG, LFP and spikes. Nat Rev Neurosci 13:407–420. CrossRef Medline

Cheyne DO (2013) MEG studies of sensorimotor rhythms: a review. Exp Neurol 245:27–39. CrossRef Medline

Crone NE, Miglioretti DL, Gordon B, Sieracki JM, Wilson MT, Uematsu S, Lesser RP (1998a) Functional mapping of human sensorimotor cortex with electrocorticographic spectral analysis: I. Alpha and beta event-related desynchronization. Brain 121:2271–2299. CrossRef Medline

Crone NE, Miglioretti DL, Gordon B, Lesser RP (1998b) Functional mapping of human sensorimotor cortex with electrocorticographic spectral analysis: II. Event-related synchronization in the gamma band. Brain 121: 2301–2315. CrossRef Medline

Dale AM, Fischl B, Sereno MI (1999) Cortical surface-based analysis: I. Segmentation and surface reconstruction. Neuroimage 9:179–194. CrossRef Medline

Darvas F, Pantazis D, Kucukaltun-Yildirim E, Leahy RM (2004) Mapping human brain function with MEG and EEG: methods and validation. Neuroimage 23:289–299. CrossRef Medline

Donner TH, Siegel M (2011) A framework for local cortical oscillation patterns. Trends Cogn Sci 15:191–199. CrossRef Medline

Elul R (1971) The genesis of the EEG. Int Rev Neurobiol 15:227–272. Medline

Engel AK, Fries P (2010) Beta-band oscillations-signalling the status quo? Curr Opin Neurobiol 20:156–165. CrossRef Medline

Engel AK, Gerloff C, Hilgetag CC, Nolte G (2013) Intrinsic coupling modes: multiscale interactions in ongoing brain activity. Neuron 80:867–886. CrossRef Medline

Fischl B (2012) FreeSurfer. Neuroimage 62:774–781. CrossRef Medline

Fischl B, Sereno MI, Tootell RB, Dale AM (1999) High-resolution intersubject averaging and a coordinate system for the cortical surface. Hum Brain Mapp 8:272–284. CrossRef Medline

Fujioka T, Trainor LJ, Large EW, Ross B (2012) Internalized timing of isochronous sounds is represented in neuromagnetic β oscillations. J Neurosci 32:1791–1802. CrossRef Medline

Gerloff C, Richard J, Hadley J, Schulman AE, Honda M, Hallett M (1998) Functional coupling and regional activation of human cortical motor areas during simple, internally paced and externally paced finger movements. Brain 121:1513–1531. CrossRef Medline

Gramfort A, Papadopoulo T, Olivi E, Clerc M (2010) OpenMEEG: open-source software for quasistatic bioelectromagnetics. Biomed Eng Online 9:45. CrossRef Medline

Hämäläinen MS, Ilmoniemi RJ (1994) Interpreting magnetic fields of the brain: minimum norm estimates. Med Biol Eng Comput 32:35–42. CrossRef Medline

Hermes D, Siero JC, Aarnoutse EJ, Leijten FS, Petridou N, Ramsey NF (2012) Dissociation between neuronal activity in sensorimotor cortex and hand movement revealed as a function of movement rate. J Neurosci 32:9736–9744. CrossRef Medline

Houweling S, Beek PJ, Daffertshofer A (2010) Spectral changes of interhemispheric crosstalk during movement instabilities. Cereb Cortex 20: 2605–2613. CrossRef Medline

Hyvärinen A (1999) Fast and robust fixed-point algorithms for independent component analysis. IEEE Trans Neural Netw 10:626–634. CrossRef Medline

Jasper HH, Penfield W (1949) Electrocorticograms in man: effect of the voluntary movement upon the electrical activity of the precentral gyrus. Arch Psychiatry Z Neurol 183:163–174. CrossRef

Jenkinson N, Brown P (2011) New insights into the relationship between dopamine, beta oscillations and motor function. Trends Neurosci 34: 611–618. CrossRef Medline

Jensen O, Gelfand J, Kounios J, Lisman JE (2002) Oscillations in the alpha band (9–12 Hz) increase with memory load during retention in a short-term memory task. Cereb Cortex 12:877–882. CrossRef Medline

Jolliffe I (2002) Principal component analysis. Encyclopedia of statistics in behavioral science. New York: Wiley.

Joundi RA, Jenkinson N, Brittain JS, Aziz TZ, Brown P (2012) Driving oscillatory activity in the human cortex enhances motor performance. Curr Biol 22:403–407. CrossRef Medline

Kybic J, Clerc M, Abboud T, Faugeras O, Keriven R, Papadopoulo T (2005) A common formalism for the integral formulations of the forward EEG problem. IEEE Trans Med Imaging 24:12–28. CrossRef Medline

Maris E, Oostenveld R (2007) Nonparametric statistical testing of EEG and MEG data. J Neurosci Methods 164:177–190. CrossRef Medline

Michel CM, Murray MM (2012) Towards the utilization of EEG as a brain imaging tool. Neuroimage 61:371–385. CrossRef Medline

Michel CM, Murray MM, Lantz G, Gonzalez S, Spinelli L, Grave de Peralta R (2004) EEG source imaging. Clin Neurophysiol 115:2195–2222. CrossRef Medline

Miller KJ, Leuthardt EC, Schalk G, Rao RP, Anderson NR, Moran DW, Miller JW, Ojemann JG (2007) Spectral changes in cortical surface potentials during motor movement. J Neurosci 27:2424–2432. CrossRef Medline

Miller KJ, Zanos S, Fetz EE, den Nijs M, Ojemann JG (2009) Decoupling the cortical power spectrum reveals real-time representation of individual finger movements in humans. J Neurosci 29:3132–3137. CrossRef Medline

Morlet J, Arens G, Fourgenau E, Glard D (1982) Wave propagation and sampling theory: I. Complex signal and scattering in multilayered media. Geophysics 47:222–236. CrossRef

Müller GR, Neuper C, Rupp R, Keinrath C, Gerner HJ, Pfurtscheller G (2003) Event-related beta EEG changes during wrist movements induced by functional electrical stimulation of forearm muscles in man. Neurosci Lett 340:143–147. CrossRef Medline

Neuper C, Pfurtscheller G (2001) Event-related dynamics of cortical rhythms: frequency-specific features and functional correlates. Int J Psychophysiol 43:41–58. CrossRef Medline

Nichols TE, Holmes AP (2002) Nonparametric permutation tests for functional neuroimaging: a primer with examples. Hum Brain Mapp 15:1–25. Medline

Nolte G, Bai O, Wheaton L, Mari Z, Vorbach S, Hallett M (2004) Identifying true brain interaction from EEG data using the imaginary part of coherency. Clin Neurophysiol 115:2292–2307. CrossRef Medline

Oostenveld R, Praamstra P (2001) The five percent electrode system for high-resolution EEG and ERP measurements. Clin Neurophysiol 112: 713–719.

Pascual-Marqui RD (2002) Standardized low resolution brain electromagnetic tomography (sLORETA): technical details. Methods Findings Exp Clin Pharmacol 24D:5–12. Medline

Pfurtscheller G, Aranibar A (1977) Event-related cortical desynchronization detected by power measurements of scalp EEG. Electroencephalogr Clin Neurophysiol 42:817–826. CrossRef Medline

Pfurtscheller G, Lopes da Silva FH (1999) Event-related EEG/MEG synchronization and desynchronization: basic principles. Clin Neurophysiol 110:1842–1857. CrossRef Medline

Pfurtscheller G, Neuper C, Andrew C, Edlinger G (1997) Foot and hand area mu rhythms. Int J Psychophysiol 26:121–135. CrossRef Medline

Pogosyan A, Gaynor LD, Eusebio A, Brown P (2009) Boosting cortical activity at beta-band frequencies slows movement in humans. Curr Biol 19:1637–1641. CrossRef Medline

Pollok B, Gross J, Müller K, Aschersleben G, Schnitzler A (2005) The cerebral oscillatory network associated with auditorily paced finger movements. Neuroimage 24:646–655. CrossRef Medline

Raichle ME (2010) Two views of brain function. Trends Cogn Sci 14:180–190. CrossRef Medline

Saleh M, Reimer J, Penn R, Ojakangas CL, Hatsopoulos NG (2010) Fast and slow oscillations in human primary motor cortex predict oncoming behaviorally relevant cues. Neuron 65:461–471. CrossRef Medline

Scherer R, Zanos SP, Miller KJ, Rao RP, Ojemann JG (2009) Classification of contralateral and ipsilateral finger movements for electrocorticographic brain-computer interfaces. Neurosurg Focus 27:E12. CrossRef Medline

Seeber M, Scherer R, Wagner J, Solis-Escalante T, Müller-Putz GR (2014) EEG beta suppression and low gamma modulation are different elements of human upright walking. Front Hum Neurosci 8:485. CrossRef Medline

Seeber M, Scherer R, Wagner J, Solis-Escalante T, Müller-Putz GR (2015) High and low gamma EEG oscillations in central sensorimotor areas are conversely modulated during the human gait cycle. Neuroimage 112:318–326. CrossRef Medline

Siegel M, Donner TH, Engel AK (2012) Spectral fingerprints of large-scale neuronal interactions. Nat Rev Neurosci 13:121–134. CrossRef Medline

Tadel F, Baillet S, Mosher JC, Pantazis D, Leahy RM (2011) Brainstorm: a user-friendly application for MEG/EEG analysis. Comput Intelligence Neurosci 2011.

Toma K, Mima T, Matsuoka T, Gerloff C, Ohnishi T, Koshy B, Andres F, Hallett M (2002) Movement rate effect on activation and functional coupling of motor cortical areas. J Neurophysiol 88:3377–3385. CrossRef Medline

Wagner J, Solis-Escalante T, Grieshofer P, Neuper C, Müller-Putz G, Scherer R (2012) Level of participation in robotic-assisted treadmill walking modulates midline sensorimotor EEG rhythms in able-bodied subjects. Neuroimage 63:1203–1211. CrossRef Medline

Wagner J, Solis-Escalante T, Scherer R, Neuper C, Müller-Putz G (2014) It's how you get there: walking down a virtual alley activates premotor and parietal areas. Front Hum Neurosci 8:93. CrossRef Medline

Yuan H, Perdoni C, He B (2010) Relationship between speed and EEG activity during imagined and executed hand movements. J Neural Eng 7:26001. CrossRef Medline

Appendix B.

Author contributions

Martin Seeber, Reinhold Scherer, Johanna Wagner, Teodoro Solis-Escalante, and Gernot R. Müller-Putz "EEG beta suppression and low gamma modulation are different elements of human upright walking." In: *Frontiers in Human Neuroscience* 8 (2014). DOI: 10.3389/fnhum.2014.00485

Martin Seeber, Reinhold Scherer, Johanna Wagner, Teodoro Solis-Escalante, and Gernot R. Müller-Putz "Corrigendum: EEG beta suppression and low gamma modulation are different elements of human upright walking." In: *Frontiers in Human Neuroscience* 9 (2015). DOI: 10.3389/fnhum.2015.00542

MS (55%), RS (15%), JW (15%), TS (10%), GM (5%)
conceptual idea: MS, RS; experimental design: RS, JW, TS, GM; recorded data: JW, TS; contributed unpublished analytic tools: MS; analyzed data: MS; wrote the paper: MS, RS, JW, TS, GM.

Martin Seeber, Reinhold Scherer, Johanna Wagner, Teodoro Solis-Escalante, and Gernot R. Müller-Putz "High and low gamma EEG oscillations in central sensorimotor areas are conversely modulated during the human gait cycle." In: *NeuroImage* 112 (2015), pp. 318–326. DOI: 10.1016/j.neuroimage.2015.03.045

MS (70%), RS (10%), JW (10%), TS (5%), GM (5%)
conceptual idea: MS, RS; experimental design: RS, JW, TS, GM; recorded data: JW, TS; contributed unpublished analytic tools: MS; analyzed data: MS; wrote the paper: MS, RS, JW, TS, GM.

Martin Seeber, Reinhold Scherer, and Gernot R. Müller-Putz "EEG Oscillations Are Modulated in Different Behavior-Related Networks during Rhythmic Finger Movements." In: *Journal of Neuroscience* 36.46 (2016), pp. 11671–11681. DOI: 10.1523/jneurosci.1739-16.2016

MS (80%), RS (10%), GM (10%)
conceptual idea: MS; experimental design: MS, GM; recorded data: MS; contributed unpublished analytic tools: MS; analyzed data: MS; wrote the paper: MS, RS, GM.

Appendix C.

List of Scientific Publications

Journal Articles

Seeber M., Scherer R., and Müller-Putz G.R. "EEG Oscillations Are Modulated in Different Behavior-Related Networks during Rhythmic Finger Movements." In: *Journal of Neuroscience* 36.46 (2016), pp. 11671–11681. DOI: 10.1523/jneurosci.1739-16.2016

Brunner C., Billinger M., Seeber M., Mullen T.R., Makeig S. "Volume Conduction Influences Scalp-Based Connectivity Estimates." In: *Frontiers in Computational Neuroscience* 10 (2016). DOI: 10.3389/fncom.2016.00121

Seeber M., Scherer R., Wagner J., Solis-Escalante T., and Müller-Putz G.R. "High and low gamma EEG oscillations in central sensorimotor areas are conversely modulated during the human gait cycle." In: *NeuroImage* 112 (2015), pp. 318–326. DOI: 10.1016/j.neuroimage.2015.03.045

Seeber M., Scherer R., Wagner J., Solis-Escalante T., and Müller-Putz G.R. "EEG beta suppression and low gamma modulation are different elements of human upright walking." In: *Frontiers in Human Neuroscience* 8 (2014). DOI: 10.3389/fnhum.2014.00485

Seeber M., Scherer R., Wagner J., Solis-Escalante T., and Müller-Putz G.R. "Corrigendum: EEG beta suppression and low gamma modulation are different elements of human upright walking." In: *Frontiers in Human Neuroscience* 9 (2015). DOI: 10.3389/fnhum.2015.00542

Conference Papers

Hehenberger L., Seeber M. and Scherer R. "Estimation of Gait Parameters from EEG Source Oscillations" In: *IEEE International Conference on Systems, Man, and Cybernetics* (2016)

Seeber M., Wagner J., Scherer R., Solis Escalante T., and Müller-Putz G.R. "Reconstructing gait cycle patterns from non-invasive recorded low gamma modulations." In: *Proceedings of the 6th International Brain-Computer Interface Conference* (2014)

Seeber M., Scherer R., Wagner J., Solis Escalante T., and Müller-Putz G.R. "Spatial-spectral identification of μ and β EEG rhythm sources during robot-assisted walking." In: *Proceedings of the BMT* (2013)

Scherer R., Solis Escalante T., Faller J., Wagner J., Seeber M., and Müller-Putz G.R. "On the use of Non-Invasive Brain-Computer Interface Technology in Neurorehabilitation." In: *Proceedings of the BMT* (2013)

Seeber M., Friedrich E., Jehna M., Müller-Putz G.R. and Scherer R. "Non-invasive functional mapping of brain activity." In: *NeuroLogisch Supplementum* (2012)

Holzinger A., Scherer R., Seeber M., Wagner J., and Müller-Putz G.R. "Computational Sensemaking on Examples of Knowledge Discovery from Neuroscience Data: Towards Enhancing Stroke Rehabilitation." In: *Lecture Notes in Computer Science* (2012)

Scientific Talks

Seeber M., Scherer R., and Müller-Putz G.R. "Linking neural oscillations and motor behavior: Modeling EEG source dynamics during human walking and rhythmic finger movements." *ANT Burgundy Neuromeeting*, Beaune, France (2016)

Seeber M., Wagner J., Scherer R., Solis Escalante T., and Müller-Putz G.R. "Reconstructing gait cycle patterns from non-invasive recorded low gamma modulations." *6th International Brain-Computer Interface Conference*, Graz, Austria (2014)

Seeber M., Wagner J., Scherer R., Solis Escalante T., and Müller-Putz G.R "The Role of β and γ EEG Oscillations during Upright Walking in Humans." *Chair Biological Psychology and Neuroergonomics*, Berlin, Germany (2014)

Seeber M., Scherer R., Wagner J., Solis Escalante T., Müller-Putz G.R. "Spatial-spectral identification of μ and β EEG rhythm sources during robot-assisted walking." *BMT*, Graz, Austria (2013)

Original Theses

Seeber M. "The Electroencephalographic Sources of Repetitive Movements." *Doctoral Thesis, Graz University of Technology* (2017)

Seeber M. "sLORETA reconstruction of EEG sources." *Diploma Thesis, Graz University of Technology* (2011)